

## SOUHRN

### Vliv intramolekulární elektronové interakce na elektrochemickou redukci a reaktivitu orthoftalaldehydu při analýze aminokyselin. Porovnání s iso- a tereftalaldehydem

Orthoftalaldehyd (OPA) se používá jako dezinfekční činidlo v nemocnicích a jako derivatizační činidlo při analýze a stanovení aminokyselin. Uvedené procesy jsou založeny na reakci OPA s nukleofily, mechanismus těchto dějů však není dosud zcela známý. Pro jeho studium jsme v rámci dlouhodobého projektu zvolili elektrochemický přístup. Ukázalo se však, že v literatuře popsané elektrochemické chování OPA ve vodném prostředí není úplné a elektrochemická redukce v nevodném prostředí není popsána vůbec. Proto hlavním cílem této diplomové práce je poprvé detailně prostudovat elektrochemickou redukci OPA v nevodném prostředí a upřesnit, případně doplnit údaje o redukovatelnosti OPA ve vodních roztocích. Pro správné aplikace OPA využívající reaktivitu této látky s nukleofily je důležité mít tyto informace k dispozici. Aby bylo možné zodpovědně interpretovat experimentální výsledky, byly pro srovnání do tohoto výzkumu zahrnutý také zbylé dva strukturní izomery - isoftalaldehyd (IPA) a tereftalaldehyd (TPA) a navíc i tři analogické *o*-, *m*- a *p*-diacetylbenzeny.

Experimenty s cílem objasnit průběh elektrochemické redukce OPA, IPA a TPA byly provedeny převážně v bezvodém acetonitrilu. Látky byly studovány pomocí elektrochemických metod (DC-polarografie, cyklická voltametrie na rtuťové a zlaté elektrodě, coulometrie a preparativní elektrolýzy) a pomocí kombinací elektrochemických a spektroskopických technik (UV/Vis a IČ spektroelektrochemie a elektronová paramagnetická rezonance spojená s *in situ* elektrochemickou generací radikálových částic). NMR spektroskopie a HPLC-MS byly použity pro identifikaci produktů preparativních elektrolýz.

Elektrochemická redukce OPA byla pro porovnání provedena i v dalších aprotických rozpouštědlech (dimethylformamid, aceton) a kromě rtuti i na dalších elektrodových materiálech jako je zlato a platina. Na základě získaných experimentálních elektrochemických a spektroelektrochemických dat a jejich interpretace byla popsána elektrochemická redukce OPA, IPA a TPA a byly navrženy mechanismy pro jejich redukci v nevodném prostředí. Elektrochemické chování ve vodních roztocích bylo sledováno v celém rozsahu pH a ukázalo se být daleko složitější, než je popsáno v literatuře. Na závěr byla elektrochemicky a spektrometricky testována reaktivita OPA vůči osmi vybraným aminokyselinám. Rozdíly v rychlosti derivatizace závisí na struktuře AAs a byly diskutovány. Zvláště pozoruhodná je otázka hydratace jakožto konkurenční reakce k adici aminů na karbonyl.

## SUMMARY

### **Effects of intramolecular electron interactions on electrochemical reduction and reactivity of orthophthalaldehyde in analysis of amino acids. Comparison with iso- and terephthalaldehyde**

Orthophthalaldehyde (OPA) is used as a disinfecting agent in hospitals and as a derivatization agent for analysis and determination of amino acids. These processes are based on the reaction of OPA with nucleophiles, however, the mechanism of these applications is not fully understood until now. For the mechanistic study, the electrochemical approach was selected. It was found that the electrochemical behavior of OPA in water solutions described in the literature is not complete, moreover, the electrochemical reduction in non aqueous solutions has not been reported at all. Therefore the main aim of the presented thesis is the first detailed investigation of electroreduction of OPA in aprotic solvents and completion or specification of experimental data for reducibility of OPA in water solutions. Its electrochemical behavior in both media has to be known prior to any application of OPA. In order to find a reliable interpretation of the experimental results, the remaining two isomeric species - isophthalaldehyde (IPA) a terephthalaldehyde (TPA) and, in addition to this, three analogous *o*-, *m*- and *p*-diacetylbenzenes were included in the research for comparison.

Experiments in order to investigate progress of electrochemical reduction of OPA, IPA, and TPA were performed mainly in non-aqueous acetonitrile. The compounds were studied using electrochemical methods (cyclic voltammetry on mercury and gold electrodes, DC-polarography, coulometry, preparative electrolyses) and combinations of electrochemical methods with spectroscopic techniques (UV/Vis, IR and electron paramagnetic resonance spectroelectrochemistry). NMR spectroscopy and HPLC-MS were used for identification of products after preparative electrolysis.

Electrochemical reduction of OPA has been performed for comparison also in other aprotic solvents (dimethylformamide, acetone) and besides mercury, gold and platinum were used as alternative electrode materials. Based on the acquired experimental electrochemical and spectroelectrochemical data and their interpretation, electrochemical reduction of OPA, IPA, and TPA was described and the probable mechanisms for their reduction in aprotic media were suggested. The electrochemical behavior of the studied compounds in aqueous solutions has been followed over the whole pH range in detail and it appeared to be much more complicated in contrast to the literature reports. At the end, the reactivity of OPA towards eight selected AAs was electrochemically and spectrometrically tested. The differences in reaction rates depend on the structure of AAs and were discussed. The question of hydration as a concurrent process to the addition of amines to carbonyl appeared to be particularly remarkable.

## **ACKNOWLEDGEMENT**

First of all, I would like to thank my supervisor Prof. Jiří Ludvík for his help during measurements and during data analysis. Also I would like to thank my colleagues from the lab (J. Heyrovský Institute of Physical Chemistry of the CAS – JHI) – Jiří Urban, Ludmila Šimková and Radka Metelková – for creating friendly and helpful working environment.

I would like to thank Dr. Jiří Klíma (JHI) and Dr. Karol Lušpaj (Faculty of Chemical and Food Technology at Slovak University of Technology) for help with measurement of EPR spectra of studied compounds, Dr. Jan Fiedler (JHI) for help with measurement of IR spectroelectrochemical experiments, Ing. Eva Hanzlová (Department of Organic Chemistry, UCT, Prague) for help with measurement of NMR spectra of products after electrolysis, doc. Igor Linhart (Department of Organic Chemistry, UCT, Prague) for help with HPLC-APCI-MS analysis of products after electrolysis, and Prof. Pavel Matějka (Department of Physical Chemistry, UCT, Prague) for consultation of measured IR spectroelectrochemical spectra.

Many thanks belong to Vít Svoboda for fruitful discussions about the obtained results and for all his understanding and love. Finally I would like to thank my family for support, caring and love during my university studies.

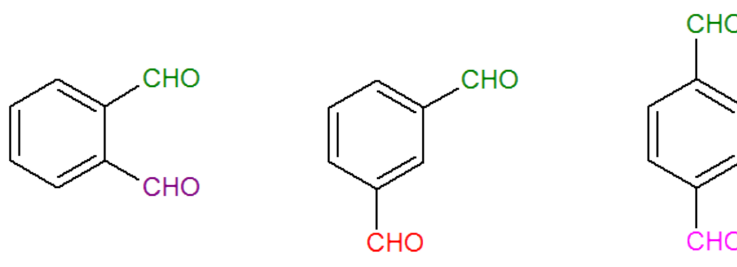
# Contents

<b>1 INTRODUCTION</b>	<b>6</b>
<b>2 LITERATURE</b>	<b>8</b>
2.1 Amino acid analysis . . . . .	8
2.2 Derivatization agents . . . . .	11
2.2.1 Ninhydrin . . . . .	11
2.2.2 Orthophthalaldehyde (OPA) . . . . .	13
2.2.3 Other derivatization agents . . . . .	15
2.3 Techniques used for analysis of AAs . . . . .	17
2.3.1 Ion-exchange chromatography (IEC) . . . . .	17
2.3.2 Liquid chromatography (LC) . . . . .	17
2.3.3 Capillary electrophoresis (CE) . . . . .	18
2.4 Electrochemical behavior of three isomeric benzenedialdehydes in aqueous and non-aqueous media . . . . .	19
2.4.1 Orthophthalaldehyde . . . . .	21
2.4.2 Isophthalaldehyde . . . . .	23
2.4.3 Terephthalaldehyde . . . . .	27
2.5 Electrochemical behavior of three isomeric diacetylbenzenes . . . . .	33
<b>3 EXPERIMENT</b>	<b>34</b>
3.1 Used techniques and instrumentation . . . . .	34
3.2 Chemicals . . . . .	38
<b>4 RESULTS AND DISCUSSION</b>	<b>40</b>
4.1 Non-aqueous media . . . . .	41
4.1.1 Orthophthalaldehyde . . . . .	41
4.1.2 Isophthalaldehyde . . . . .	48
4.1.3 Terephthalaldehyde . . . . .	53
4.1.4 Comparison of behavior of benzenedialdehydes in non-aqueous media . . . . .	60
4.1.5 Electrochemical behavior of studied benzenedialdehydes in DMF and acetone . . . . .	62

4.2 Aqueous media . . . . .	66
4.3 Reactivity of OPA, IPA and TPA with nucleophiles . . . . .	68
<b>5 CONCLUSION</b>	<b>71</b>
<b>List of abbreviations</b>	<b>73</b>
<b>List of Figures</b>	<b>75</b>
<b>List of Tables</b>	<b>78</b>
<b>SUPPLEMENTARY MATERIAL</b>	<b>79</b>
<b>A Tables</b>	<b>79</b>
<b>B UV/Vis SEC</b>	<b>83</b>
<b>C Electrochemical behavior of diacetylbenzenes in ACN, DMF and acetone</b>	<b>85</b>
<b>BIBLIOGRAPHY</b>	<b>91</b>

# 1 INTRODUCTION

Three isomeric benzenedialdehydes - orthophthalaldehyde (OPA), isophthalaldehyde (IPA) and terephthalaldehyde (TPA) - belong among biologically active substances whose active part is a carbonyl group. The most important one is OPA. Its biological activity manifests itself in two ways: as a disinfecting preparation and as a derivatization agent for analysis and determination of AAs. Therefore the literary part deals with brief description of several techniques which are used for analysing samples that contain amino acids – ion-exchange chromatography (IEC), reversed-phase high performance liquid chromatography (RP-HPLC) and capillary electrophoresis (CE). The literary part describes also other derivatization agents: ninhydrin, naphthalene-2,3-dicarboxaldehyde, 3-(2-furoyl)quinoline-2-carboxaldehyde, 3-(4-carboxybenzoyl)quinoline-2-carboxaldehyde, 3-(4-bromobenzoyl)quinoline-2-carboxaldehyde and 3-(4-chlorobenzoyl)quinoline-2-carboxaldehyde.



ortho<sup>phthalaldehyde (OPA)</sup>    isop<sup>phthalaldehyde (IPA)</sup>    ter<sup>phthalaldehyde (TPA)</sup>

**Figure 1:** Structures of OPA, IPA and TPA.

Although the derivatization of AAs by OPA is already long time widely used for AAs analysis, the detailed mechanism is still not fully understood.<sup>1</sup> It is necessary to mention that the derivatization is based on the condensation reaction of the dialdehyde with the primary amine group of AAs. In contrast to expectations the condensation reaction of the *o*-dialdehyde is complicated by several simultaneous and follow-up reactions, including intramolecular ones, not only with amines, but also with water as a nucleophile. Although water is much weaker nucleophile than amines, its high excess makes its reaction with OPA significant (hydration).

For analysis of the reaction mechanism a method should be applied which enables to follow the starting molecule of OPA, intermediates and products. Due to the presence of two carbonyl groups, the three benzenedialdehydes are electrochemically reducible, that means, electrochemical approach is very suitable as a tool for monitoring of the reaction course under various conditions. For this purpose the detailed and fundamental investigation of redox properties of the title dialdehyde and its isomers is necessary. In case of benzenedialdehydes there are two electron-withdrawing groups which can interact with each other.

Studied benzenedialdehydes have different electrochemical behaviour due to diverse resonance and/or inductive intramolecular electron interactions of both carbonyl groups. In literature their electroreduction is described only in aqueous solutions. In this media electrochemical reduction is affected by covalent hydration (mentioned above) caused by nucleophilic attack of water molecules. This fact complicates the reduction mechanisms.

In living organisms there are also non-aqueous parts (e.g. lipid bilayers and adipocytes) in which these compounds can penetrate and be active. However electrochemical behavior of the three benzenedialdehydes in non-aqueous aprotic media, i.e. in media where addition of water (hydration) to the carbonyl group is impossible, is not reported in any article. The presented thesis is therefore focused on the investigation of electrochemical reduction of benzenedialdehydes in non-aqueous aprotic media and on its comparison with the results obtained in aqueous buffered solutions. For more general conclusions, the methylated analogues (1,2-diacetylbenzene, 1,3-diacetylbenzene and 1,4-diacetylbenzene) were also investigated.

All compounds were studied using DC-polarography, cyclic voltammetry (CV), coulometry, preparative electrolyses, UV/Vis and IR spectroelectrochemistry and electron paramagnetic resonance (EPR) coupled *in situ* with electrolysis. NMR spectroscopy and HPLC coupled with MS were used for identification of products of electrochemical reduction.

## 2 LITERATURE

### 2.1 Amino acid analysis

Amino acids (AAs) belong among the most important natural compounds. They take part in many physiological processes, either in their free form or as a part of peptides and proteins.<sup>2</sup> Common proteins in living organisms consist of 19 AAs and of one imino acid – proline. These AAs are called proteinogenic AAs and they are  $\alpha$ -AAs – the amino group is on the  $\alpha$ -carbon. Rarely two more AAs are present in organisms - selenocysteine and pyrolysine.<sup>3</sup>

Analysis of AAs is based on the detection of amino group. The process of analysis depends on the type of AAs which are subject to analysis. Free AAs in a sample can be analyzed right after their extraction from matrix.<sup>3</sup> For determination of AAs bound in peptides and proteins, hydrolysis of the peptide bond has to be performed before the actual analysis.

Hydrolysis conditions differ depending on the type of a sample. The hydrolysis time depends on the used temperature, on the primary structure of AAs, on stability of functional groups, on strength of the peptide bond and on a sample matrix. According to the official AOAC (Association of Analytical Communities) method, hydrolysis is recommended for 24 hours at 110 °C in 6M HCl as a compromise between hydrolysis effect and stability of AAs.<sup>3,4</sup> Microwave radiation is used also for protein hydrolysis. High temperatures are reached in short times (up to 180 °C) and hydrolysis is finished after 5 minutes. It is performed in acid or basic conditions in a special equipment that is resistant to high temperature and pressure.

When desired AAs are obtained, next step is their detection. Basic detection of AAs without possibility to distinguish individual AAs can be performed by UV spectroscopy at wavelengths 200–210 nm (absorption maximum of carboxyl group COOH).<sup>5</sup> This method is direct, almost nondestructive and it detects primary and secondary AAs at one time, however its sensitivity and selectivity is very low. Aromatic AAs can be detected in region between 250 and 280 nm, but in more complex matrix this detection is not possible.

The solution to the problem of AA detection is a derivatization reaction during which amino group (both primary and secondary) selectively reacts with a derivatization agent. By this reaction a compound is formed which can be detected with better limits of detection thanks to its properties. After separation of derivatives, the content of individual AAs can be determined. The first used derivatization agent for determination of AAs was ninhydrin.<sup>6</sup> In 1910 Siegfried Ruhemann discovered that after heating of a solution of ninhydrin with primary amines a purple compound is formed which was later named as Ruhemann's purple.

In 1958 the first automatic chromatograph was made by Sanford Moore and William H. Stein. It was capable of both qualitative and quantitative analysis of AAs based on ion-exchange chromatography (IEC) of derivatives with ninhydrin.<sup>7</sup> Since then the method went through many improvements<sup>8-11</sup> – sample preparation, protein hydrolysis, determination of unstable AAs, higher sensitivity or other derivatization agent. Compared to the original method, the analysis time is now shortened from one day to less than five minutes.<sup>12</sup> In last decades, high-performance liquid chromatography (HPLC) has become more popular than IEC.<sup>7,12</sup> The disadvantage compared to IEC is that samples determined by this technique have to be much purer otherwise the column is destroyed. IEC is not so much sensitive to sample impurities because uncharged contaminants pass through the system quickly and they don't interfere during post-column derivatization and during detection. Next, capillary electrophoresis (CE) is also used for analysis of AAs.<sup>12</sup> It is used mostly for on-line analysis of small sample volumes on a chip connected with microdialysis.

Today, amino acid derivatization is performed in three ways – before separation of AAs, so called pre-column derivatization, directly during separation, so called on-column derivatization, or after separation of AAs and before their detection, so called post-column derivatization. Each of them has its own advantages and disadvantages. If pre-column derivatization is used, a mixture of AAs reacts with a derivatization agent.<sup>5</sup> After some specified time the derivatives are applied on a column with a nonpolar sorbent and separation is carried out. Detection is made by UV/Vis spectroscopy, fluorescence or electrochemical detectors. Disadvantages

of pre-column derivatization include simultaneous derivatization reaction with all present AAs therefore it's not possible to quantify AAs in a solution because the derivatization reaction can have different conversion with different AAs; instability of derivatives and interference of other solution components.

If post-column derivatization is used, a mixture of AAs is separated using some separation method, then derivatization is carried out and the derivatives are detected by UV/Vis spectroscopy or by fluorescence.<sup>5</sup> Advantages of post-column derivatization are easy performance with great quantification, simple automation and reaction only with an eluted AA (no interferences with other matrix components). Disadvantages of post-column derivatization include necessary miscibility of the mobile phase with the derivatization agent and high consumption of the agent. Unreacted derivatization agent shouldn't have response in the same region as derivatives with AAs and reagent excess in the system can cause higher background signal which can lead to lower analyte signal. In general pre-column methods are used in laboratories with fundamental and applied research where hydrolyzates are often used. Post-column methods are used in laboratories ensuring quality where huge amounts of samples are analyzed and where the need for sample preparation before analysis is very small.

On-column derivatization is used mostly in capillary electrophoresis.<sup>13</sup> Advantages are small consumption of reagents and samples, short reaction time and possibility of automation. Also no special equipment is needed. Several modes of on-column derivatization have been published. Zone-passing derivatization is based on different electrophoretic mobilities of samples and reagents. It is necessary to apply first a solution with lower electrophoretic mobility. After applying solutions on column, separating voltage is applied. The solution with higher electrophoretic mobility starts to pass through the zone of the solution with lower electrophoretic mobility and by that the derivatization reaction proceeds. When throughout-capillary derivatization is used, the capillary is filled with a buffer in which a derivatization agent is dissolved. Sample components therefore react with the derivatization agent during separation. In case of inlet derivatization, short zones of a sample and a reagent are applied at the capillary inlet, low voltage is applied for some specified time and solutions react before application of separation voltage.

## 2.2 Derivatization agents

As was mentioned in previous section, there are no general methods by which AAs can be simply detected. For their detection, a derivatization reaction has to be performed that transforms AAs to better detectable substances. For this purpose, several derivatization agents are used. The choice of the agent depends on the technique used for separation of AAs.

### 2.2.1 Ninhydrin

Ninhydrin (structure in Fig. 2) is used for more than one hundred years for determination of primary and secondary amino groups, guanidine, amide and thiol groups and also cyanide ions.<sup>6</sup> It is used in post-column derivatization after reversed-phase HPLC .

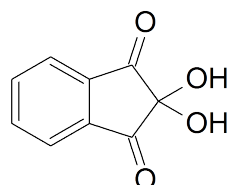


**Figure 2:** Structure of ninhydrin.

The derivatization reaction is usually performed at slightly acidic pH (5.5) and at higher temperature. The reaction product is a soluble chromophore which includes a nitrogen atom from the amine. This chromophore is the same for all amines that react with ninhydrin - amines, AAs, peptides, proteins and ammonia. The chromophore is not chemically bound to the determined protein or to other insoluble material therefore it is still present in the solution after filtration of the substrate.

Friedman<sup>6</sup> studied in detail the mechanism of the reaction of ninhydrin with  $\alpha$ -AAs at 30 and 100 °C and he observed dependence on basicity and steric vicinity of amino group. As the rate-determining step, the replacing of OH group in ninhydrin by unprotonated amino group was determined (Fig. 3). This step is affected by steric accessibility of the amino group and by the ratio of protonated

and unprotonated amino group in the solution. It was found out that the reaction involves two molecules of ninhydrin and one molecule of amino acid. The reaction product causing the change of color is Ruhemann's purple (the final product in Fig. 3).

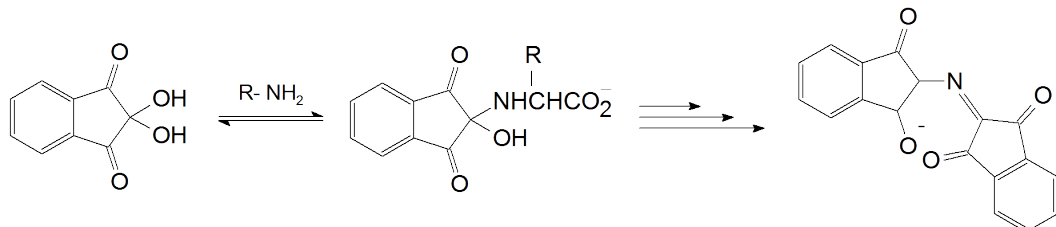


**Figure 3:** The reaction of ninhydrin with  $\alpha$ -AAs and with primary amines, Ruhemann's purple is formed.

The presence of Ruhemann's purple is detected by UV/Vis spectrophotometry.<sup>6</sup> Spectra are strongly influenced by used solvent. In non-polar aprotic solvents (e.g. DMSO, DMF) the compound absorbs most around 605 nm, in non-polar aprotic solvents which can participate in acid-base equilibria (e.g. pyridine) it absorbs most around 550 nm, and in non-aqueous protic solvents (e.g. formamide) around 575 nm.

Ninhydrin is used also as an universal agent for the determination of latent fingerprints on porous materials (e.g. paper). This method is often used in forensic sciences.<sup>6</sup> The principle of this method is either a reaction of ninhydrin with free AAs from left sweat and wax or creation of metal complexes between Ruhemann's purple and added metal salts (cadmium, europium, iron, zinc). These metal complexes are strongly fluorescent under blue-green light of argon laser. Ruhemann's purple is generated slowly at room temperature therefore often higher temperature is applied for the development of colour.<sup>14</sup> A problem can occur with the reaction of ninhydrin with additives in paper at higher temperatures. By that fingerprints can be destroyed.

## 2.2.2 Orthophthalaldehyde (OPA)

Reactivity of OPA with amino acids was published in 1971 by Marc Roth.<sup>15</sup> Reaction of OPA with AAs was performed in basic solution in the presence of another nucleophile – 2-mercaptoethanol. By this reaction strongly fluorescent compounds are formed. The advantage, compared to the reaction with ninhydrin, is that the reaction mixture does not have to be heated and fluorescence is detectable after 5 minutes from mixing reagents. The determination with OPA is more sensitive than with ninhydrin because it is a fluorometric determination which generally gives limits of detection lower by several orders of magnitude than spectrophotometric determinations. The disadvantage is that imino acids (e.g. proline) and cysteine don't react with OPA and therefore they can't be detected by this derivatization agent.

The highest yields of fluorescence are obtained when a strong reducing agent is added to the reaction mixture of OPA and AAs, e.g. 2-mercaptoethanol. Also other thiol compounds have been tested.<sup>16</sup> 2-mercaptoethanol, ethanethiol and 3-mercaptopropionic acid are used mostly. The ratio OPA/thiol in the derivatization solutions is in most cases 1/3 for 3-mercaptopropionic acid (MPA), N-acetylcysteine (NAC) and 2-mercaptoethanol (MCE), or 1/10 for ethanethiol (ET). OPA is used in excess (20-120fold) against AAs. The derivatization solution is kept in a refrigerator at 4 °C and it is used for several days.<sup>17</sup> Fluorescence is measured usually at these wavelengths:  $\lambda_{ex} = 340$  nm and  $\lambda_{em} = 455$  nm.<sup>15</sup> OPA is used mostly in a pre-column derivatization reaction with one of these reducing agents before RP-HPLC.<sup>2,18-24</sup> There were also attempts to develop methods using capillary electrophoresis for separation of the derivatives.<sup>25-28</sup>

Intensity of fluorescence is influenced also by the order of mixing of reactants. If first OPA is mixed with 2-mercaptoethanol and then a sample with AAs is added to the solution, fluorescence is higher than if OPA is first mixed with AAs and after that 2-mercaptoethanol is added. This dependence is caused by the fact that OPA alone also reacts with AAs but the products are not fluorescent compounds.

The fluorescence reaction is also dependent on pH. Aliphatic AAs and AAs with a second carboxyl group, with thiol or hydroxy group give the highest fluorescence yields between pH 8.0 and 11.0. Lysine gives the highest fluorescence in slightly acidic pH, between 6.0 and 7.0. Intensity of fluorescence is influenced by the type of buffer, too. In borate buffer at pH 8.0 fluorescence was higher than in phosphate buffer at same pH. Intensity of fluorescence reaches its maximum about 5 minutes after mixing reagents. After 25 minutes, significant decline in fluorescence occurs caused by instability of formed fluorescent compounds.

The structure of these fluorescent compounds was determined in 1970's as an isoindole derivative (see Fig. 4). This compound is unstable and it undergoes further reactions. The reaction mechanism is still unknown. One of suggested reaction mechanisms of the reaction of OPA with ammonia and with glycine is in Fig. 5 and 6.

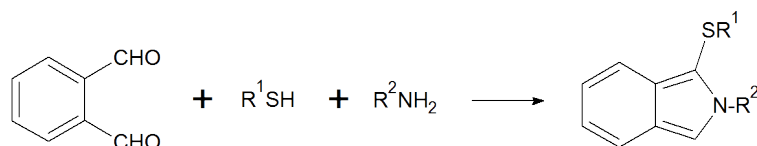


**Figure 4:** The reaction of OPA with a thiol and an amine, an isoindole derivative is formed (a fluorescent compound).<sup>16</sup>

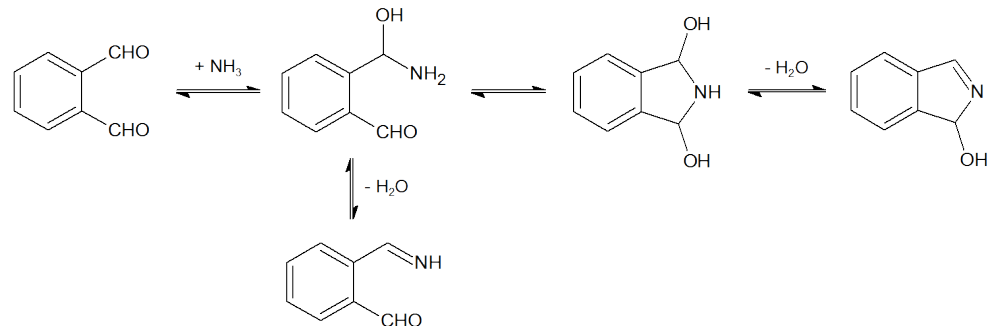


**Figure 5:** The suggestion for mechanism of reaction of OPA with ammonia.<sup>29</sup>

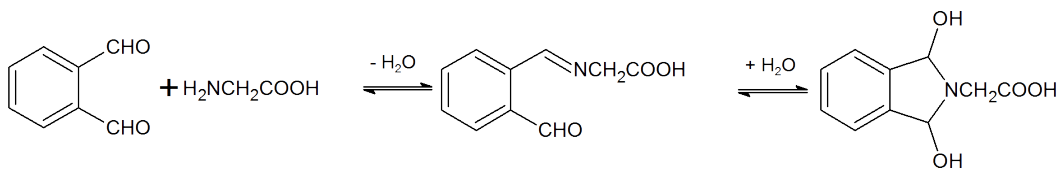


**Figure 6:** The suggestion for mechanism of reaction of OPA with glycine.<sup>29</sup>

The conditions for analytical determination of AAs with OPA have been obtained only empirically. The summary about the derivatization with OPA in various publications is in table 6 (see Appendix A). The composition of agents and conditions differ greatly in individual cases. There have been many attempts to clarify the reaction mechanism in order to develop the best agent composition and ideal derivatization conditions. However none of them gives satisfactory explanations about the influence of some factors on the reaction course (e.g. the order of mixing the reactants) given the complexity of the entire system. The main complication at defining the reaction mechanism is hydration of OPA in aqueous solutions. More about this problem is stated in Section 2.4.1.

### 2.2.3 Other derivatization agents

In last years naphthalene-2,3-dicarboxaldehyde (NDA, sometimes called inaccurately naphthalene-1,2-dicarboxaldehyde) is used as an alternative to OPA.<sup>16,30</sup> Instead of thiols, cyanide ions are used (the reaction scheme is in Fig. 7). The summary about the derivatization with NDA in various publications is in table 7 (see Appendix A).

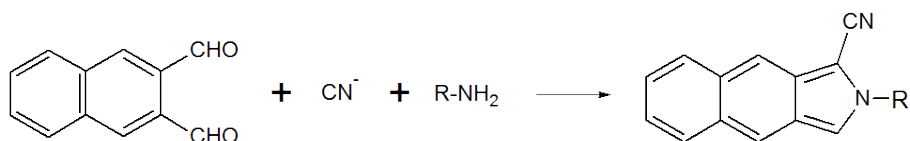


**Figure 7:** The reaction of NDA with an amine and cyanide ions.

Formed isoindole derivatives are more stable than derivatives formed in the reaction with OPA and they give higher fluorescence intensity. The principle of the reactions is the same as with OPA but NDA is less hydrated in aqueous solutions. The price of this reagent is however much higher than the price of OPA.

Derivatives formed in reactions with OPA or NDA do not have excitation maxima near lines of lasers used for laser-induced fluorescence (LIF; He/Cd – 442 nm, Ar – 488 nm).<sup>31</sup> Therefore 3-(2-furoyl)quinoline-2-carboxaldehyde (FQ, FQCA)<sup>13,31</sup>, 3-(4-carboxybenzoyl)quinoline-2-carboxaldehyde (CBQCA)<sup>32</sup>, 3-(4-bromobenzoyl)quinoline-2-carboxaldehyde (Br-BQCA)<sup>33</sup> and 3-(4-chlorobenzoyl)-quinoline-2-carboxaldehyde (Cl-BQCA)<sup>34</sup> have been developed in various research groups directly for detection by LIF. They are also used in combination with another nucleophile compound, mostly with potassium cyanide KCN. The general reaction scheme for these agents is in Fig. 8.

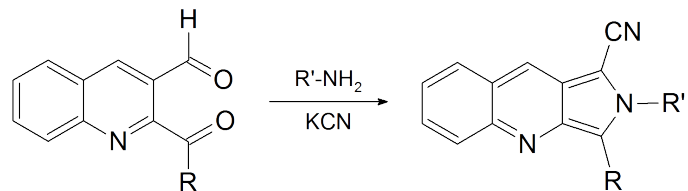


**Figure 8:** The scheme of reaction for FQCA, CBQCA, Br-BQCA and Cl-BQCA with cyanide ions and an amine.

## **2.3 Techniques used for analysis of AAs**

### **2.3.1 Ion-exchange chromatography (IEC)**

Ion-exchange chromatography (IEC) was the first method that was used for amino acid analysis.<sup>7</sup> It comprised a combination of IEC with post-column derivatization with ninhydrin. The method was later automated and it is still used. By this method up to 38 AAs can be separated during 2 hours.<sup>10</sup> Time consumption, instability of derivatization solution and interference of other sample components are the main disadvantages of IEC with post-column derivatization with ninhydrin.

AAs are separated by IEC usually in sodium or lithium buffer.<sup>7</sup> Separation of AAs is usually performed with temperature gradient for better separation of some AAs. A copolymer of styrene and divinylbenzene (8 %) is used as the stationary phase. Benzene rings are sulfonated and sulfonate groups work as cation exchangers. After exiting the column, the eluate is mixed with ninhydrin and it continues to a part where the solution is heated (e.g. a teflon coil submerged in a boiling water bath). In this part the derivatization reaction takes place and the coloured complex is made – Ruhemann’s purple. Then there is detection of the complex in a flow spectrophotometer.

### **2.3.2 Liquid chromatography (LC)**

Reversed-phase high-performance liquid chromatography (RP-HPLC) with pre-column derivatization is nowadays the most used technique for separation and determination of AAs.<sup>12</sup> Analysis using RP-HPLC is usually simpler, faster and it has higher sensitivity than analysis using IEC.<sup>3,7</sup> As the stationary phase, reversed-phase C<sub>8</sub> or C<sub>18</sub> silica-based columns are typically used.<sup>3</sup> In most cases, OPA in the presence of a thiol is used as derivatization agent.<sup>2,10,18–24</sup> Derivatives are detected using spectrofluorimetry, nonfluorescent derivatives can be detected using amperometry. The derivatization time is usually from 1 to 10 minutes. The analysis time ranges from 13 minutes (separation of 23 analytes) to 95 minutes (separation of 38 analytes).

### 2.3.3 Capillary electrophoresis (CE)

Capillary electrophoresis (CE) is the newest technique used for the analysis of AAs. In most cases capillary zone electrophoresis (CZE) is used.<sup>3</sup> Also micellar electrokinetic capillary chromatography (MECC) is often used. The mass detection limits are lower than in the case of HPLC but the concentration detection limits are higher because the injection volume is in the order of nl.<sup>35</sup> In order to increase the method sensitivity, an appropriate fluorescence agent is used. The agent has to be hydrophilic enough so that it is not adsorbed on the capillary wall. In capillary electrophoresis, laser-induced fluorescence (LIF) is used with argon or helium-cadmium laser. In last years, more expensive gas lasers are replaced with cheaper light-emitting diodes (LED) or with solid lasers.<sup>36</sup>

The CE-LIF system can be easily connected to a microdialysis probe through a flow interface.<sup>35</sup> Microdialysis can be used in order to observe changes in concentrations of analytes directly in tissues of living organisms or in body fluids. On-column derivatization with the derivatization agent NDA is used in most cases.<sup>36</sup> In some methods, a combination of CE with MS is used in which the derivatization step is left out.<sup>10</sup>

It was found out that D-AAs are present at very small concentrations (compared to L-AAs) in brain and other nerve tissues (eye tissues, lens).<sup>28,35,37</sup> For example, the concentration of D-serine increases in eye tissues during light stimulation. Because of low concentration of D-AAs, very sensitive methods using CE-LIF are under development for their detection.<sup>28,37</sup>

## 2.4 Electrochemical behavior of three isomeric benzenedi-aldehydes in aqueous and non-aqueous media

As stated in Section 2.2.2 and 2.3.2, AAs are determined using RP-HPLC in combination with the derivation agent OPA with a thiol. The reaction mechanism between the agent and AAs has been investigated in many studies by electrochemical techniques since aldehydic groups of OPA as well as the possible imine – or carbonyl intermediates or products – are electrochemically reducible. However, the reduction mechanism of OPA itself in various solutions is still not much clarified. Therefore the main purpose of this thesis is elucidation of the electrochemical reduction of OPA in aqueous and non-aqueous solvents. Its position isomers IPA and TPA were also investigated under same conditions in order to explain effects of resonance, induction, and/or steric interactions between both carbonyl groups depending on the position on the benzene ring.

In aqueous solvents nucleophilic addition of water to the carbonyl group takes place. Most of carbonyl compounds are hydrated only from a small part. Hydration of a carbonyl group is a reversible reaction and it can be acid- or base-catalyzed (Fig. 9 and 10).<sup>38</sup>

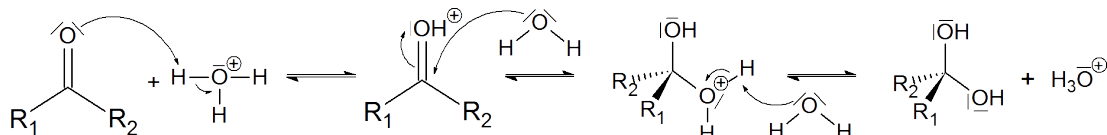


**Figure 9:** Acid-catalyzed hydration of a carbonyl group.

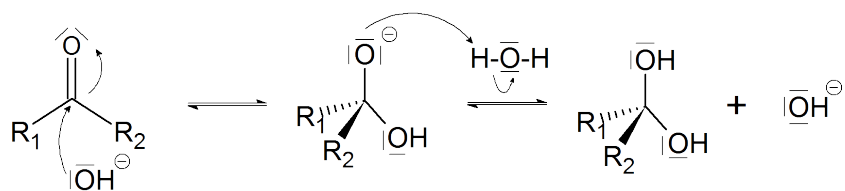


**Figure 10:** Base-catalyzed hydration of a carbonyl group.

The geminal diol which is a product of hydration is electroinactive. Dehydration is generally faster than diffusion of molecules to the surface of an electrode therefore reduction of carbonyl compounds is controlled by diffusion.<sup>39</sup> At some conditions like a certain range of pH dehydration is slower than diffusion and then reduction of a carbonyl group is controlled by kinetics of this dehydration.<sup>40</sup>

In protic solvents there are two forms of carbonyl group that can be reduced - an unprotonated carbonyl group or a protonated one. Antecedent protonation occurs on partly negatively charged oxygen atom. The protonated form of carbonyl group is reduced more easily, i.e. at less negative potentials than the unprotonated form. Reduction of the protonated form is pH-dependent. The potential of its reduction is shifted to more negative values with increasing pH due to decreasing rate of protonation. Reduction of the unprotonated form is pH-independent, i.e. the potential of reduction of the unprotonated form is constant over the pH range where the unprotonated form is present. Pre-protonation of a carbonyl group mainly occurs in acidic, neutral and slightly basic pH and it is not significant in basic pH.

In general, the first step of reduction of a carbonyl group is reversible addition of an electron either to preprotonated species yielding a neutral radical or to unprotonated parent species when a highly reactive radical anion is formed (Fig. 11).<sup>40</sup> The radical anion is less reactive in case of an aromatic carbonyl compound due to delocalization of the electron over the conjugated  $\pi$ -system. Formed radical anion can be reversibly protonated on oxygen atom giving rise to the same neutral radical like the pre-protonated species. This radical can react with another protonated radical and a pinacol is formed (dimerization). Formation of a pinacol is a very slow reaction and it can be suppressed in protic solvents. A pinacol is formed also by a reaction of a radical and a radical anion followed by protonation. Instead of dimerization, the neutral radical can be reduced further to an alcohol.

As indicated in Introduction, aromatic aldehydes also undergo covalent hydration in aqueous media (formally a nucleophilic addition to the C=O double bond) which complicates course of reduction. Benzaldehyde is in aqueous solvents mostly present in the non-hydrated form (more than 97 %).<sup>39,41</sup> Majority of benzaldehydes substituted with an electron-donating group are also present in the non-hydrated

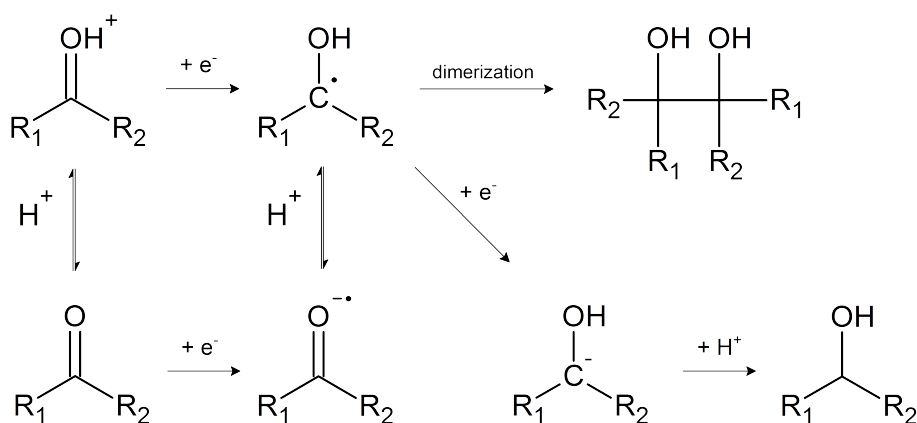


**Figure 11:** General scheme for reduction of a carbonyl compound.

form.<sup>42</sup> In contrast to that, benzaldehydes with an electron-withdrawing group are typically subject to hydration.<sup>41,43</sup> Also benzenedialdehydes undergo hydration in aqueous solutions. Their hydration and electrochemical behaviour is discussed in following three chapters.

#### 2.4.1 Orthophthalaldehyde

Orthophthalaldehyde (benzene-1,2-dicarboxaldehyde, OPA) is in aqueous solvents present in three forms due to its hydration: electroactive unhydrated form, electroactive monohydrated form and electroinactive cyclic hemiacetal form (Fig. 12). Published percentages quite vary - 10 % of unhydrated form, 20 % of monohydrated form, and 70 % of cyclic hemiacetal form<sup>39</sup>; or 20 % of unhydrated form, 8 % of monohydrated form, and 72 % of cyclic hemiacetal form<sup>30</sup>. These differences are caused by reversibility of hydration (Fig. 12) when the equilibrium is shifted with pH and in case of electrochemical monitoring, only electroactive species are consumed. The resulting data depend on the rate of re-establishing of the equilibria.

Electrochemical behavior of OPA in aqueous solutions was first described in 1954.<sup>44</sup> More detailed description was published more than fifty years later.<sup>45</sup> According to the published reports, electrochemical reduction of OPA occurs in two waves. The currents (height of the waves) are pH-dependent. The first wave is assigned to a two-electron reduction of the protonated unhydrated form (Fig. 13).

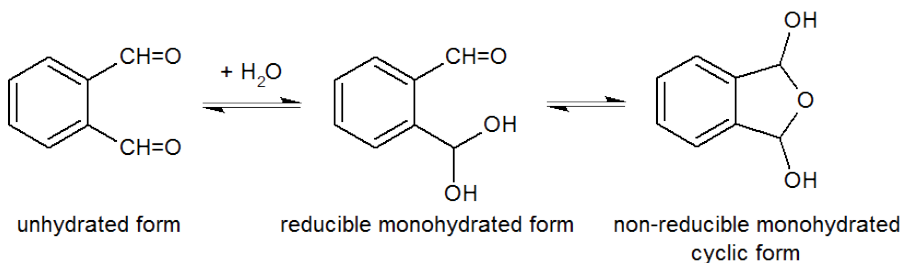


**Figure 12:** Hydration of OPA in aqueous solvents.<sup>29</sup>

Due to strong resonance interaction between two carbonyl groups in *ortho* position there is a difference in potentials at which the first wave appears and at which it is predicted. The first reduction occurs at potential 300 mV more positive than the second reduction step.

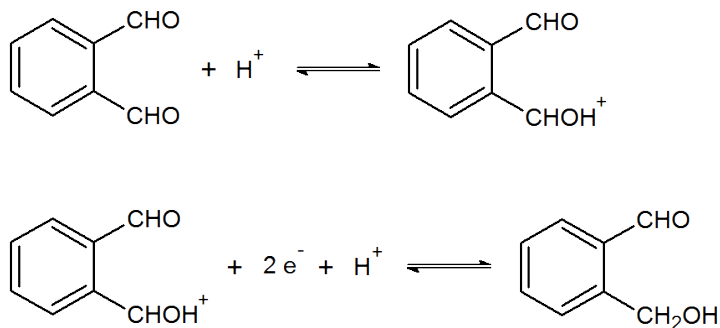


**Figure 13:** The first reduction step of OPA.<sup>45</sup>

At pH < 3 the current of the first wave increases as acid-catalyzed dehydration of hydrated OPA takes place. Between pH 4 and 8 the current of the first wave is very low due to the hydration resulting in the stable, electrochemically inactive isobenzofuran derivative. At pH > 8 there is an increase of the current of the first wave due to base-catalyzed dehydration. At pH > 10 addition of hydroxide ions (Fig. 14) occurs leading to decrease of the current of the first wave.

The second reduction step is in the range of potentials where a two-electron reduction of most of monosubstituted benzaldehydes occurs. The polarographic wave comprises reduction of the product of the first reduction step and also reduction of the acyclic monohydrated form (Fig. 15).

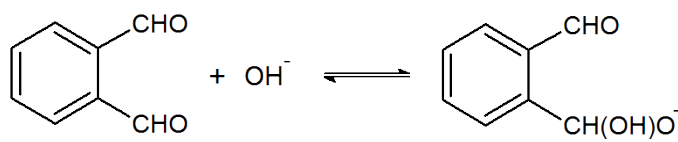


**Figure 14:** Addition of hydroxide ions to OPA yielding a geminal diol anion.<sup>45</sup>

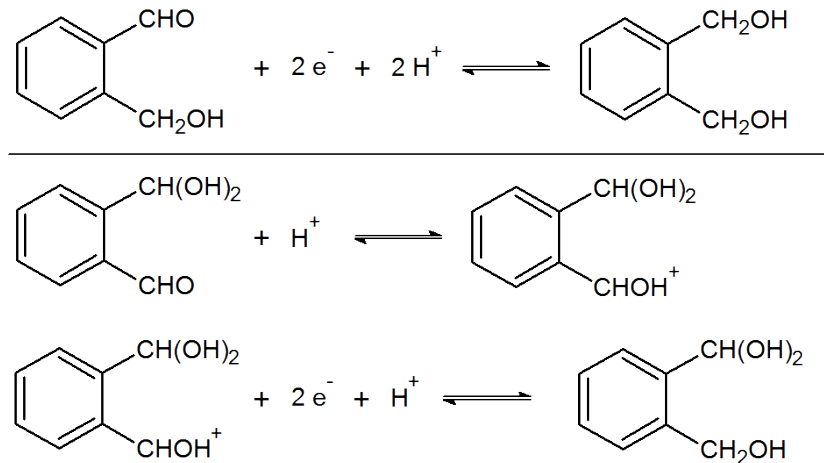


**Figure 15:** The second reduction step of OPA.<sup>45</sup>

Generally currents of the both reduction waves in the pH region 4 – 8 are much smaller than the limiting current of a two-electron reduction should be. It is due to strong hydration of the carbonyl groups.

Electrochemical behavior in non-aqueous solutions is mentioned in the study concerning EPR spectroscopy of substituted benzaldehydes anions.<sup>46</sup> Polarography of OPA in DMSO gives two waves with half-wave potentials  $-1.27$  and  $-1.97$  V. The first wave is attributed to the one-electron reduction of OPA yielding a radical anion. No other reports are available.

#### 2.4.2 Isophthalaldehyde

Isophthalaldehyde (benzene-1,3-dicarboxaldehyde, IPA) is in aqueous solutions present in less than 3 % in the hydrated form because the second carbonyl group in *meta* position does not influence hydration of the first carbonyl group.<sup>39,42</sup>

Course of reduction of IPA is dependent on pH.<sup>42</sup> In acidic pH IPA is reduced like benzaldehyde at twice the concentration. Reduction pathway suggested in the literature is shown on Fig. 16. First step is protonation of both carbonyl groups followed by simultaneous reduction by two electrons (one electron per carbonyl group), it is expressed as a two-electron wave. At pH < 4 the half-wave potential of this reduction is pH-dependent. It becomes pH-independent at pH > 5. At pH > 4 a second two-electron wave appears and its half-wave potential is pH-independent. In the second step a diradical is reduced by other two electrons, it reacts with other two protons under formation of a diol.

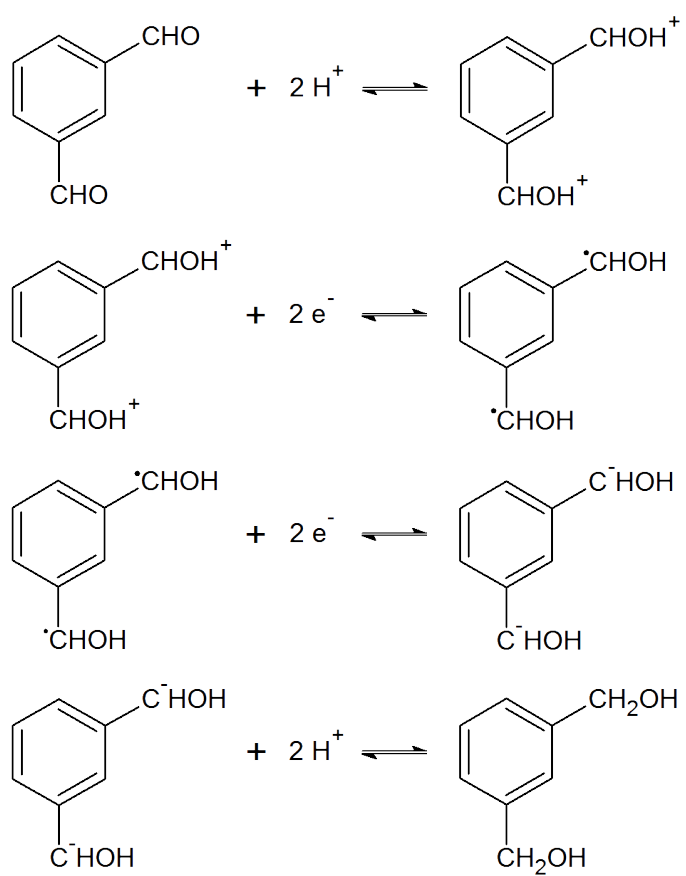


**Figure 16:** Reduction of IPA in acidic pH (pH < 5).<sup>42</sup>

In the range of pH from 5 to 10, one of carbonyl groups is protonated. According to the literature, the first step is reduction of the protonated carbonyl group by two electrons to  $\text{CH}_2\text{OH}$  group – a two-electron wave. In the second step the unprotonated carbonyl group is reduced by other two electrons – another two-electron wave. Half-wave potentials of both these waves are pH-dependent. The limiting current remains constant in this pH range. The process is shown on Fig. 17.

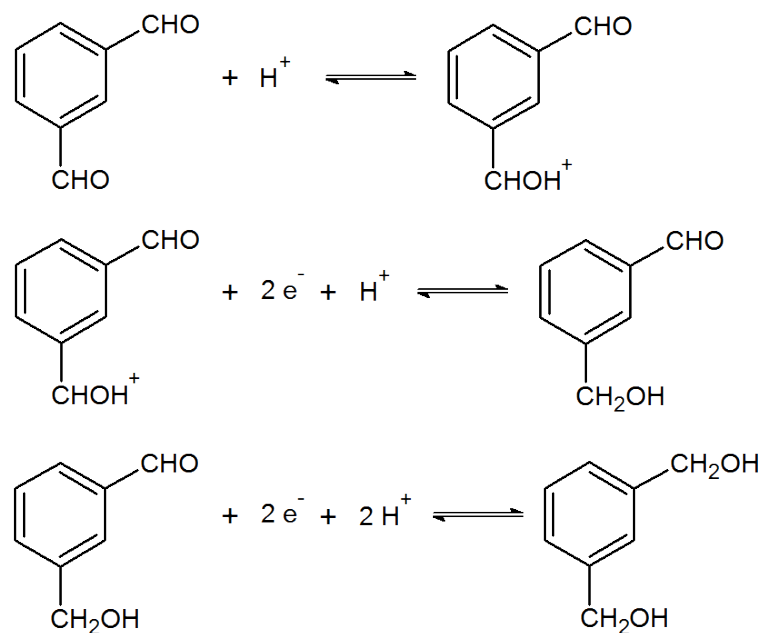


**Figure 17:** Reduction of IPA in the range of pH 5 to 10.<sup>42</sup>

At  $\text{pH} > 10$  the limiting current of both waves decreases and half-wave potentials are pH-independent. Protonation of carbonyl group is slow and therefore also the unprotonated form is reduced which is confirmed by appearance of the third most negative wave (Fig. 18).

At  $\text{pH} > 11$  addition of hydroxide ions to unhydrated carbonyl groups in IPA is expected (Fig. 19). Formed geminal diol ions are not reducible in the available potential range. This process is accompanied by decreasing of the third wave.

Electrochemistry of IPA in non-aqueous media is not published. There can be found only a mention that polarography of IPA in DMSO indicated one one-electron wave at potential  $-1.45 \text{ V}$ .<sup>46</sup>

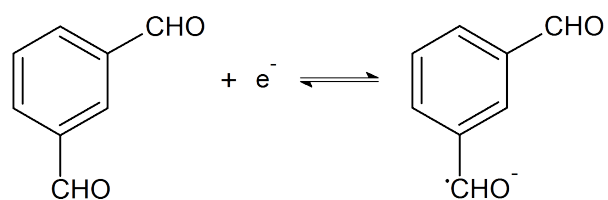


**Figure 18:** Reduction of IPA at pH > 10.<sup>42</sup>

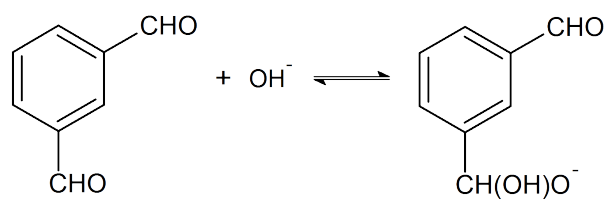


**Figure 19:** Addition of hydroxide ions to IPA at pH > 11.<sup>42</sup>

### 2.4.3 Terephthalaldehyde

Terephthalaldehyde (benzene-1,4-dicarboxaldehyde, TPA) is also subject to hydration in aqueous solutions where it is present from about 23 % as a geminal diol.<sup>47</sup> It was thought that *p*-nitrobenzaldehyde should be the most hydrated species among the substituted benzaldehydes but it was found out that the effect of second carbonyl group in *para* position is larger than the effect of *p*-nitro group. Stronger hydration is the result of strong resonance interaction between two carbonyl groups on the benzene ring which leads to increase of the partial positive charge on one carbonyl carbon. The carbonyl group bearing this carbon atom is then attacked by a water molecule (nucleophilic addition).

TPA is reduced in two two-electron waves over a large pH range (pH 0 – 11.5).<sup>48</sup> The species reduced in these steps differ according to pH of the solution. At pH from 1 to 5 the diprotonated form of TPA is reduced by two electrons and a diradical is formed (Fig. 20). This diradical is stabilized by quinoidie structure and can be converted into an aldol (Fig. 21). The half-wave potential of the first wave shifts to more negative values with increasing pH. It indicates that the reduced species is a protonated form of TPA.

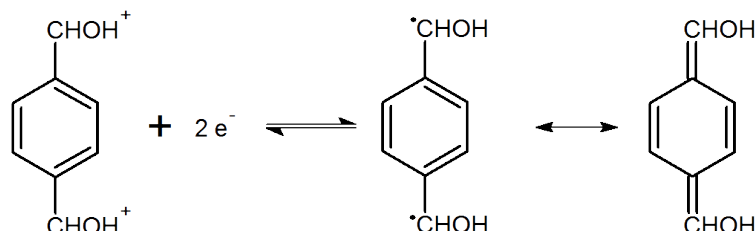


**Figure 20:** Reduction of the diprotonated form of TPA in the range of pH from 1 to 5.<sup>48</sup>

The product of the conversion in Fig. 21 is reduced in the second wave (Fig. 22). The height of the second wave increases with increasing pH due to the accelerated conversion.

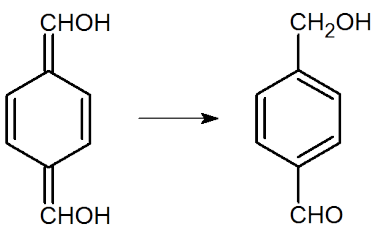


**Figure 21:** Conversion of the product of the first reduction step of TPA in pH from 1 to 5 to an aldol.<sup>48</sup>

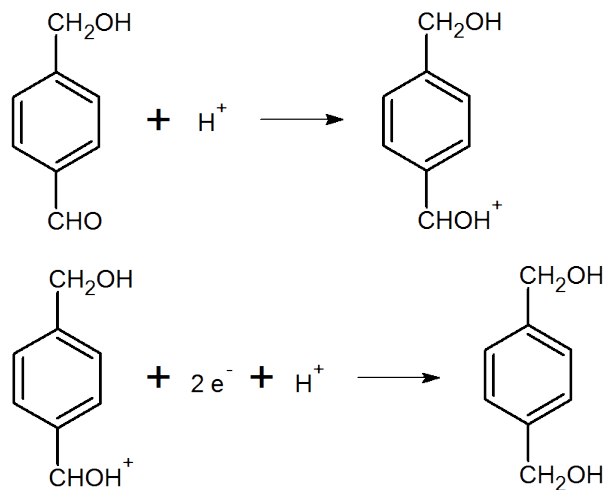


**Figure 22:** Second step of reduction of TPA at pH from 1 to 5.<sup>48</sup>

In the range of pH from 5 to 8.5, the limiting current of the first wave is constant. In this step the monoprotonated form is reduced by two electrons (Fig. 23). The half-wave potential of the first wave is pH-dependent and the dependence corresponds to transfer of one proton before reduction. The current of this wave is only 85 % of the theoretical value that would be caused by diffusion controlled reduction of this species. Therefore in aqueous solution 15 % of TPA should be present in the monohydrated form.

In the second wave in the range of pH from 5 to 8.5, totally three species are reduced according to the literature.<sup>48</sup> The first one is product of the first step of reduction, then the protonated monohydrated form is reduced at the same time and also protonated product of the first reduction step (Fig. 24).

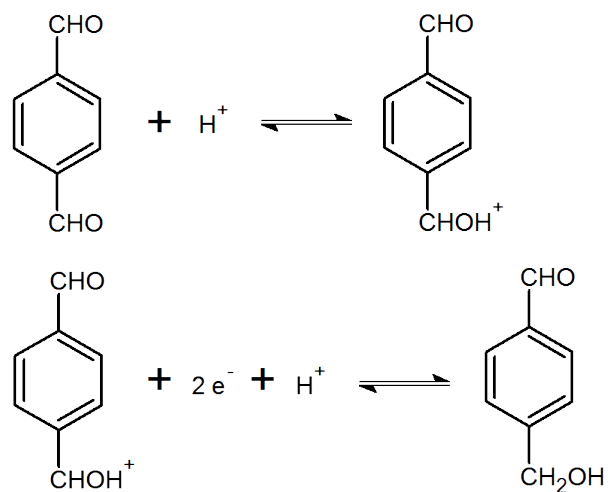


**Figure 23:** First step of reduction of TPA at pH from 5 to 8.5.<sup>48</sup>

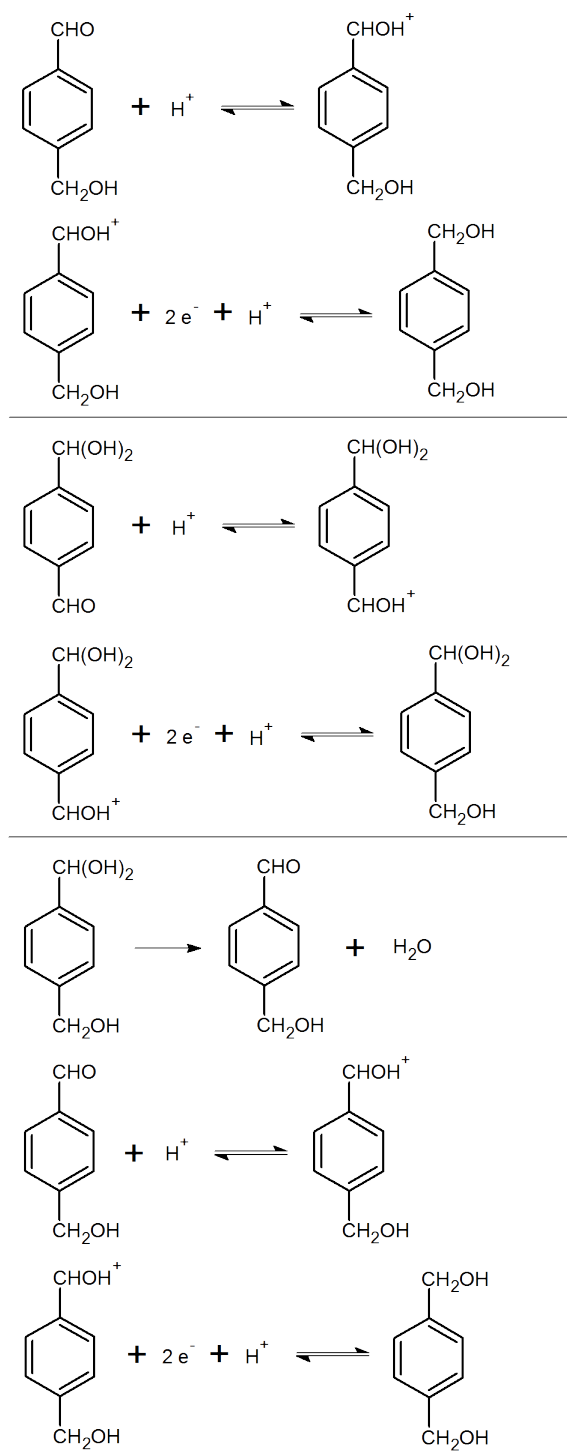


**Figure 24:** Second step of reduction of TPA at pH from 5 to 8.5.<sup>48</sup>

It is further reported that at  $\text{pH} > 8.5$  reduction of TPA occurs also in two steps. Half-wave potentials of both two-electron waves are pH-independent which means that in this pH range the unprotonated form is reduced (Fig. 25 and 26). Current of the first wave is higher than in previous pH range. It is caused by base-catalyzed dehydration of the original monohydrated form. At  $\text{pH} > 10$  there is a decrease of both waves due to addition of hydroxide ions to a carbonyl group (Fig. 27).

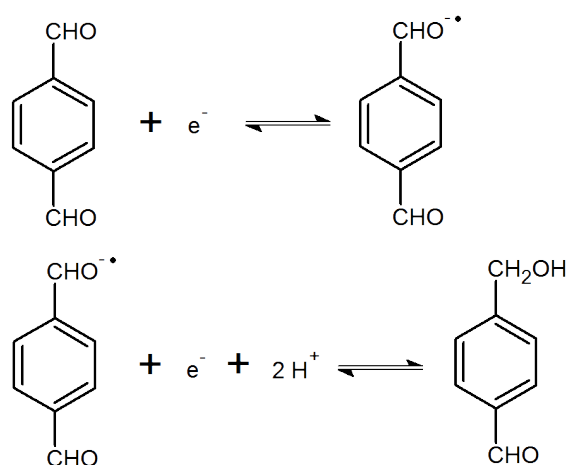


**Figure 25:** First step of reduction of TPA at  $\text{pH} > 8.5$ .<sup>48</sup>

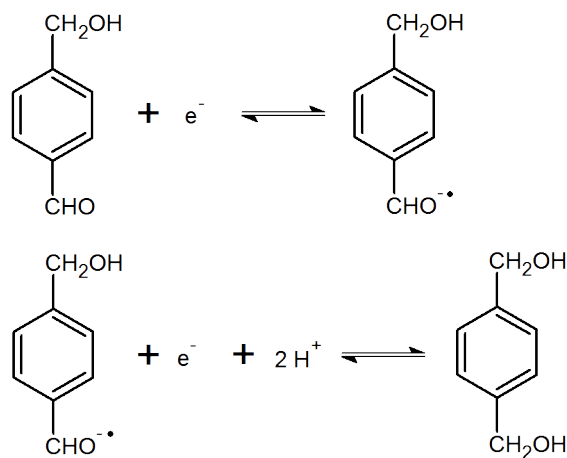


**Figure 26:** Second step of reduction of TPA at  $\text{pH} > 8.5$ .<sup>48</sup>

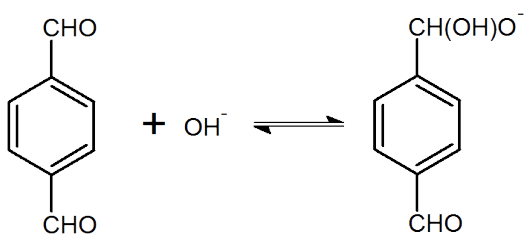


**Figure 27:** Addition of hydroxide ions to TPA at pH > 10.<sup>48</sup>

Electrochemistry of TPA in non-aqueous solutions is mentioned in a work of Stone and Maki<sup>46</sup> which deals with EPR study of rotamers of substituted benzaldehyde anions. A radical anion of TPA was generated at potential  $-1.5$  V (vs. a modified calomel electrode; the first reduction step) in DMSO.

In DMF, the reduction potentials were determined as  $-0.67$  and  $-1.21$  V (vs. mercury pool), both steps are one-electron waves and they are reversible.<sup>49</sup> The reduction is described as formation of anion radicals and dianions which are stabilized by a quinoid structure in which the negative charges can be delocalized. Another work<sup>50</sup> reports reduction of TPA in DMF at potentials  $-0.62$  and  $-1.10$  V (vs. mercury pool). No other information from the literature is available.

## 2.5 Electrochemical behavior of three isomeric diacetylbenzenes

This chapter describes electrochemical behavior of 1,3-diacetylbenzene (*m*-diacetylbenzene, *m*-DAB), and 1,4-diacetylbenzene (*p*-diacetylbenzene, *p*-DAB). Behavior of 1,2-diacetylbenzene (*o*-diacetylbenzene, *o*-DAB) is not published at all. These ketones were chosen for comparison with OPA, IPA and TPA.

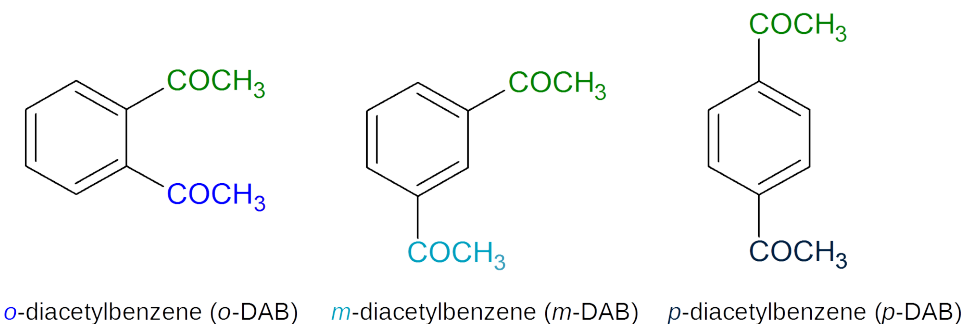


**Figure 28:** Structures of *o*-DAB, *m*-DAB and *p*-DAB.

The electrochemical reduction in aqueous solutions is described only for *p*-DAB.<sup>51</sup> At pH 2 – 5 it is reduced in the diprotonated form in a reversible two-electron step. At pH below 2 or above 5 reversibility of reduction of the diprotonated form is perturbed by an acid- and base-catalyzed reaction, respectively. At pH > 5 a monoprotonated form is reduced in two consecutive irreversible steps.

According to literature, reduction of *m*-DAB takes place at potential –1.81 V (vs. SCE) in DMF.<sup>52</sup> Its anion-radicals are not stabilized with conjugated π-system therefore they are not stable.

Two works of Kargin et al.<sup>49,50</sup> state reduction of *p*-DAB in DMF at potentials –0.95 and –1.41 V, and –0.81 and –1.24 V, respectively (both vs. mercury pool). Both reduction steps are one-electron and reversible. Pragst et al.<sup>53,54</sup> reported reduction of *p*-DAB in DMF in two different works, at potential –1.52 V, and at potential –1.56 V (vs. SCE), respectively.

## 3 EXPERIMENT

### 3.1 Used techniques and instrumentation

DC-polarography is a linear scan voltammetry with a dropping mercury electrode (DME) as the working electrode.<sup>55</sup> The DME is a capillary tube with inner diameter approx. 50 µm which is connected with the mercury reservoir. The height of the mercury column is between 30 and 100 cm. Mercury drops are formed at the capillary orifice and a special "hammer" controls the drop time (usually 1 – 2 seconds). The advantage of polarography in comparison with other voltammetric techniques is that the surface of the working electrode is absolutely smooth and is renewed with every new mercury drop formed at the end of the capillary tube. A three-electrode system was used – a saturated calomel electrode (SCE) was used as the reference electrode and a platinum wire was used as the auxiliary electrode. The drop time was 1 second, scan rate was 10 mV/s.

Cyclic voltammetry (CV) is a linear scan voltammetry which is characteristic with faster scan rate (from 50 to 100 mV/s for standard analytical working electrodes with the size about 1 mm<sup>2</sup>) which makes the experiment time-dependent.<sup>56</sup> At certain vertex potential the voltage scan direction is reversed and the electrode is turned to its starting condition. It was measured either with a hanging mercury drop working electrode (HMDE) or with a gold working electrode. During one measurement the surface of the electrode is constant in contrast to DC-polarography therefore the number of peaks on CV can be different from the number of polarographic waves due to presence of adsorption peaks and of peaks of some minor products.

For measuring CV before and after electrolysis, a mercury "pseudodrop" electrode was used. It consists of a platinum wire which has a small sphere at one end with diameter approx. 1 mm. The rest of the wire is sealed into a glass tube and used as a contact. The small sphere is immersed into a saturated solution of AgNO<sub>3</sub> together with a counter electrode. Electrolysis is performed at potential –1 V for 5 min and by that the sphere is covered with silver. After that the electrode is immersed into mercury and silver amalgam is formed at the surface

of the sphere. For renovation of the mercury surface, the tip of the electrode is again immersed into mercury. After several tens of measurements the sphere has to be renewed. For that, electrolysis is performed in a 10% solution of  $\text{HNO}_3$  at potential 1 V, by that the silver sphere dissolves and it can be created again.

Electrolyses were performed under potentiostatic conditions in a special cell with a frit separating anodic and cathodic part (see Fig. 29). The solution of the electrolyzed substance was stirred and bubbled with argon during whole process. The potential for electrolysis was set approx. 100 mV behind the cathodic peak potential taken from CV.

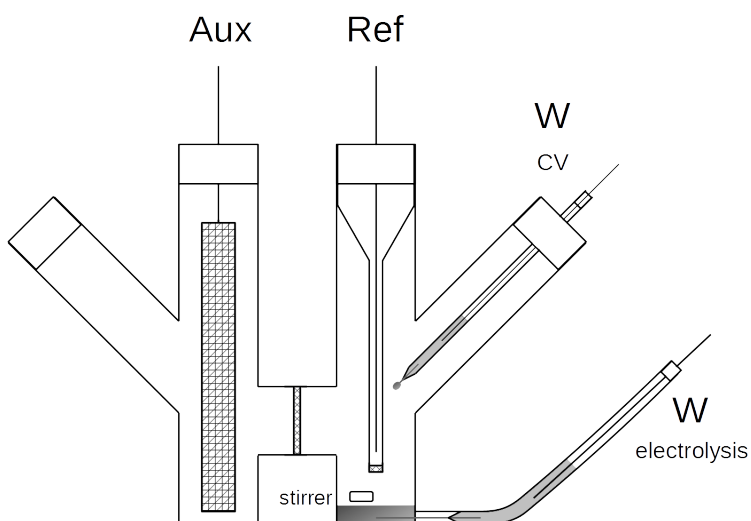


**Figure 29:** A cell used for electrolysis of studied substances. Aux – auxiliary electrode, Ref – reference electrode, W – working electrode.

Solutions intended for identification of electrolysis products were handled in the following way. The solution from the cathodic part of the cell was taken outside the cell into a 100 ml separating funnel. 40 ml of water was added and a second, organic phase created. The solution was then extracted with diethylether (three times), the organic phases were collected and dried with  $\text{MgSO}_4$ . After several hours of drying, the magnesium sulphate was filtered and diethylether was removed from the solution on a rotary evaporator. A sample of the solid which was left in the flask was then dissolved in chloroform and it was separated on a TLC (thin layer chromatography) plate in order to find a suitable mobile phase (various ratios of chloroform and ethanol). Then a preparative TLC plate (20 x 20 cm, SIL

G-200 UV<sub>254</sub>, layer 2.0 mm, Macherey-Nagel, Germany) was used for separation of the products of electrolysis. Separated stripes on the preparative TLC plate (visible under a UV lamp) were scratched from the underlying glass and desired substances were obtained from the solid phase by washout with ethanol. The ethanolic solution was then evaporated and the solid left in the flask was analyzed either by NMR spectroscopy or by HPLC-MS. <sup>1</sup>H NMR spectra were recorded on a Varian NMR spectrometer (300 MHz) in CDCl<sub>3</sub> (99.8 %, Alfa Aesar).

Samples for LC-MS analysis were dissolved in aqueous acetonitrile (ACN). They were injected on a Hypersil Gold C<sub>18</sub> column (50 x 3 cm, particle size 5 µm) and eluted by gradient elution – 0.1% formic acid in aqueous ACN, ACN concentration was linearly increased from 12.5 % to 90 % during 10 min, then constant for 2 min – with the flow 0.4 mL/min. Analytes were detected using a PDA detector (200 – 400 nm) and using a mass spectrometer Thermo Scientific LXQ with atmospheric pressure chemical ionization (APCI) in the positive mode. Capillary temperature was 200 °C, voltage was 5 kV. The nebulizer gas was nitrogen. Samples for LC-MS analysis were detected also after transformation to hydrazides for better detection with APCI-MS. A reaction mixture – 0.6 mL of a sample solution and 25 µL of hydrazine hydrate – was after 15 min evaporated in vacuum and it was dissolved for analysis.

UV/Vis and IR spectroelectrochemistry (SEC) was used for spectroscopic characterization of reduction processes. During slow cyclic voltammetry (scan rate 1.25 mV/s for UV/Vis SEC), UV/Vis and IR spectra were collected and the change in the absorbance caused by the electrochemical reduction was observed. UV/Vis SEC was measured with a spectrophotometer UV-1800 Schimadzu. The scheme of the used UV/Vis spectroelectrochemical cell is in Fig. 30). A thin-layer quartz cell with width 2 mm was used. The working and auxiliary electrodes were platinum meshes. The reference electrode was a silver wire. The light beam went through the platinum working electrode. Measured potentials were related to the ferrocene system Fc<sup>+</sup>/Fc. Its cyclic voltammogram and UV/Vis spectra can be found in Appendix B. IR SEC was measured with an IR spectrophotometer Nicolet iS50 FT-IR. An optically transparent thin-layer electrochemical (OTTLE) cell with a three electrode system was used.<sup>57</sup> The working and auxiliary electrodes were platinum meshes and the reference electrode was a silver wire.

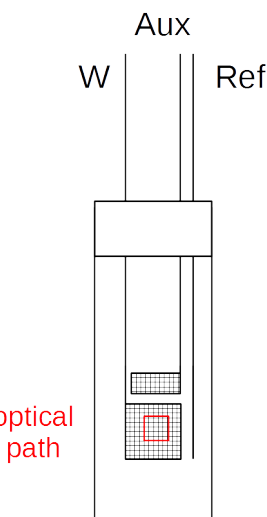


**Figure 30:** A cell used for UV/Vis SEC of studied substances. Aux – auxiliary electrode, Ref – reference electrode, W – working electrode. Optical path of the light beam is marked by the red square.

Instruments used for electrochemical measurements were the analog potentiostat PA3 and PA4 (Laboratorní přístroje Praha) with an XY recorder for DC-polarography and CV and the digital potentiostats PGSTAT101 and PGSTAT30 (with current booster for up to 10 A) from Metrohm Autolab B.V. for electrolyses. The pH was measured by pH/ORP Meter Hanna Instruments HI 3220.

Radical anions formed during electrochemical reduction were detected and characterized by electron paramagnetic resonance (EPR) spectroscopy. They were generated *in situ* in the EPR cavity (EPR SEC) in a special glass spectroelectrochemical cell (an example of the cell on Fig. 31). OPA radicals were generated in the three-electrode setup (W – mercury, Aux – a platinum mesh, Ref – a silver wire). TPA and *p*-DAB radical anions were generated either in the two-electrode setup (WE – a platinum mesh, CE – a glassy carbon electrode) or in the three-electrode setup (W – a platinum mesh, Aux – a glassy carbon, Ref – a silver wire). EPR spectra were measured on an EPR spectrometer Varian E4 (OPA radicals) in J. Heyrovsky Institute of Physical Chemistry of the CAS and on an EPR spectrometer Bruker EMX (TPA and *p*-DAB radical anions) at the Faculty of Chemical and Food Technology at Slovak University of Technology in Bratislava. The used potentiostat was HEKA PG 285 (HEKA Elektronik, Germany).

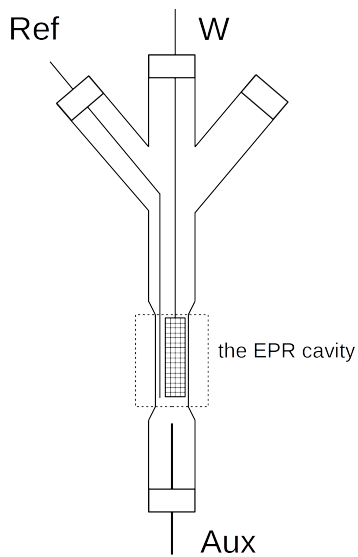


**Figure 31:** A cell used for *in situ* generation of radicals in the EPR cavity. Aux – auxiliary electrode, Ref – reference electrode, W – working electrode.

### 3.2 Chemicals

The basic chemicals were: orthophthalaldehyde ( $\geq 97\%$ , Sigma–Aldrich), isophthalaldehyde (97 %, Sigma–Aldrich), terephthalaldehyde (99 %, Sigma–Aldrich), 1,2-diacetylbenzene (99 %, Sigma–Aldrich), 1,3-diacetylbenzene (97 %, Sigma–Aldrich), 1,4-diacetylbenzene (99 %, Sigma–Aldrich), tetrabutylammonium hexafluorophosphate ( $\text{Bu}_4\text{NPF}_6$ ,  $> 98.0\%$ , TCI EUROPE N.V.), glycine (p.a., Lachema), alanine (Roanal Budapest),  $\alpha$ -aminobutyric acid,  $\alpha$ -aminoisobutyric acid ( $> 99\%$ , Fluka), valine (Lachema), norvaline (VEB Berlin-Chemie), leucine (Roanal Budapest), isoleucine (purum, Lachema) lysine ( $\geq 98\%$ , Sigma). Chemicals used for buffer preparation were orthophosphoric acid (purum, Lachema), sodium dihydrogenphosphate dihydrate (p.a., Lachema), sodium hydrogenphosphate dodecahydrate (p.a., Lachema) and sodium hydroxide (puriss. p.a., Fluka). For isolation of products after electrolysis were used magnesium sulphate (Lachema) and diethylether (Merck). For measurement of radicals by EPR spectrometry

were used dried acetonitrile (SeccoSolv<sup>®</sup>, max. 0.005 % H<sub>2</sub>O, Merck) and dried tetraethylammonium hexafluoroborate (99 %, Aldrich Chemical Company, Inc.) for preparation of indifferent electrolyte. ACN was supplied by Fisher Scientific ( $\geq$  99.9 %), acetone by Lachner (p.a.).

Bu<sub>4</sub>NPF<sub>6</sub> was recrystallized from hot ethanol and dried in a micro-wave device to obtain highly pure and dry salt for preparation of indifferent non-aqueous electrolyte. Dimethylformamide (DMF) was purified by a two-step distillation process to obtain high purity suitable for electrochemistry on mercury electrodes. The first step is azeotropic distillation of DMF with water and benzene. During this step low-boiling impurities are eliminated from the solution as water and benzene are distilled. The second step is a slow rectification under reduced pressure during which highly pure and dry DMF is obtained. Mercury for polarographic measurements and for electrolyses was cleaned by washing with hot water, ethanol and acetone (several times) and then by filtration through a filtration paper with a small hole (removing impurities from the mercury surface).

## 4 RESULTS AND DISCUSSION

As is stated in Section 2.2.2, OPA is used in many applications for determination of AAs. The electrochemical behavior of OPA in aqueous solutions was first investigated in paper of Furman and Norton.<sup>44</sup> In that paper, a two-step polarographic reduction of OPA was described. My bachelor thesis<sup>58</sup> was devoted to the study of reactivity of OPA with individual AAs. Surprisingly, it was shown that previously described electrochemical behavior of OPA is incorrect. Therefore our investigation of reactivity of OPA with AAs was strongly limited and influenced by up-to-then unknown electrochemical behavior of OPA. Despite this fact, some preliminary results were obtained and are summarized in Section 4.3. For more details, readers are kindly directed to my bachelor thesis.<sup>58</sup>

Newly observed redox behavior of OPA is partly different from that reported in literature. This fact led us to focus ourselves into detailed reinvestigation of electrochemical reduction of OPA, its analogues and models under various conditions since the new findings may have consequences in interpretation of reactivity of OPA with nucleophiles including AAs. In this work, several attempts to untangle this behavior were performed. In the first part, electrochemical reduction of OPA in non-aqueous media is described in detail. To stress out importance of the mutual position of carbonyl functional groups, two structural isomers of OPA, i.e. IPA and TPA, were studied in the same manner. This effort finally allows to propose possible reduction mechanisms for OPA and its structural isomers. Furthermore, cathodic reduction of all three benzenedialdehydes was investigated also in aqueous media. Due to the interaction of studied compounds with water molecules, the electrochemical behavior is much more complicated compared to non-aqueous media. Therefore the detailed understanding of the role of water in overall reactivity of OPA requires further study which is currently running.

## 4.1 Non-aqueous media

Non-aqueous media can be characterized as media that do not allow protonation of reduced compounds. The reduction usually proceeds in one-electron steps:  $A + e^- \rightleftharpoons A^{\cdot-}$  (formation of a radical anion),  $A^{\cdot-} + e^- \rightleftharpoons A^{2-}$  (formation of a dianion).<sup>59</sup> On the other hand, in aprotic conditions reactive radical intermediates are stabilized enabling another type of electrochemically initiated reactions. In any case the electrochemical behavior in aprotic solutions is partly simplified compared to aqueous media. Electrochemical reduction of OPA, IPA and TPA was investigated using several techniques (DC-polarography, CV, electrolysis, coulometry, UV/Vis SEC, IR SEC, EPR SEC) in ACN. For comparison specific experiments were done also in other aprotic solvents (DMF, acetone). Data obtained from such experiments are summarized in Section 4.1.5.

### 4.1.1 Orthophthalaldehyde

According to DC-polarography, OPA is in ACN reduced in two steps at potentials  $-1.47$  and  $-2.01$  V, respectively. The value of both reduction currents is dependent on concentration therefore both currents are diffusion-controlled. The first step corresponds to the uptake of one electron/molecule. The second step corresponds to approx. half of the height of the first one, meaning that approx. a half of molecules reduced in the first step were not reduced in the second step and thus they have to undergo some consecutive reaction.

Based on CV, OPA is reduced in two steps. A typical cyclic voltammogram can be seen in Fig. 32. The first reduction step at peak potential  $-1.51$  V is not completely reversible because the anodic counter peak appears only at higher scan rates. It was observed that presence of traces of water in ACN strongly influences reversibility of the first reduction step. If the supporting electrolyte is well-dried beforehand, reversibility is higher. The primary radical anion formed during the first step undergoes a relatively slow consecutive reaction. The second step is then either a reduction of the formed product (so called mechanism ECE – electron-chemical reaction-electron) or the direct reduction of the primary radical anion to a dianion (mechanism EE).

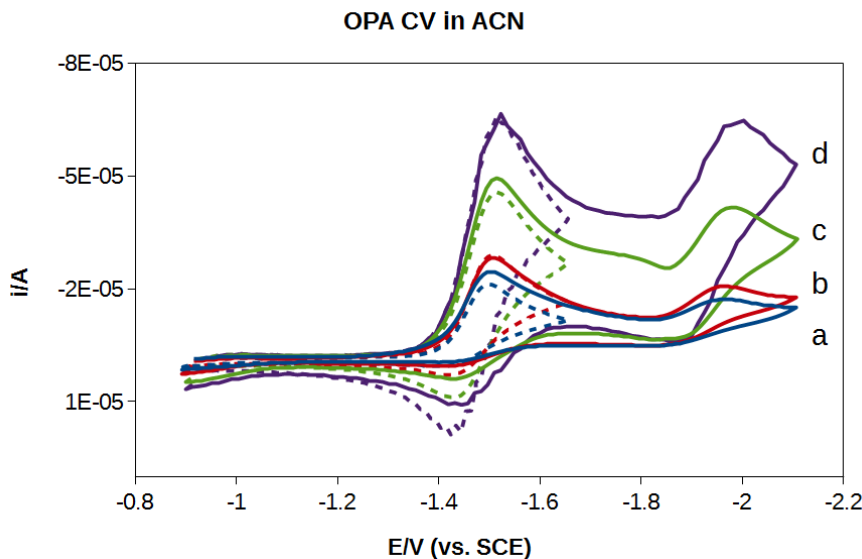


**Figure 32:** CVs of OPA in ACN at different scan rates: (a) 100 mV/s, (b) 200 mV/s, (c) 500 mV/s, (d) 1 V/s. CV measured only for the first reduction step is plotted by a dashed line. Potentials are related to the SCE.

For determination of the electron consumption during individual reduction steps, electrolysis of OPA was performed at potentials  $-1.6$  and  $-2.0$  V, respectively. In the case of a simple reduction mechanism, the decrease of current in time during electrolysis should be an exponential function. However here the current decay at certain time does not follow the theory as can be seen in Fig. 33. In addition to this, the consumption of electrons during electrolysis is less than 1 electron/molecule. The deviation on the  $i$ - $t$  curve as well as the low number of consumed electrons can be explained by existence of side consecutive reactions besides the reversible behavior of the primary radical anion.

In the case of OPA, the electron consumption at potential  $-1.6$  V is approx. 0.4 electron/molecule. This result can be understood with help of combined information from CV and the  $i$ - $t$  curve. Because CV tells us that reversibility increases with scan rate and on the contrary, final electron consumption is quite low,

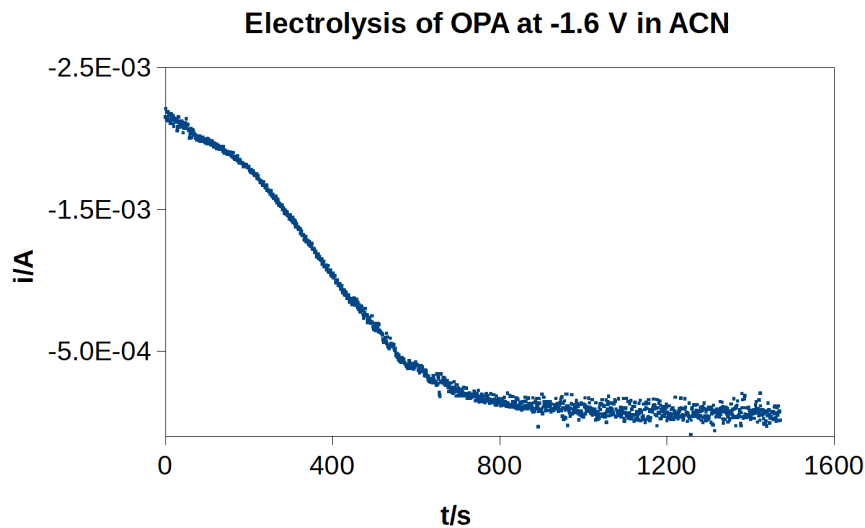


**Figure 33:** The dependence of current in time during electrolysis of OPA in ACN at potential  $-1.6$  V (vs. SCE).

one can conclude that the OPA reduction is accompanied by some "father-son" reaction, where the primary radical anion reacts e.g. with the parent compound under formation of some kind of dimeric species. Therefore subsequent experiments were focused only on the first reduction step.

The progress of the first reduction step was monitored by spectroelectrochemical techniques which can clarify the reduction mechanism itself. Spectra corresponding to the first reduction step studied by UV/Vis SEC are shown in Fig. 34. During the reduction two peaks at 220 and 258 nm corresponding to  $\pi \rightarrow \pi^*$  and  $n \rightarrow \pi^*$  transitions in benzene ring and carbonyl groups disappear from the spectra. Peak at 220 nm undergoes blue shift towards 200 nm which corresponds to the change of  $\pi$ -bonds in the molecule by the reduction. After re-oxidation the spectrum does not change back to its original form. This confirms the observation from CV that the first reduction step is not fully reversible.

The first reduction step was also studied by IR SEC. The spectra can be seen in Fig. 35. During the electrochemical reduction, peaks at  $1696$  and  $1721\text{ cm}^{-1}$  related to the coupled vibrations  $\nu(\text{C=O})$  of carbonyl groups and peak at  $2760\text{ cm}^{-1}$  related to the vibration  $\nu(\text{C-H})$  of carbonyl group disappear. The electrochemical

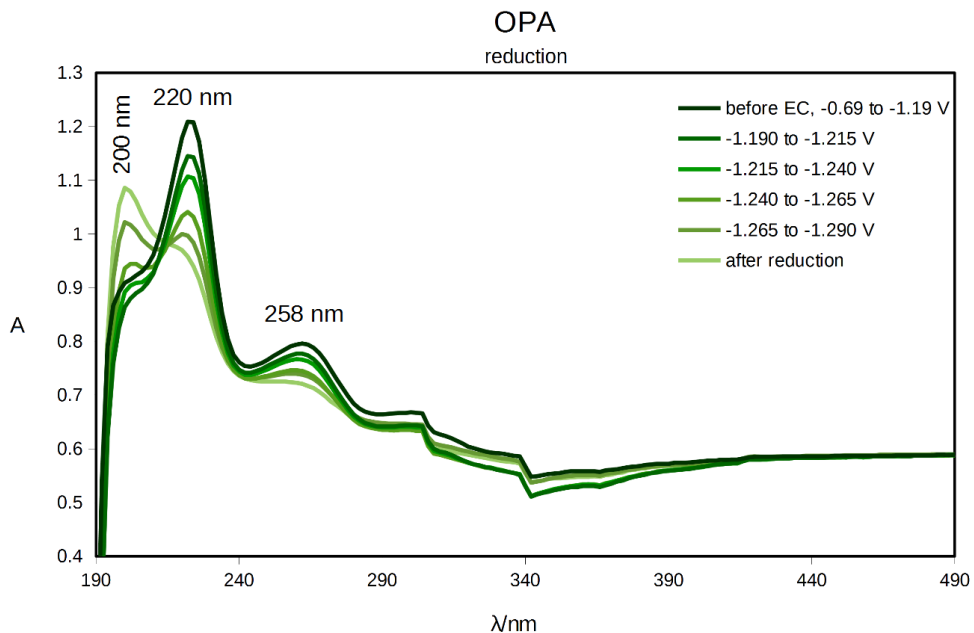


**Figure 34:** Change in UV/Vis spectra of OPA during the first reduction step in ACN. Potentials are related to the ferrocene system  $\text{Fc}^+/\text{Fc}$ .

reduction evidently intervenes into the  $\pi$ -electron distribution in benzene ring. This can be traced as diminishing and broadening of peaks at  $1595\text{ cm}^{-1}$  related to the benzene quadrant stretch vibration  $\nu(\text{C}=\text{C})$  and  $1577\text{ cm}^{-1}$  related to the benzene stretching vibration  $\nu(\text{C}=\text{C})$  caused by conjugation of benzene ring with a functional group. On the other hand, new peaks at  $2880$  and  $2925\text{ cm}^{-1}$  related to the stretching vibrations  $\nu_s(\text{C-H})$  and  $\nu_{as}(\text{C-H})$  from  $\text{CH}_2$  group appear which is connected with formation of a product. Another new peaks at  $1248$ ,  $1151$  and  $1110\text{ cm}^{-1}$  corresponding to vibrations of a carbon atom  $\text{C}_{sp^2}$  bonded to an oxygen or a nitrogen atom, usually in a cycle, appear. This gives us more detailed information about the structure of the product. In addition to this, peak at  $2150\text{ cm}^{-1}$  corresponding to the stretching vibration  $\nu(\text{C}\equiv\text{N})$  emerges in the spectra pointing to some participation of ACN in the reduction mechanism.

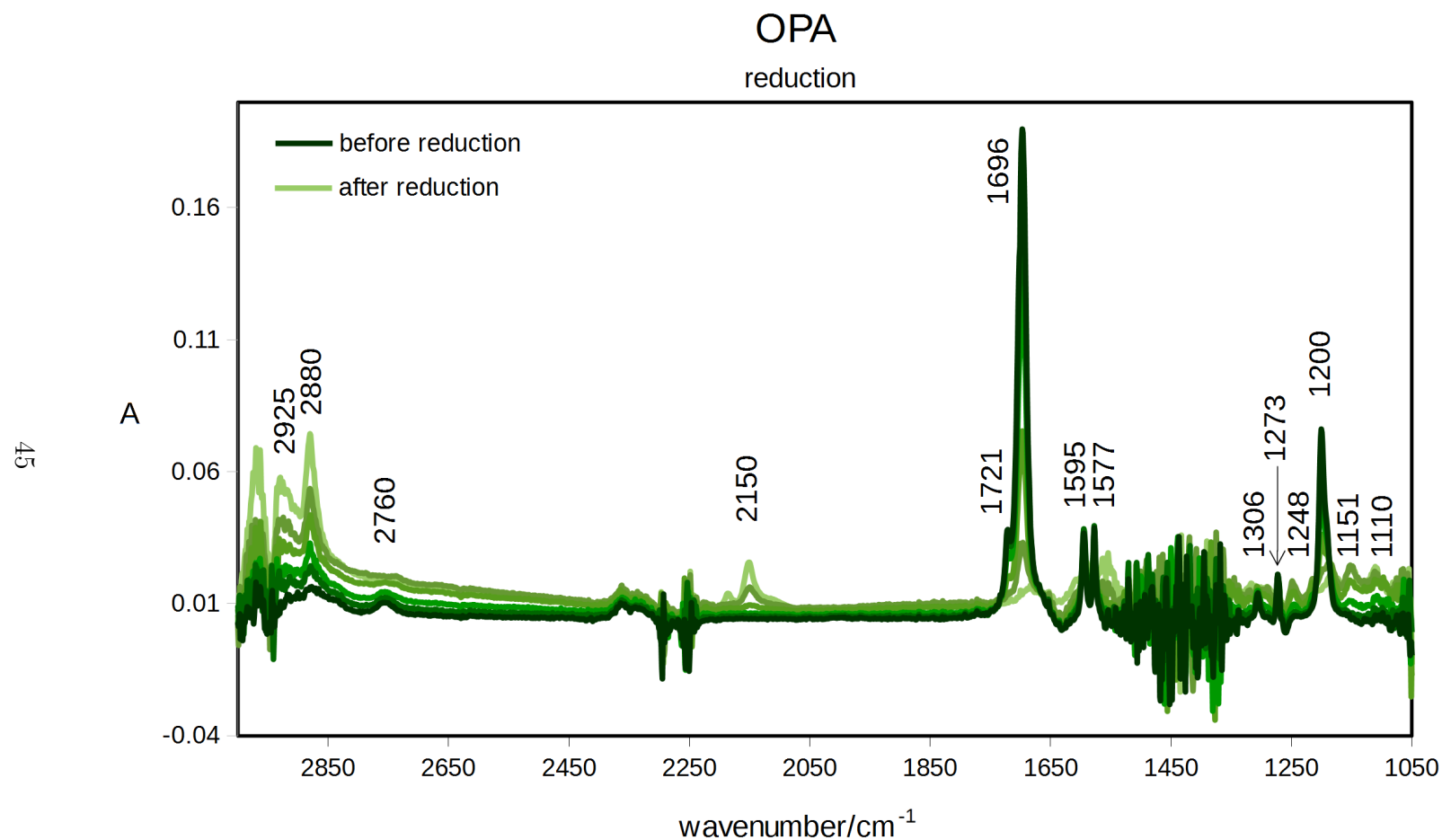


**Figure 35:** Change in IR spectra of OPA during the first reduction step.

Based on the possible structure of the product and on other obtained information, a probable reduction mechanism can be drawn (Fig. 36). The first expected step is a one-electron reduction followed by an intramolecular proton transfer to one of oxygen atoms in carbonyl groups which leads to disruption of benzene ring. In next steps some consecutive reactions take place during which 1,3-dihydroisobenzofuran (phthalan) is formed as a final product. The structure of the product may be confirmed by the fact that the final spectra after UV/Vis and IR SEC correspond to known spectra of phthalan which can be found in some chemical database (e.g. Reaxys).

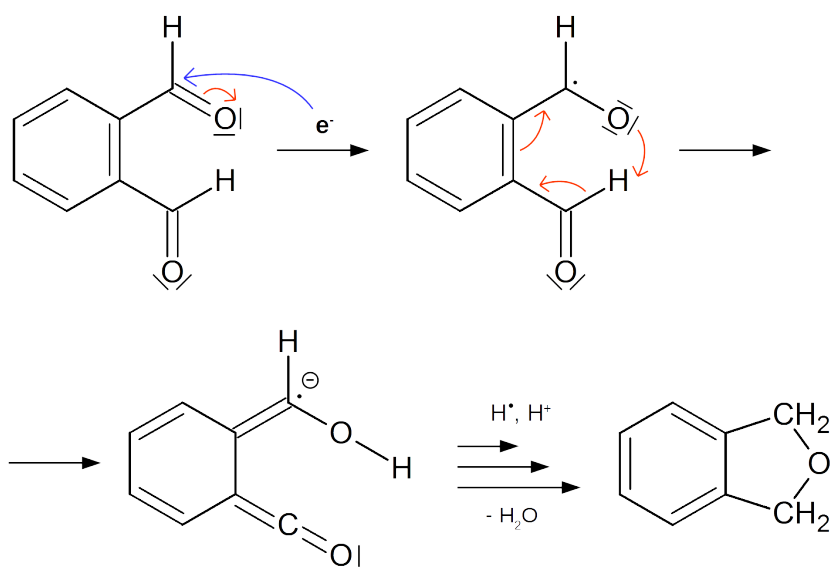


**Figure 36:** A proposed mechanism for the first step of the OPA reduction.

The presence of a relatively stable radical anion of OPA was confirmed by EPR SEC. The EPR spectrum should be symmetric about the center – peaks at left and right part of the spectra should be of the same height. During the EPR scan of approx. 20 seconds, left-right assymetry of the spectrum is observed where the signal at the end of the scan is smaller than that at the beginning. This behavior suggests that the radical anion is not fully stable and its concentration decreases in time (Fig. 37). The spectrum consists of even number of lines (in the center of the spectrum there is no line (marked in the Fig. 37 by a cross) which corresponds to the fact that OPA has six inequivalent hydrogen atoms with their own coupling constant. Altogether the spectrum should consist of 64 ( $2^6$ ) lines

but due to resolution of the used EPR spectrometer only a half of them can be identified. The smallest coupling constant which can be identified is 0.5 G. Then consecutively other coupling constants were identified as 2.2, 3.0, 3.8 and 4.7 G. The spectrum width deduced from the measured spectrum is 14.5 G whereas the sum of all identified coupling constants is 14.2 G. Therefore the last unidentified constant has to be 0.3 G and in our spectrum measured with certain resolution it causes only broadening of lines. Obtained coupling constants are comparable to the literature ones<sup>46</sup> with standard deviation less than 5 %. These data could be used by theoreticians as input parameters for advanced radical structure QM simulation.

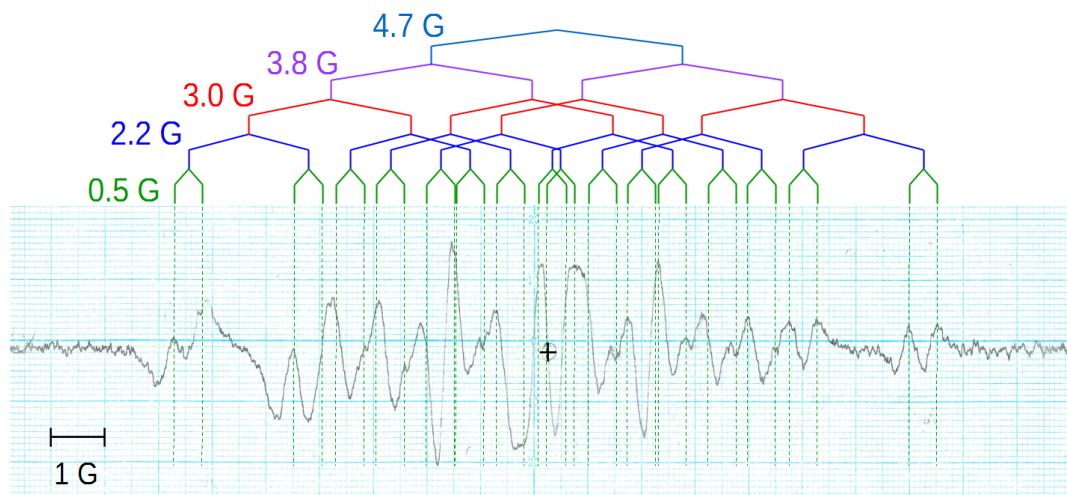


**Figure 37:** EPR spectrum of OPA radical generated electrochemically *in situ* in the EPR cavity. Derived coupling constants are displayed above. The center of the spectrum is marked by a cross.

#### 4.1.2 Isophthalaldehyde

IPA is a structural isomer of OPA having the second carbonyl group in *m*-position. Therefore it is reasonable to assume that electrochemical behavior will be different. In polarographic experiment, IPA is reduced in ACN in three steps at potentials  $-1.65$ ,  $-2.00$ , and  $-2.54$  V. The steps are diffusion-controlled and the first one corresponds to a one-electron reduction. The second and the third step are less than one-electron as in the case of OPA meaning that some portion of the radical anion formed during the first reduction step underwent a consecutive reaction therefore it could not be reduced in the next reduction steps.

On CV in Fig. 38, two completely irreversible peaks at  $-1.68$  and  $-2.04$  V can be distinguished. Their irreversibility does not change with increasing scan rate. It implies that a rather fast consecutive reaction of the primary radical anion takes place which cannot be outrun with CV at scan rates up to 1 V/s.

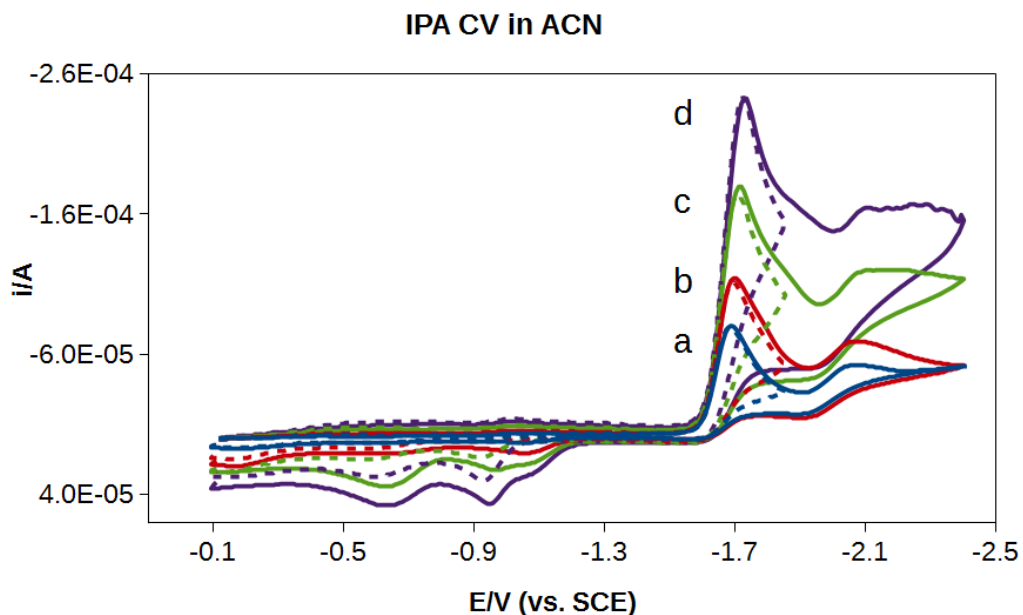


**Figure 38:** CVs of IPA in ACN at different scan rates: (a) 100 mV/s, (b) 200 mV/s, (c) 500 mV/s, (d) 1 V/s. CV measured only for the first reduction step is plotted by a dashed line. Potentials are related to the SCE.

Electrolysis of IPA was performed at potentials  $-1.8$  and  $-2.2$  V, respectively. Similarly like during the reduction of OPA, the decrease of current in time shown in Fig. 39 for electrolysis of IPA at potential of the first wave does not have a typical exponential shape. After approx. 400 s the slope of the  $i$ - $t$  curve increases. The electron consumption after the reduction on the first wave is approx. 0.8 electron/molecule. The solution turns yellow during electrolysis. From CV follows that the radical anion undergoes a fast consecutive reaction. A possible explanation is either a polymer chain reaction or an autocatalytic process. From the electron consumption during electrolysis on the first wave it can be reasonably concluded that a polymer chain reaction occurs. Because the polymer chain reaction is the case meaning that the structure of the radical anion changes in each polymerization step, measurement of EPR spectrum does not make sense because such a spectrum would be just a superposition of all intermediate radicals. Moreover, this confirms total irreversibility of IPA measured at CV.

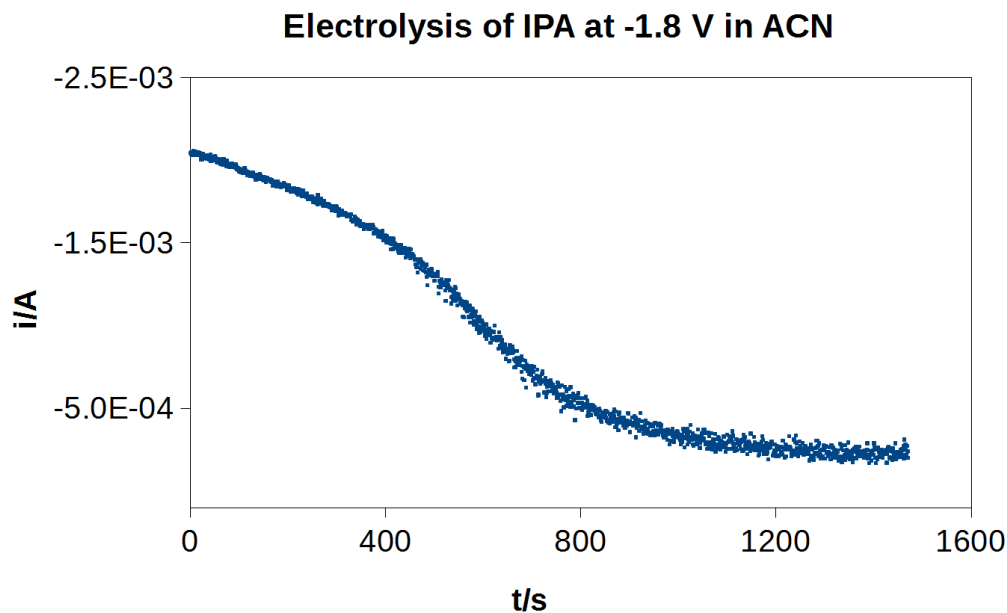


**Figure 39:** The dependence of current in time during electrolysis of IPA in ACN at potential  $-1.8$  V (vs. SCE).

In Fig. 40 there are UV/Vis spectra of IPA recorded during the first reduction step. From the figure it can be seen that the  $\pi$ -bond character changes during the reduction. This change can be traced using peak at 224 nm corresponding to  $\pi \rightarrow \pi^*$  transitions in conjugated double bonds. New peak at 430 nm appears ( $\pi \rightarrow \pi^*$  transitions in conjugated double bonds) which is related to formation of a yellow product seen during preparative electrolysis.

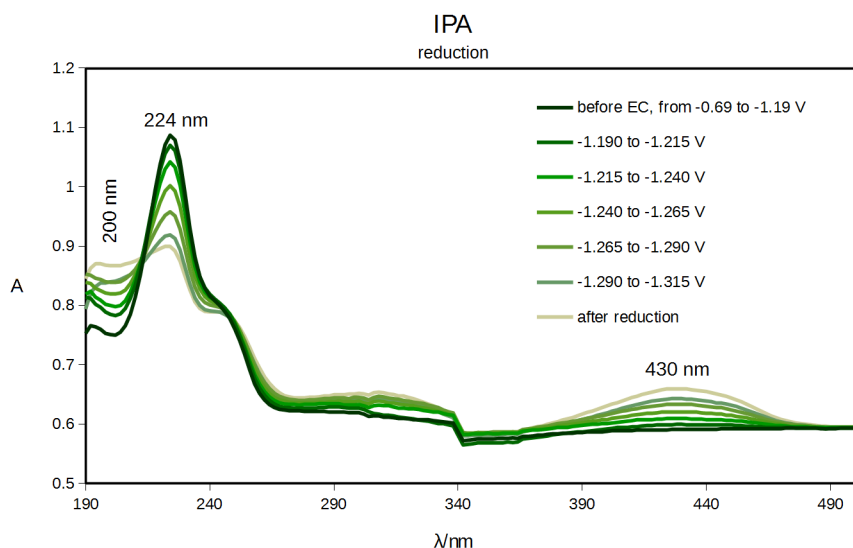


**Figure 40:** Change in UV/Vis spectra of IPA during the first reduction step in ACN. Potentials are related to the ferrocene system  $\text{Fc}^+/\text{Fc}$ .

The changes in IR spectra during the first reduction step of IPA are shown in Fig. 41 . From the doublet at  $1707$  and  $1699\text{ cm}^{-1}$  related to the coupled vibrations  $\nu(\text{C=O})$  from carbonyl groups, peak at  $1707\text{ cm}^{-1}$  disappears and peak at  $1699\text{ cm}^{-1}$  diminishes. Peak at  $2736\text{ cm}^{-1}$  related to the vibration  $\nu(\text{C-H})$  in carbonyl group is preserved and broadened. From the obtained changes in peaks it can be concluded that one carbonyl group perishes and the other one stays in the molecule in some form. Peaks at  $1616$ ,  $1606$  and  $1500\text{ cm}^{-1}$  are related to vibrations  $\nu(\text{C=C})$  in benzene ring. New peak at  $1572\text{ cm}^{-1}$  corresponds to vibrations  $\nu(\text{C=C})$  of benzene ring which is connected to some electronegative species – e.g. to an oxygen atom.

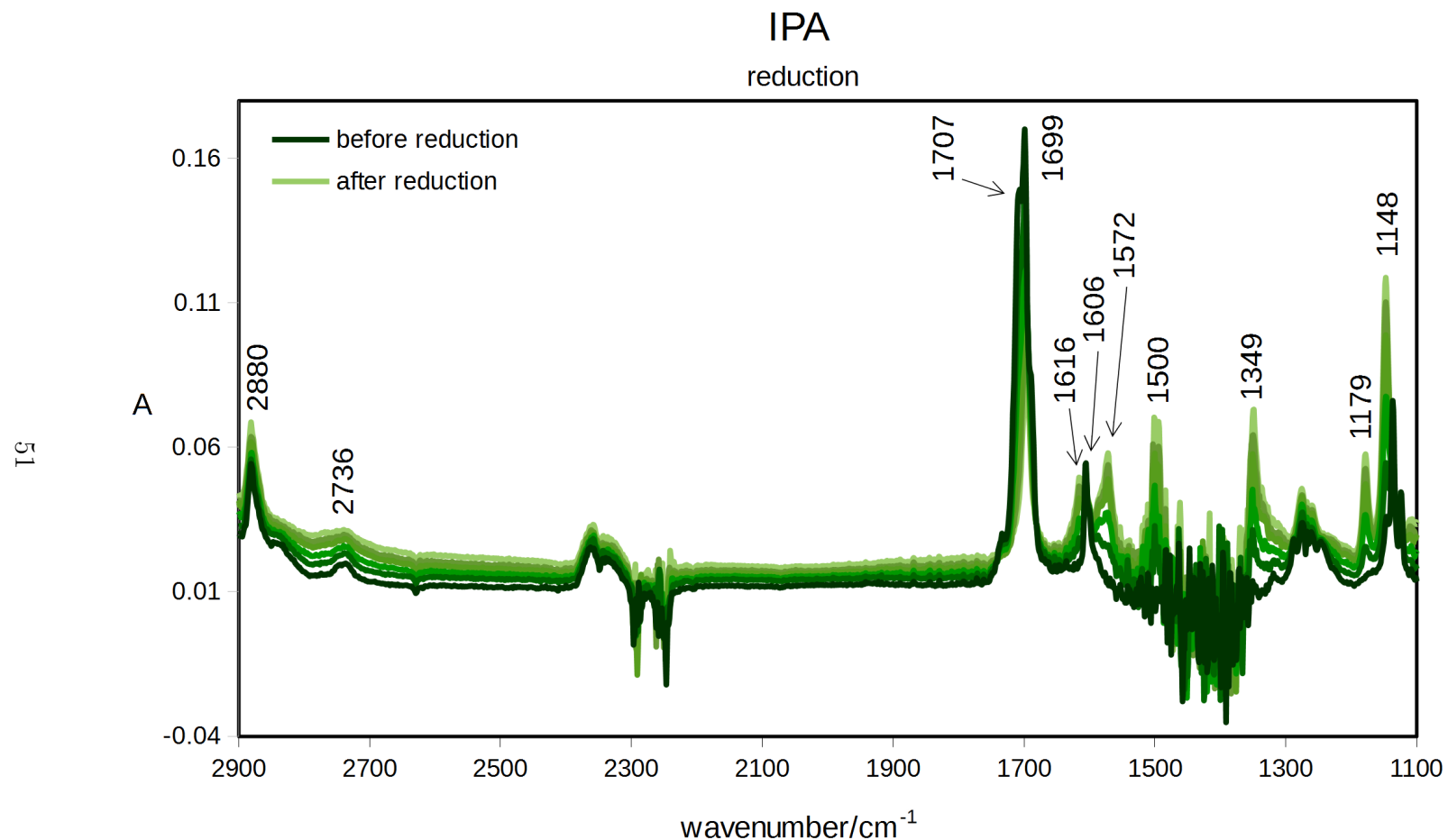


**Figure 41:** Change in IR spectra of IPA during the first reduction step.

Gathered information from IR SEC, CV and electrolysis allow us to draw a mechanism of proposed polymer chain reaction. The mechanism in Fig. 42 is started by a one-electron reduction. The negatively charged oxygen in the original carbonyl group attacks another IPA molecule on a partly positively charged carbon atom in benzene ring and a dimer is formed. The negatively charged oxygen atom in the dimer could attack another IPA molecule and by this mechanism a polymer structure can be created. A possible mechanism for rearomatization of one structural unit of the oligomer is proposed in Fig. 43. The structure of an oligomer in turn is supported by appearance of peaks at 1148, 1179, and 1349 cm<sup>-1</sup> related to vibrations  $\nu(\text{CO})$  and  $\nu(\text{CC})$  and 2880 cm<sup>-1</sup> related to vibrations  $\nu(\text{C-H})$  of aliphatic C<sub>sp<sup>3</sup></sub>. These vibrations could be found in the linking bridge in the dimer proposed in the mechanism.

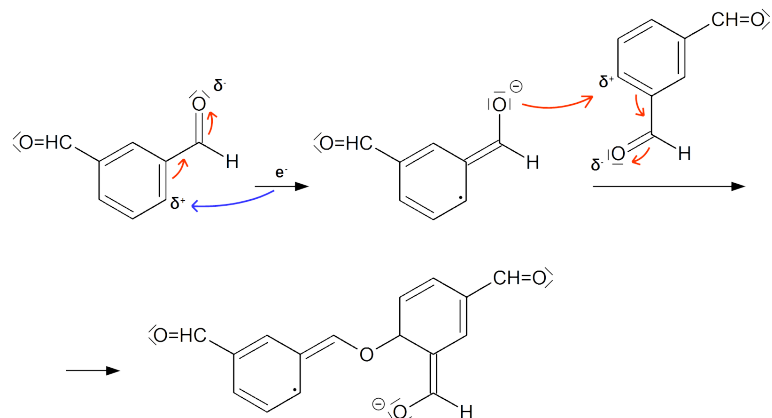


**Figure 42:** The proposed mechanism for the first reduction step of IPA leading to formation of a dimer.

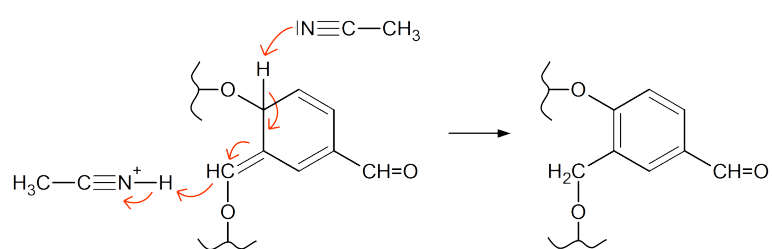
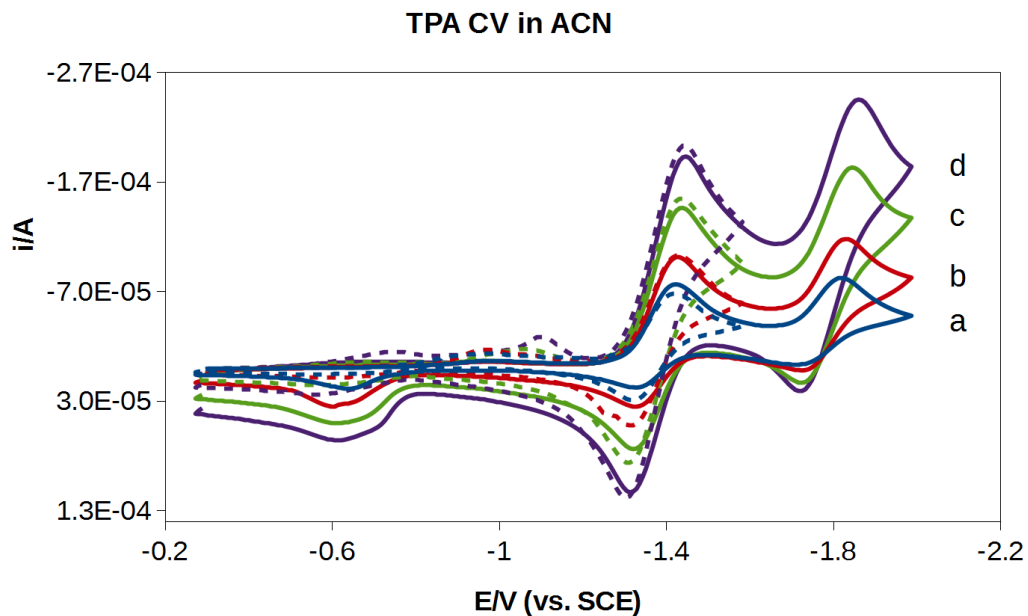


**Figure 43:** A proposed mechanism for rearomatization of one structural unit in formed oligomer of IPA with the participation of the solvent.

#### 4.1.3 Terephthalaldehyde

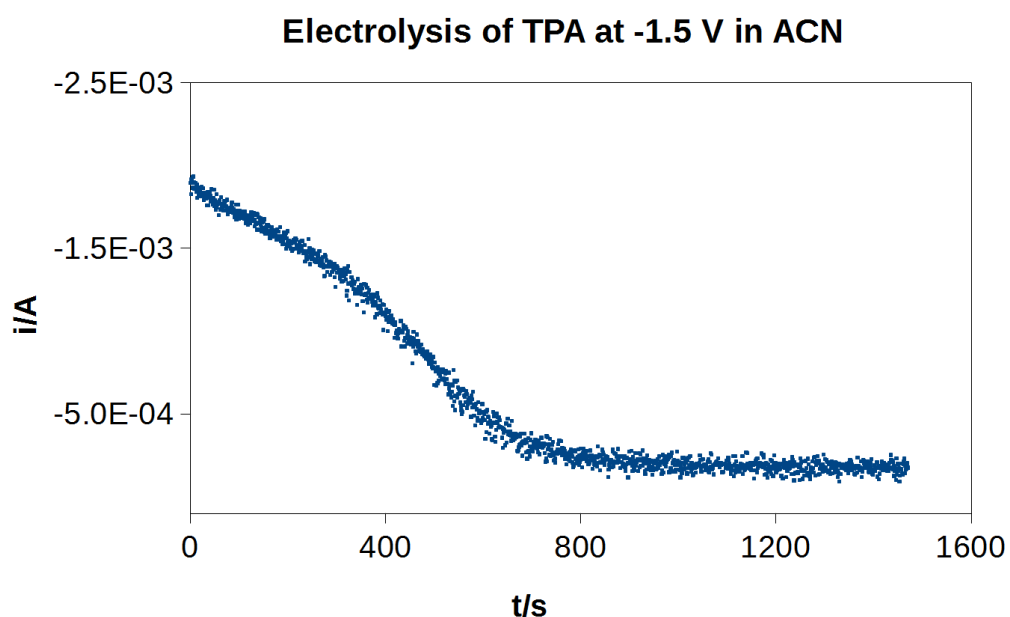
TPA is a structural isomer of OPA with carbonyl groups in *p*-position. It was studied by the same techniques as previous two substances. TPA is reduced in two steps at  $-1.40$  and  $-1.88$  V in DC-polarography. Both steps are diffusion-controlled and they represent an uptake of one electron each. Therefore during the first step a primary radical anion is formed which undergoes another one-electron reduction.

On CV in Fig. 44, one can see two completely reversible reductions independently on scan rate at peak potentials  $-1.44$  and  $-1.90$  V. During the first reduction step, a stable blue radical anion is formed. By the second reduction, a stable dianion is most probably formed.



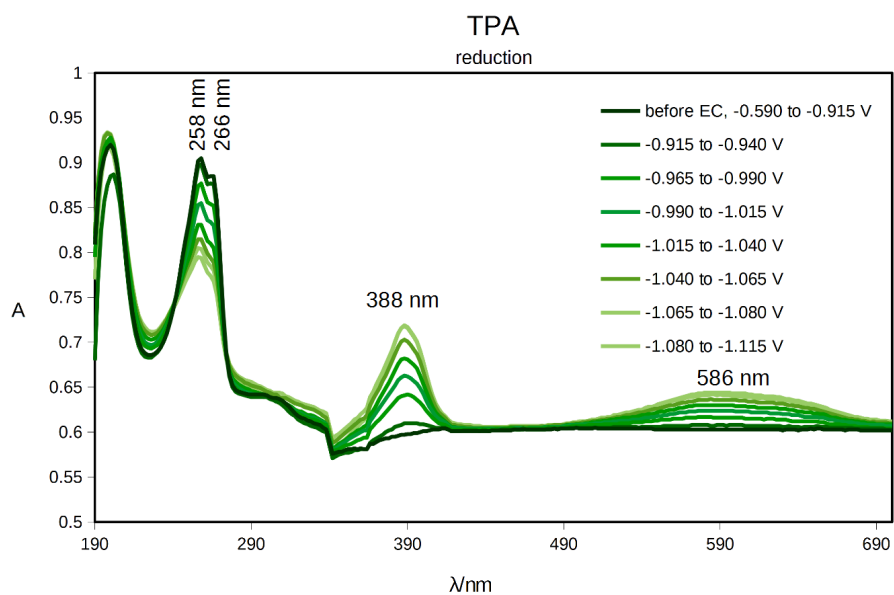
**Figure 44:** CVs of TPA in ACN at different scan rates: (a)  $100\text{ mV/s}$ , (b)  $200\text{ mV/s}$ , (c)  $500\text{ mV/s}$ , (d)  $1\text{ V/s}$ . CV measured only for the first reduction step is plotted by a dashed line. Potentials are related to the SCE.

The blue radical anion was observed also during electrolysis at potential  $-1.5$  V. The time dependence of current is shown in Fig. 45. In the first 400 s after the start of the electrolysis, the slope of the  $i$ - $t$  curve is constant. Then suddenly the slope starts to increase similarly to OPA and IPA. The electron consumption during electrolysis on the first wave is approx. 0.35 electron/molecule which is similar to OPA. It can be caused by high reversibility of the reduction steps.

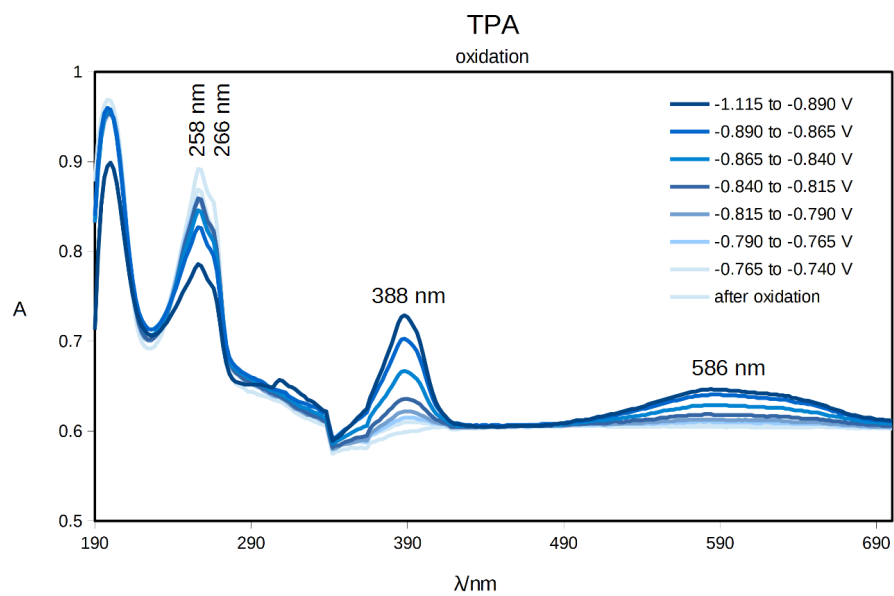


**Figure 45:** The dependence of current in time during electrolysis of TPA in ACN at potential  $-1.5$  V (vs. SCE).

Next, UV/Vis SEC of IPA was measured. Spectra can be seen in Fig. 46. While the doublet at 258 and 266 nm related to  $\pi \rightarrow \pi^*$  transitions in carbonyl groups diminishes, two new peaks at 388 and 586 nm emerge ( $\pi \rightarrow \pi^*$  transitions in conjugated double bonds). Peak at 586 nm is related to formation of the blue radical anion. It was also proved that the first reduction step is reversible – the UV/Vis spectrum after the re-oxidation is the same as before the reduction meaning that peaks that were formed during the reduction disappear during the re-oxidation and diminished peaks return to their original height (Fig. 47).



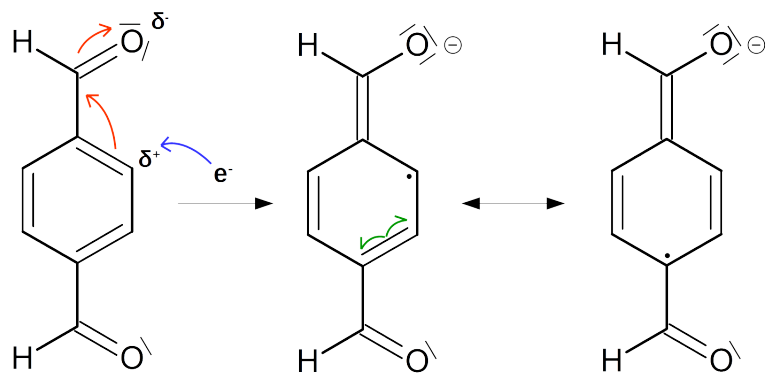
**Figure 46:** Change in UV/Vis spectra of TPA during the first reduction step in ACN. Potentials are related to the ferrocene system  $\text{Fc}^+/\text{Fc}$ .



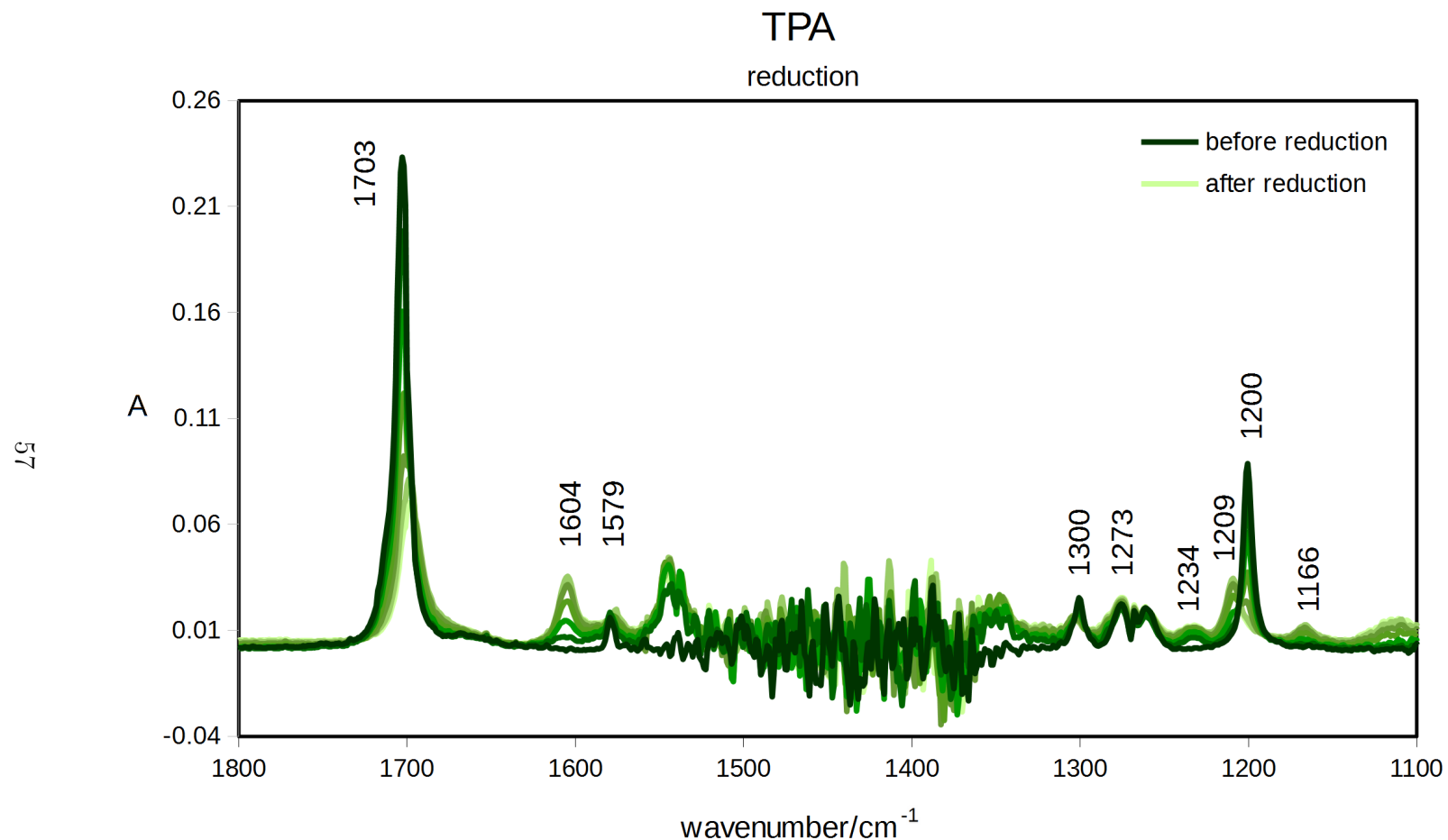
**Figure 47:** Change in UV/Vis spectra of TPA during oxidation in ACN. Potentials are related to the ferrocene system  $\text{Fc}^+/\text{Fc}$ .

Fig. 48 represents the spectra obtained during IR SEC of TPA. Peak at  $1703\text{ cm}^{-1}$  related to the vibration  $\nu(\text{C=O})$  from carbonyl groups diminishes as well as peak at  $1579\text{ cm}^{-1}$  associated with the benzene stretching vibration  $\nu(\text{C=C})$ , caused by conjugation of benzene ring with a functional group, which means that a carbonyl group was reduced. New peak at  $1604\text{ cm}^{-1}$  is related to formation of a planar quinoid structure with coupled vibrations  $\nu(\text{C=C})$  between carbon atoms forming double bonds in the cycle. Position of peak at  $1200\text{ cm}^{-1}$  related to the vibration  $\nu(\text{C-C-H})$  between one carbon atom from benzene ring, to which is attached a carbon atom from the original carbonyl group, shifts to  $1209\text{ cm}^{-1}$ . New peaks at  $1234$  and  $1273\text{ cm}^{-1}$  related to vibrations  $\delta(\text{C-H})$  on benzene ring emerge in the spectra.

Combined information from UV/Vis and IR SEC and from electrochemical methods allow to draw the most probable reduction mechanism. The reduction mechanism and the structure of the assumed quinoid species is in Fig. 49. The mechanism is started by a one-electron reduction on benzene ring. By that the  $\pi$ -electron distribution in the molecule is changed and the quinoid structure is formed.



**Figure 49:** A planar quinoid structure of a radical anion formed during the first reduction step of TPA.



**Figure 48:** Change in IR spectra of TPA during the first reduction step.

The presence of the quinoid radical anion of TPA formed during the first reduction was confirmed by EPR SEC. The measured EPR spectrum shown in Fig. 50 represents a superposition of two spectra of the *cis* and *trans* rotamer of the radical anion. The *cis* and *trans* rotamers are resonance hybrids of two resonance structures from Fig. 51. In the case of both rotamers, the signal is split by three pairs of equivalent hydrogen atoms. In the spectrum of each rotamer there should be nine triplets –  $3^3$ , altogether 27 lines. The highest coupling constant is in both spectra approx. the same with the value of 3.95 G and it is most probably caused by hydrogen atoms in original carbonyl groups because they have approx. the same chemical surroundings. Hydrogen atoms on benzene ring are different in *cis* and *trans* rotamer therefore they have different coupling constants. The measured EPR spectrum is easily interpretable. The spectrum width is 6.7 G. The form I has coupling constants 3.95, 2.10 and 0.75 G, for the form II it is 3.95, 1.55 and 1.10 G. Assignment of coupling constants to individual rotamers could be made with help of QM simulations.

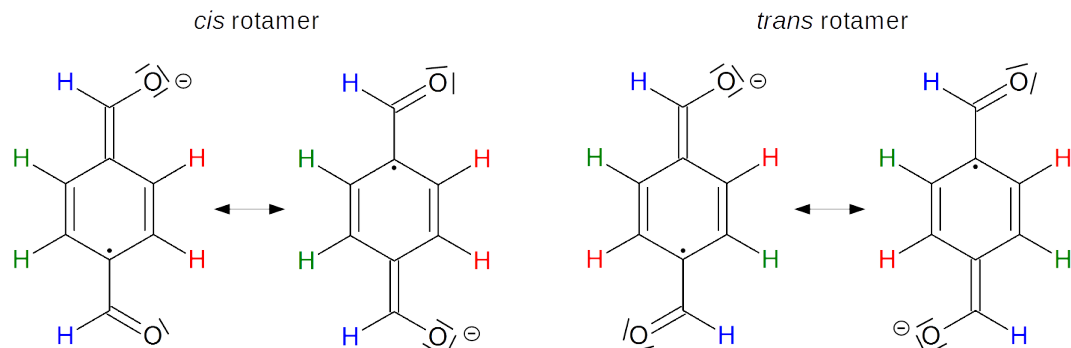


**Figure 51:** *Cis* and *trans* rotamers of the TPA radical anion.

### EPR spectrum of the TPA radical anion

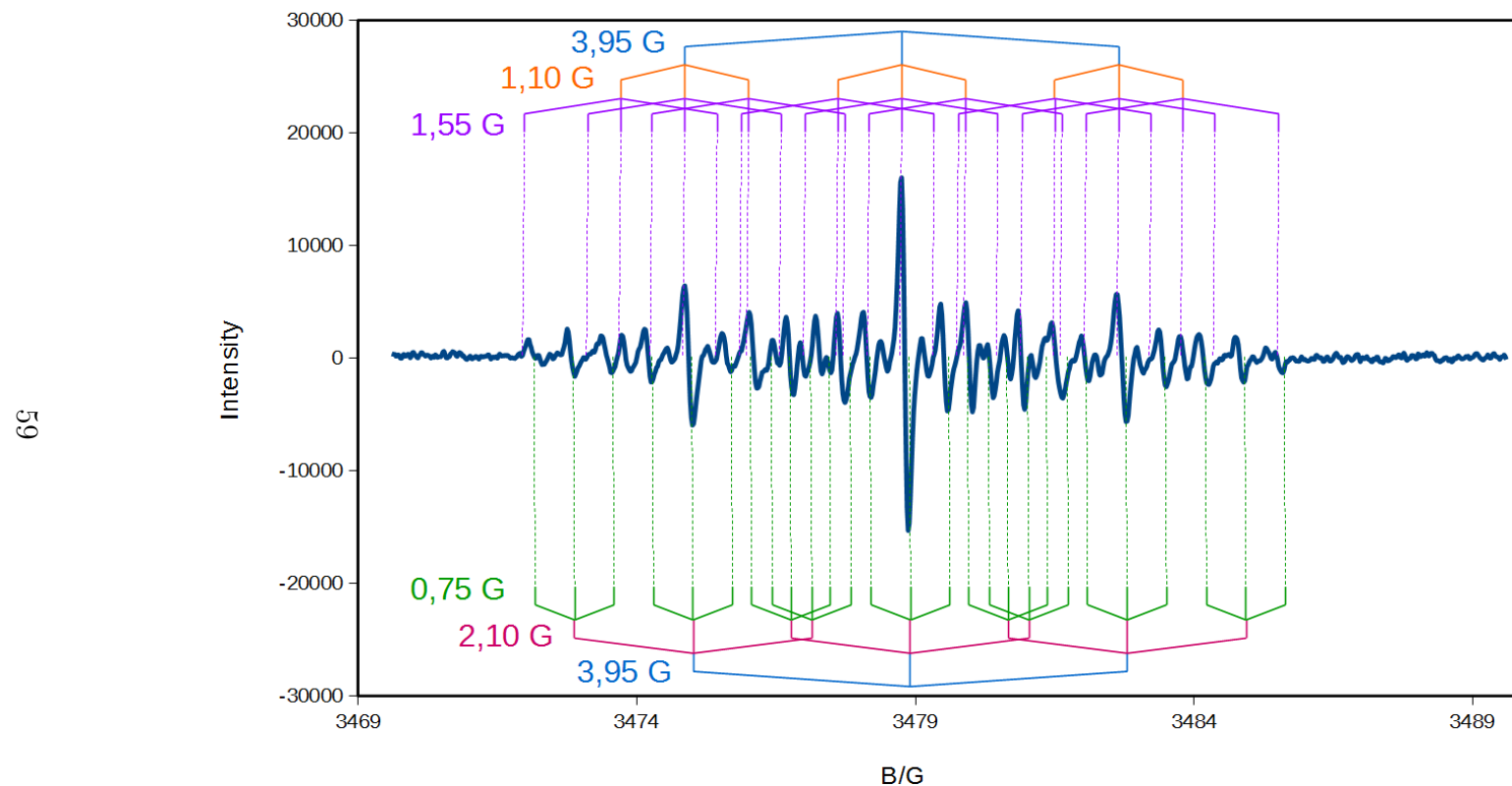


**Figure 50:** EPR spectrum of the TPA radical anion generated electrochemically *in situ* in the EPR cavity. Derived coupling constants for the *cis* and *trans* rotamer are displayed above and below the spectrum.

#### 4.1.4 Comparison of behavior of benzenedialdehydes in non-aqueous media

In the previous sections, electrochemical behavior of three isomeric benzenedialdehydes in non-aqueous aprotic media was investigated. In ACN, benzenedialdehydes are reduced usually in two steps. Table 1 summarizes reduction potentials and the electron consumptions in both steps. For comparison of the reduction behavior, the value of reduction potential of benzaldehyde is given.

**Table 1:** Reduction potentials and the electron consumptions for studied benzenedialdehydes in ACN and comparison with benzaldehyde (BA).

	$E_{red}^1/V$	$z_1$	$E_{red}^2/V$	$z_2$	$E_{red}^3/V$
OPA	-1.51	0.40	-2.02	1	(-2.20)
IPA	-1.68	0.80	-2.04	> 1	-
TPA	-1.46	0.35	-1.90	< 1	-
BA <sup>60</sup>			-2.00		

The most significant is always the first reduction potential. Its value should reflect the induction effect of the neighbor groups and substituents, and simultaneously the energy of the LUMO, that means the extent of electron delocalization and simultaneously the level of intramolecular electron communication. TPA is most easily reduced (-1.46 V) because, besides the induction effect of the second aldehydic electron-withdrawing group which lowers electron density in the molecule, a very important role is played by the *p*-mutual position of the two aldehydes on the phenyl ring. This *p*-isomer offers the most extended, symmetric and planar delocalized quinoid-like system which substantially shifts the reduction potential to less negative values.<sup>61</sup>

Although the induction and resonance effects in OPA are operating in the same way like TPA, the *o*-effect is weaker, moreover, the steric influence plays also a role. Therefore OPA is reduced slightly more negatively than TPA at -1.51 V. The reduction potential of IPA is the most negative from all three benzenedialdehydes because the resonance effect plays only marginal role and only induction effect takes place. The latter, however, is important even here. The influence of the *m*-substitution is evident from the comparison of the reduction potential of IPA

(-1.68 V) and benzaldehyde (aprox. -2.0 V), where is no substitution in the position 3 and where the induction effect is missing. The appropriateness of this comparison is supported also by the fact that the potential of the second reduction wave of OPA and IPA is -2.02 and -2.04 V, respectively, hence, close to that of benzaldehyde.

In the case of OPA and TPA, during the first reduction step, a relatively stable radical anion is formed which was detected by cyclic voltammetry and which was intercepted and characterized by EPR. The first reduction step in IPA is, however, irreversible, but from the comparison of the potentials of all three benzenedialdehydes and from their shape of the CV curve, one can expect that even in IPA first the radical anion is formed. However, its stability is low because it undergoes fast follow-up reaction(s), most probably with the traces of protons present in the solvent (leading to a simple reduction) or with the starting substance (the "father - son" mechanism) resulting in dimers or oligomers. Therefore the radical anion of IPA could not be confirmed by EPR technique. The partly limited reversibility of OPA is probably the same reason for not very good EPR spectrum.

The TPA radical anion formed in the first reduction step is reduced more easily also in the second step, the second reduction potential is only -1.90 V. Due to prevailing *p*-mesomeric effect the interaction between both carbonyl groups is so pronounced that carbonyl groups lose their original properties. They form a new symmetric and planar electron-delocalized quinoid system together with benzene ring and this system can be reduced more easily at both reduction steps. This fact is consistent with nearly total reversibility of both steps.

The structure of products of OPA, IPA, and TPA electrolysis in ACN at potentials corresponding to the first and to the second reduction step was investigated using NMR spectroscopy and HPLC-APCI-MS. Despite many efforts to obtain the highest purity, measured NMR spectra of the products were not suitable for determination of their structure because spectra contained peaks belonging to different impurities (e.g. salt from supporting electrolyte, impurities from used chemicals). Therefore products were analyzed by HPLC-APCI-MS technique. Regrettably, no substances present in the samples were ionized by the APCI technique therefore no products were identified. Although the APCI technique provides weak ionization of analytes, after their conversion to hydrazides they should be detectable. Absence of

any ions corresponding to the analyzed substances indicates that primarily formed products after electrolysis undergo consecutive reactions that lead to a mixture of oligomers which cannot be ionized by the APCI technique. This is consistent with the proposed mechanism of the first reduction step of IPA (Fig. 42) during which a dimer is formed which can undergo other follow-up polymerisation reactions. It is also consistent with the shapes of  $i$ - $t$  curves obtained during electrolysis of all three substances which indicate that some reactions of the intermediate with the starting material takes place yielding oligomers.

#### 4.1.5 Electrochemical behavior of studied benzenedialdehydes in DMF and acetone

As stated before, electrochemical behavior of the three benzenedialdehydes was also studied in different solvents. In DMF at HMDE (Table 2), OPA is reduced in two steps at potentials  $-1.41$  and  $-2.10$  V. Both steps on CV are reversible. At the gold working electrode, the potential range in which the reduction of analyzed substances can be observed is limited to approx.  $-2$  V therefore only the first reduction step is accessible. It occurs at potential  $-1.44$  V and it is completely reversible under these conditions. This correspondence with the results obtained in ACN confirms that the reduction potentials are reliable. Higher stability of primary radical anion in DMF than in ACN is caused by protophilicity of DMF which effectively lowers activity of the traces of protons.

In acetone, the cyclic voltammogram changes after the first scan and the final peaks are not related to the reduction of OPA. Even after making a new surface of the working electrode, the positions of peaks on CV remain the same as on the last scan of the first measurement. OPA probably somehow reacts with the solvent therefore electrochemical data in this medium were not obtained.

IPA is in DMF at DME reduced polarographically in three steps at potentials  $-1.58$ ,  $-2.00$ , and  $-2.40$  V. All steps are diffusion-controlled and the first one is equal to a one-electron reduction as in ACN. The second wave has very small current compared to the first one. The third step is of the same height as the first step therefore it also corresponds to a one-electron reduction. On CV (Table 3), five peaks with indication of reversibility at  $-1.64$ ,  $-2.07$ ,  $-2.59$ ,  $-2.74$ , and  $-2.90$  V

**Table 2:** Reduction potentials from CV for OPA in ACN, DMF and acetone and on mercury and gold electrode. Potentials are related to the SCE.

solvent/ electrode	$E_{pc}^1/V$	$E_{pa}^1/V$	$\Delta E^1/mV$	$E_{pc}^2/V$	$E_{pa}^2/V$	$\Delta E^2/mV$	$E_{pc}^3/V$
ACN/Hg	-1.51	-1.45	60	-2.02	-	-	-2.20
DMF/Hg	-1.41	-1.35	60	-2.10	-2.02	80	-
DMF/Au	-1.44	-1.37	70	-	-	-	-
acetone/Hg	the substance probably reacts with the solvent						

can be distinguished. Their degree of reversibility does not change with increasing scan rate. They can be attributed to reduction of carbonyl groups present in some consecutive products. At gold working electrode, only the first one step is observable, at -1.63 V. In acetone, IPA is reduced in two completely irreversible steps at -1.63 and -1.96 V.

**Table 3:** Reduction potentials from CV for IPA in ACN, DMF and acetone and on mercury and gold electrode. Potentials are related to the SCE.

solvent/ electrode	$E_{pc}^1/V$	$E_{pc}^2/V$	$E_{pc}^3/V$	$E_{pc}^4/V$	$E_{pc}^5/V$
ACN/Hg	-1.68	-2.04	-	-	-
DMF/Hg	-1.64	-2.07	-2.59	-2.74	-2.90
DMF/Au	-1.63	-	-	-	-
acetone/Hg	-1.65	-1.96	-	-	-

TPA in DMF under polarographic conditions (DME) undergoes two reduction steps at potentials -1.30 and -1.89 V. Both steps are diffusion-controlled and one-electron reductions like in ACN. CV in DMF (Table 4) show two completely reversible reductions as well, at potentials -1.34 and -1.90 V (Fig. 52 and 53). During the re-oxidation part of the cycle, there is not only one anodic peak corre-

sponding to the oxidation of the primary radical anion formed during the reduction but at more positive potentials there are other peaks. They are probably caused by numerous adsorption and reduction of products on the surface of the hanging mercury drop working electrode.

**Table 4:** Reduction potentials from CV for TPA in ACN, DMF and acetone and on mercury and gold electrode. Potentials are related to the SCE.

solvent/ electrode	$E_{pc}^1/V$	$E_{pa}^1/V$	$\Delta E^1/mV$	$E_{pc}^2/V$	$E_{pa}^2/V$	$\Delta E^2/mV$
ACN/Hg	-1.44	-1.37	70	-1.90	-1.84	60
DMF/Hg	-1.34	-1.29	50	-1.90	-1.83	70
DMF/Au	-1.35	-1.28	70	-1.93	-1.84	70
acetone/Hg	the substance probably reacts with the solvent					

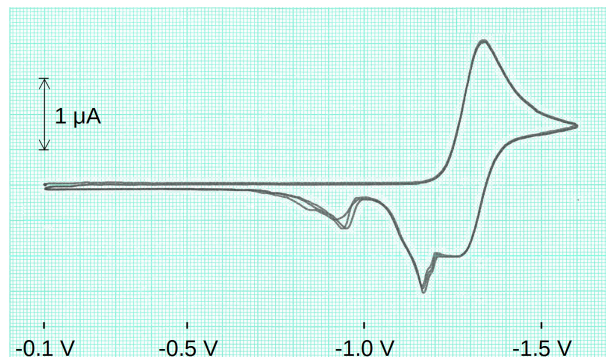


**Figure 52:** Cyclic voltammogram of TPA in DMF on hanging mercury drop working electrode, only the first reduction step. Potentials are related to the SCE.

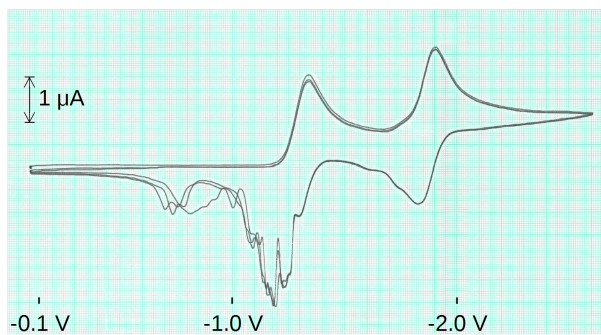


**Figure 53:** Cyclic voltammogram of TPA in DMF on hanging mercury drop working electrode, both reduction steps. Potentials are related to the SCE.

At gold working electrode, the reduction potentials are very similar,  $-1.35$  and  $-1.93$  V, both steps are completely reversible and only anodic peaks corresponding to oxidation of the species reduced in the reduction part of the cycle are present. This means that the numerous peaks seen on CV on hanging mercury drop working electrode are related somehow to the specific surface of this "liquid" electrode. As in the case of OPA, in acetone the cyclic voltammogram changes during individual scans in the first measurement. In the next measurements the voltammogram does not correspond to the first one and there are only peaks from final scans of the first CV meaning that TPA reacts somehow with the solvent.

## 4.2 Aqueous media

Electrochemical reduction of the three benzenedialdehydes was investigated also in buffered aqueous solutions. In this media, the reduction proceeds at more positive potentials than in non-aqueous solutions.<sup>59</sup> This is caused either by antecedent protonation of heteroatoms (here the carbonyl oxygen) when the positively charged protonated species is reduced more easily; or by the presence of protons in the solution (depending on pH), availability of which shifts the equilibrium of the protonation of primary radical anion to the right side and thus makes the reaction more energetically profitable. Many organic compounds undergo a two-electron reduction in the protic solutions according to the ECEC mechanism:  $A + e^- \rightarrow A^{\cdot-}$ ,  $A^{\cdot-} + H^+ \rightarrow AH^{\cdot}$ ,  $AH^{\cdot} + e^- \rightarrow AH^-$ ,  $AH^- + H^+ \rightarrow AH_2$ . The position of the reduction potential is dependent on pH and acid-base properties of used solutions. The number of hydrogen ions that participate in the reduction can be determined from the dependence of the polarographic half-wave potential or peak potential on pH.

Electrochemical reduction of OPA, IPA and TPA is treated in many articles (cf. Section 2.4). However results from classic electrochemical literature concerning the reduction of the three benzenedialdehydes are not precise. In the literature, a two-step electrochemical reduction of all three benzenedialdehydes is described but the more detailed and more systematic results obtained during this thesis and also during other experiments in our group do not fully correlate with the published ones. The reason is higher resolution used on both the voltage and the current range and more detailed approach.

In Fig. 54 and 55, there is a pH dependence of half-wave potentials and of limiting currents, respectively, for reduction of OPA in aqueous buffered solutions obtained by DC-polarography (like in the literature). The analysis of curves revealed that the reduction of OPA occurs in totally four waves over the entire pH range. It concerns the reduction of diprotonated, monoprotonated and unprotonated form. Also the reduction of IPA and TPA in aqueous media proceeds in more than two steps, in contrast to literature where only two steps in the whole pH

range are reported. A serious interpretation and understanding of the electrochemical behavior in aqueous solutions and the assignment of individual polarographic waves to reducing substances requires further investigation which is still running and is beyond the scope of this thesis.

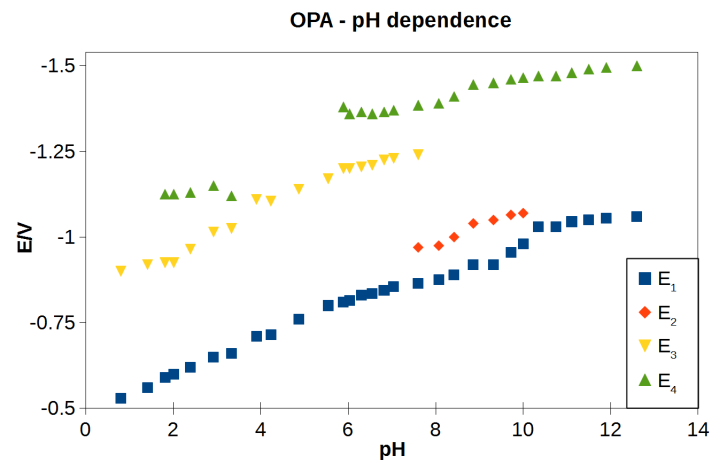


**Figure 54:** The dependence of half-wave potentials on pH for reduction of OPA in aqueous phosphate buffers. Potentials are related to the SCE.

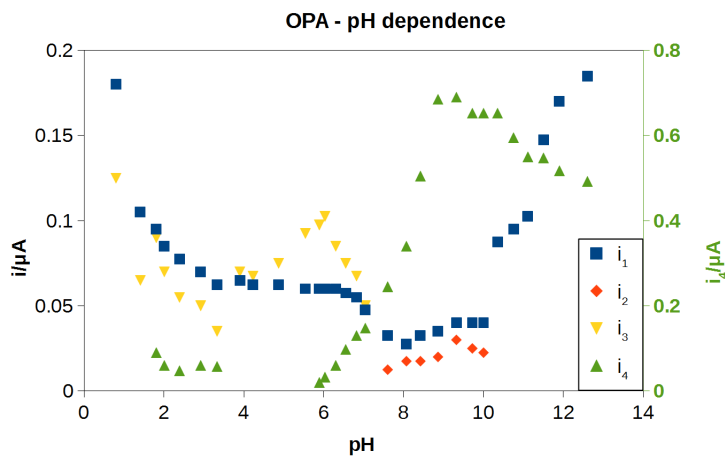


**Figure 55:** The dependence of limiting currents on pH for reduction of OPA in aqueous phosphate buffers.

### 4.3 Reactivity of OPA, IPA and TPA with nucleophiles

In analytical chemistry, reactions of OPA with nucleophiles are used for many decades.<sup>58</sup> OPA undergoes hydration in aqueous solutions where totally three forms are present: unhydrated, monohydrated and cyclic hydrate form (see Section 2.4.1). As mentioned above, OPA is used in analytical methods for determination of AAs but the progress of this procedure was developed only empirically. Therefore a study of the reactivity of OPA with AAs was carried out.<sup>58</sup>

It was found out that the reactivity of OPA depends strongly on the structure of the AA. The course of the reaction of OPA with AAs was followed by measuring the decrease of the limiting current in time at constant potential corresponding to a reduction of the first wave. During the reaction, the concentration of free OPA in a solution decreases and therefore from the dependence od the limiting current on time, the reaction kinetics for individual AAs can be evaluated.

In Table 5, the obtained slopes of linear parts of dependences of logarithm of limiting currents on time are shown. Glycine is the simplest AA and it reacts the fastest. On the other hand,  $\alpha$ -aminoisobutyric acid was the AA with the greatest steric hindrance and it was found out that it almost does not react with OPA. Other used AAs (alanine, valine, norvaline, leucine, isoleucine,  $\alpha$ -aminobutyric acid) react in the similar rate. Lysine as an AA with two amino groups react very fast, in basic pH the reaction is finished almost immediately.

The reaction of OPA with AAs was also studied by UV/Vis spectrophotometry. It was found out that the course of the reaction differs in various used OPA stock solutions. If aqueous OPA stock solution is used – where OPA is already in equilibrium with the monohydrated and the cyclic hydrate form – on UV/Vis spectra we can observe immediate increase in absorbance due to a reaction with an AAs. If OPA is dissolved in ACN where only unhydrated OPA is present, at first there is a decrease in spectra due to hydration of OPA and then an increase follows like in the previous case but the reaction proceeds slower. The examples of obtained UV/Vis spectra for reaction of isoleucine with the aqueous and the non-aqueous stock solution of OPA are in Fig. 56 and 57, respectively.

**Table 5:** Slopes from  $\ln(i)$ - $t$  curves for the ratio AA:OPA 3:1

AA:OPA 3:1	slope: $\frac{d\ln(i)}{dt} \cdot 10^3$	
amino acid	pH 7.86	pH 11.22
glycine	-3.20	-3.65
alanine	-2.00	-5.10
$\alpha$ -aminobutyric acid	-1.70	-4.70
$\alpha$ -aminoisobutyric acid	-0.04	-0.20
valine	-1.40	-2.70
norvaline	-1.70	-4.25
leucine	-1.75	-3.80
isoleucine	-1.40	-2.90

This finding is probably very important because it suggests that not the di-aldehydic form but some hydrated form of OPA is really reacting with AAs. This problem requires further proofs because if confirmed it will change the fundamental view on the reactivity of OPA with nucleophiles generally and on the mechanism of AAs analysis specifically.

For comparison of the reactivity of the studied *o*-benzenedialdehyde with AAs, same experiments were performed also with the *m*- and *p*-isomer (IPA and TPA). It was found out however that the reaction conversion is so small (if any at all) that the decrease of concentration in time cannot be observed using DC-polarography. It implies that the *o*-position of the two carbonyl groups in OPA is necessary for the reaction to occur. Also the presence of water seems to be important for the progress of the reaction.

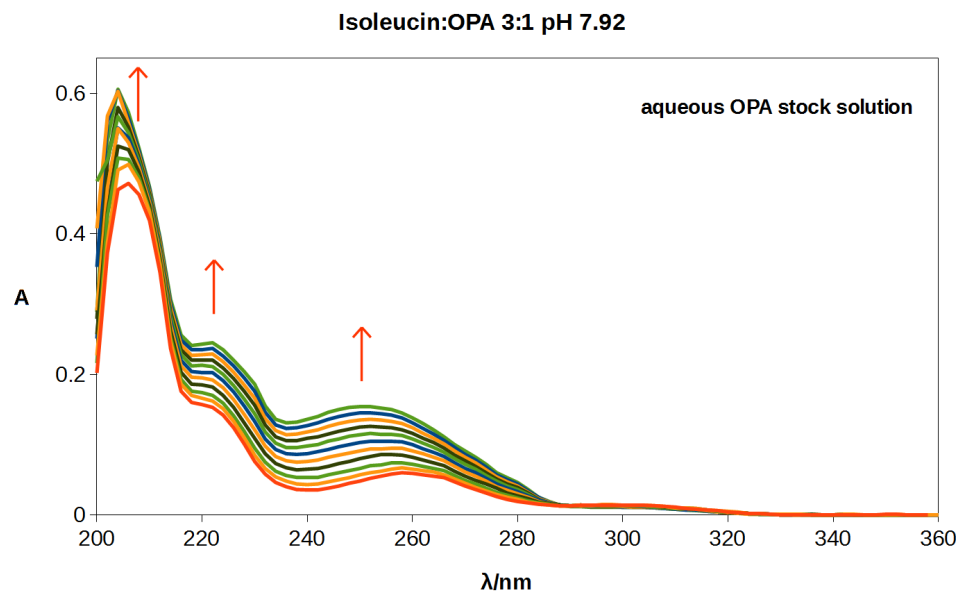


**Figure 56:** UV/Vis spectra for reaction of hydrated OPA with isoleucine in ratio 1:3 in pH 7.92.

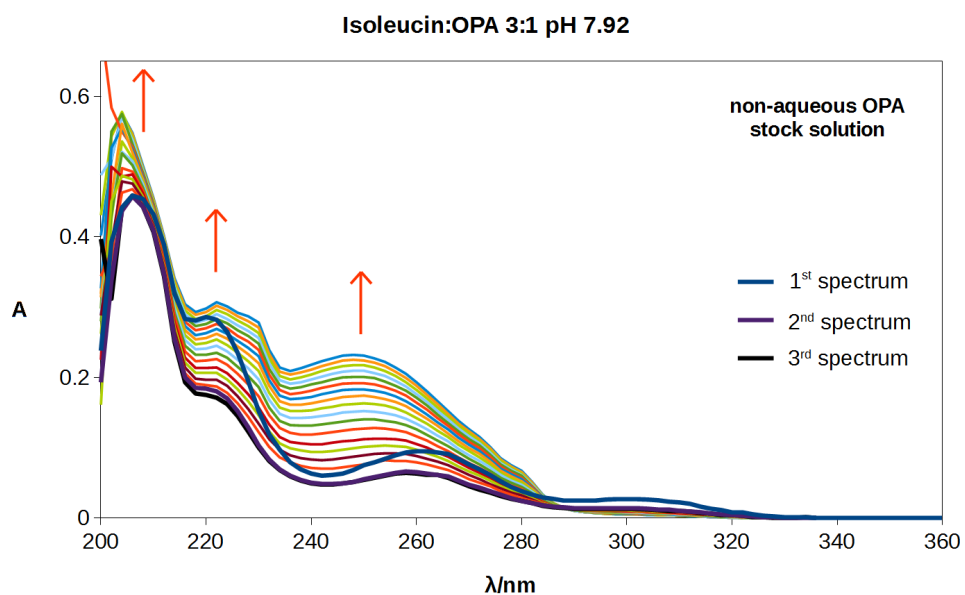


**Figure 57:** UV/Vis spectra for reaction of unhydrated OPA with isoleucine in ratio 1:3 in pH 7.92.

## 5 CONCLUSION

This thesis presents description of electrochemical reduction behavior of orthophthalaldehyde (OPA), isophthalaldehyde (IPA) and terephthalaldehyde (TPA) in non-aqueous media. More detailed description is provided for the first reduction step which was studied using spectroelectrochemical techniques and the reduction mechanism is proposed.

OPA is reduced in two steps at potential  $-1.51$  and  $-2.02$  V (peak potentials). The first step is reversible with increasing scan rate meaning that a consecutive reaction with the reduced substance takes place. The first step is a one-electron reduction. A neutral radical is formed and the final product of the first reduction step after some consecutive reactions is assumed to be 1,3-dihydro-isobenzofuran (phthalan). The presence of the relatively unstable radical was confirmed by EPR spectroelectrochemistry.

In the case of IPA, both reduction steps at  $-1.68$  and  $-2.04$  V are completely irreversible. The primary radical anion formed in the first reduction step undergoes a very fast consecutive reaction. It is assumed that the radical anion reacts with the starting substance and a mixture of oligomers is formed. This assumption is consistent with the fact that no products were identified using HPLC-MS technique with atmospheric pressure chemical ionization and that on CV there are small peaks that could correspond to reduction of individual products of these consecutive reactions.

The first reduction step of TPA occurs at the most positive potential ( $-1.46$  V) because of the *p*-position of both carbonyl groups which offers the highest induction and resonance effects. A planar quinoid radical anion is formed and its stability is confirmed by total reversibility of the first reduction step on CV. The second reduction step is also highly reversible.

Electrochemical reduction of the studied benzenedialdehydes was also studied in other solvents, namely in DMF and acetone. The results obtained in DMF corresponds to those from ACN which confirms reliability of reduction potentials. Electrochemical data for OPA and TPA in acetone were not obtained because the substances probably somehow react with the solvent. IPA is in acetone reduced at similar potentials as in ACN and DMF.

The comparison of the three benzenedialdehydes with the analogous diacetyl derivatives (text in Supplementary material C) demonstrate the electronic similarity of the two types of compounds. More negative reduction potentials in diacetylbenzenes reflect the induction effect of the present methyl groups, observed higher degree of reversibility (namely in *m*-DAB in contrast to IPA) points to higher stability of the primary radical anions, and thus to their lower reactivity caused by the strong C(O)-CH<sub>3</sub> bond preventing the di- and oligomerization.

Study about reactivity of OPA, IPA and TPA with AAs brings important findings. It suggests that not the dialdehydic form but some hydrated form of OPA is reacting with AAs. This finding needs more investigation because it would change the view on reactivity of OPA with nucleophiles.

## LIST OF ABBREVIATIONS

2-ME	2-mercptoethanol
2-MPT	2-methylpropane-2-thiol
AA	amino acid
AAs	amino acids
ACN	acetonitrile
AOAC	Association of Analytical Communities
APCI	atmospheric pressure chemical ionization
BA	benzaldehyde
Br-BQCA	3-(4-bromobenzoyl)chinoline-2-carboxaldehyde
CBQCA	3-(4-carboxybenzoyl)chinoline-2-carboxaldehyde
CE	capillary electrophoresis
LED	light-emitting diode
LEDIF	LED-induced fluorescence
LIF	laser-induced fluorescence
CE	counter electrode
Cl-BQCA	3-(4-chlorobenzoyl)chinoline-2-carboxaldehyde
CV	cyclic voltammetry
CZE	capillary zone electrophoresis
DAB	diacetylbenzene
DC	direct current
DMF	dimethylformamide
DMSO	dimethylsulfoxide
ET	ethanethiol
EPR	electron paramagnetic resonance
FQCA	3-(2-furoyl)chinoline-2-carboxaldehyde
HPLC	high-performance liquid chromatography
IEC	ion-exchange chromatography
IPA	isophthalaldehyde
IR	infrared
LC	liquid chromatography
MCE	2-mercptoethanol

<i>m</i> -DAB	<i>m</i> -diacetylbenzene
MECC	micellar electrokinetic capillary chromatography
MPA	3-mercaptopropionic acid
MS	mass spectrometry
NAC	N-acetylcysteine
NDA	naphthalene-2,3-dicarboxaldehyde
NMR	nuclear magnetic resonance
<i>o</i> -DAB	<i>o</i> -diacetylbenzene
OPA	orthophthalaldehyde
<i>p</i> -DAB	<i>p</i> -diacetylbenzene
QM	quantum mechanics
RP-HPLC	reversed-phase high-performance liquid chromatography
SEC	spectroelectrochemistry
SCE	saturated calomel electrode
TPA	terephthalaldehyde
UPLC	ultra-performance liquid chromatography
UV	ultraviolet light
Vis	visible light
WE	working electrode

## List of Figures

1	Structures of OPA, IPA and TPA . . . . .	6
2	Structure of ninhydrin. . . . .	11
3	The reaction of ninhydrin with $\alpha$ -AAs and with primary amines. . . . .	12
4	The reaction of OPA with a thiol and an amine. . . . .	14
5	The suggestion for mechanism of reaction of OPA with ammonia. <sup>29</sup> . . . . .	14
6	The suggestion for mechanism of reaction of OPA with glycine. <sup>29</sup> . . . . .	15
7	The reaction of NDA with an amine and cyanide ions. . . . .	15
8	The scheme of reaction for FQCA, CBQCA, Br-BQCA and Cl-BQCA. . . . .	16
9	Acid-catalyzed hydration of a carbonyl group. . . . .	19
10	Base-catalyzed hydration of a carbonyl group. . . . .	19
11	General scheme for reduction of a carbonyl compound. . . . .	21
12	Hydration of OPA in aqueous solvents. <sup>29</sup> . . . . .	22
13	The first reduction step of OPA. <sup>45</sup> . . . . .	22
14	Addition of hydroxide ions to OPA yielding a geminal diol anion. <sup>45</sup> . . . . .	23
15	The second reduction step of OPA. <sup>45</sup> . . . . .	23
16	Reduction of IPA in acidic pH (pH < 5). <sup>42</sup> . . . . .	24
17	Reduction of IPA in the range of pH from 5 to 10. <sup>42</sup> . . . . .	25
18	Reduction of IPA at pH > 10. <sup>42</sup> . . . . .	26
19	Addition of hydroxide ions to IPA at pH > 11. <sup>42</sup> . . . . .	26
20	Reduction of the diprotonated form of TPA in the range of pH from 1 to 5. <sup>48</sup> . . . . .	27
21	Conversion of the product of the first reduction step of TPA in pH from 1 to 5 to an aldol. <sup>48</sup> . . . . .	28
22	Second step of reduction of TPA at pH from 1 to 5. <sup>48</sup> . . . . .	28
23	First step of reduction of TPA at pH from 5 to 8.5. <sup>48</sup> . . . . .	29
24	Second step of reduction of TPA at pH from 5 to 8.5. <sup>48</sup> . . . . .	30
25	First step of reduction of TPA at pH > 8.5. <sup>48</sup> . . . . .	31
26	Second step of reduction of TPA at pH > 8.5. <sup>48</sup> . . . . .	31
27	Addition of hydroxide ions to TPA at pH > 10. <sup>48</sup> . . . . .	32
28	Structures of <i>o</i> -DAB, <i>m</i> -DAB and <i>p</i> -DAB. . . . .	33
29	A cell used for electrolysis of studied substances. . . . .	35

30	A cell used for UV/Vis SEC of studied substances. . . . .	37
31	A cell used for <i>in situ</i> generation of radicals in the EPR cavity. . . . .	38
32	CVs of OPA in ACN. . . . .	42
33	The dependence of current in time during electrolysis of OPA on the first wave. . . . .	43
34	Change in UV/Vis spectra of OPA during the first reduction step. . . . .	44
35	Change in IR spectra of OPA during the first reduction step. . . . .	45
36	A proposed mechanism for the first step of the OPA reduction. . . . .	46
37	EPR spectrum of OPA radical. . . . .	47
38	CVs of IPA in ACN . . . . .	48
39	The dependence of current in time during electrolysis of IPA on the first wave. . . . .	49
40	Change in UV/Vis spectra of IPA during the first reduction step. . . . .	50
41	Change in IR spectra of IPA during the first reduction step. . . . .	51
42	The proposed mechanism for the first reduction step of IPA. . . . .	52
43	A proposed mechanism for rearomatization of one structural unit in formed oligomer of IPA with the participation of the solvent. . . . .	52
44	CVs of TPA in ACN. . . . .	53
45	The dependence of current in time during electrolysis of TPA on the first wave. . . . .	54
46	Change in UV/Vis spectra of TPA during the first reduction step. . . . .	55
47	Change in UV/Vis spectra of TPA during oxidation. . . . .	55
49	A planar quinoid structure of a TPA radical anion. . . . .	56
48	Change in IR spectra of TPA during the first reduction step. . . . .	57
51	<i>Cis</i> and <i>trans</i> rotamers of the TPA radical anion. . . . .	58
50	EPR spectrum of the TPA radical anion. . . . .	59
52	Cyclic voltammogram of TPA in DMF, the first step. . . . .	64
53	Cyclic voltammogram of TPA in DMF, the second step. . . . .	65
54	The dependence of half-wave potentials on pH for reduction of OPA in aqueous phosphate buffers. . . . .	67
55	The dependence of limiting currents on pH for reduction of OPA in aqueous phosphate buffers. . . . .	67
56	UV/Vis spectra for reaction of hydrated OPA with isoleucine. . . . .	70

57	UV/Vis spectra for reaction of unhydrated OPA with isoleucine. . .	70
58	CV of ferrocene in ACN in UV/Vis SEC cell. . . . .	83
59	Change in UV/Vis spectra of ferrocene during reduction. . . . .	84
60	Change in UV/Vis spectra of ferrocene during oxidation. . . . .	84
61	Change in UV/Vis spectra of <i>o</i> -DAB during the first reduction step.	86
62	Change in UV/Vis spectra of <i>m</i> -DAB during the first reduction step.	87
63	Change in UV/Vis spectra of <i>p</i> -DAB during the first reduction step.	89
64	Change in UV/Vis spectra of <i>p</i> -DAB during oxidation. . . . .	89
65	EPR spectrum of the <i>p</i> -DAB radical anion. . . . .	90

## List of Tables

1	Reduction potentials and the electron consumptions for studied benzene dialdehydes in ACN and comparison with benzaldehyde (BA) . . . . .	60
2	Reduction potentials from CV for OPA in ACN, DMF and acetone and on mercury and gold electrode. Potentials are related to the SCE. . . . .	63
3	Reduction potentials from CV for IPA in ACN, DMF and acetone and on mercury and gold electrode. Potentials are related to the SCE. . . . .	63
4	Reduction potentials from CV for TPA in ACN, DMF and acetone and on mercury and gold electrode. Potentials are related to the SCE. . . . .	64
5	Slopes from $\ln(i)-t$ curves for the ratio AA:OPA 3:1 . . . . .	69
6	The composition of the derivatization agents with OPA. . . . .	79
7	The composition of the derivatization agents with NDA. . . . .	81
8	Reduction potentials and currents from DC-polarography for studies compounds in ACN. Potentials are related to the SCE. . . . .	82
9	Reduction potentials and currents from DC-polarography for studies compounds in DMF. Potentials are related to the SCE. . . . .	82
10	Reduction potentials and currents from CV for <i>o</i> -DAB in different solvents and working electrodes. For comparison values for OPA are presented. Potentials are related to the SCE. . . . .	85
11	Reduction potentials and currents from CV for <i>m</i> -DAB in different solvents and working electrodes. For comparison values for IPA are presented. Potentials are related to the SCE. . . . .	87
12	Reduction potentials and currents from CV for <i>p</i> -DAB in different solvents and working electrodes. For comparison values for TPA are presented. Potentials are related to the SCE. . . . .	88

# SUPPLEMENTARY MATERIAL

## A Tables

**Table 6:** The composition of the derivatization agents with OPA.

literature	separation method	composition of derivatization solution	pH	detection	reaction time	notes
McKenzie et al. <sup>19</sup>	capillary LC	0.54 % (w/v) OPA, 0.45 % (w/v) 2-MPA	10.5	electrochemically (cyclic voltammetry)	5 min	simultaneous determination of catecholamines, kept at room temperature
Meussen et al. <sup>20</sup>	UPLC	0.40 % (w/v) OPA, 0.42 % (w/v) ET	10.5	spectrophotometry (338 nm)		every second day a new solution
Hanczkó et al. <sup>21</sup>	HPLC	1.14 % (w/v) OPA, 0.44 % (w/v) ET	9.3 – 11.3	spectrophotometry (between 190 and 400 nm), spectrofluorimetry (excitation 337 nm, emission 454 nm)	1 min	solutions were used after 90 min, storage max. 2 days, at 4 °C
Asadpoor et al. <sup>2</sup>	HPLC	OPA/MPA in methanol	9.5	spectrofluorimetry (excitation 330 nm, emission 450 nm)	1 min	
Dai et al. <sup>4</sup>	HPLC	0.39 % (w/v) OPA, 0.43 % (w/v) 2-ME	9.5	spectrofluorimetry (excitation 340 nm, emission 455 nm)	1 min	storage at 4 °C, solutions used max. 36 hod
Tian et al. <sup>25</sup>	CE	0.13 % (w/v) OPA, 2.23 % (w/v) 2-ME	10	spectrophotometry (340 nm)		

Continued on next page

**Table 6 – continued from previous page**

literature	separation method	composition of derivatization solution	pH	detection	reaction time	notes
Roth <sup>15</sup>	-	0.016 % (w/v) OPA, 0.009 % (w/v) 2-ME	9.5	spectrofluorimetry (excitation 340 nm, emission 455 nm)	5 – 25 min	stable 1 day at room temperature
Körös <sup>22</sup>	HPLC	0.11 % (w/v) OPA, 0.50 % (w/v) ET		spectrophotometry, spectrofluorimetry	2 min	
Boyd et al. <sup>23</sup>	capillary LC	40 mM OPA, 50 mM 2-MPA	10.6 ± 0.1	electrochemically	2 min	if precipitates were present, a new solution was prepared
Sandlin et al. <sup>26</sup>	CE	10 mM OPA, 40 mM 2-ME	9.5	LIF	< 2 min	
Cellar et al. <sup>27</sup>	CE	10 mM OPA, 40 mM 2-ME	9.5	LIF	1 min	
Pereira et al. <sup>24</sup>	RP-HPLC	250 mg dissolved in 1.5 ml of ethanol, borate buffer added to total volume 10 ml, 200 µl of 2-ME added	10.5	spectrofluorimetry (excitation 335 nm, emission 440 nm)	3 min	used after 90 min, storage in dark glass bottles at 4 °C, max. 9 days
Ravindran et al. <sup>18</sup>	IEC	1.2 g OPA in 15-20 ml of ethanol, 2.4 ml 3-MPA and 10 ml of Brij-35 solution added, then diluted to 1 l with a buffer		spectrofluorimetry		
Ptolemy et al. <sup>28</sup>	CE	100 mM OPA	9.5	spectrophotometry (340 nm)		

**Table 7:** The composition of the derivatization agents with NDA.

literature	separation method	composition of derivatization solution	pH	detection	reaction time	notes
Nandi et al. <sup>62</sup>	CE	7 mM NDA, 10 mM NaCN	9.2	LIF	3 - 15 min	
Chang et al. <sup>63</sup>	CE	NDA/CN <sup>-</sup>	9.5	LEDIF		
Kao et al. <sup>64</sup>	CE	0.3 mM NDA, 0.3 mM NaCN	9.0	LEDIF	40 min	
Chang et al. <sup>65</sup>	CE	0.1 mM NDA, 0.1 mM NaCN	9.3	LEDIF	30 min	storage at 4 °C for one week
Yassine et al. <sup>66</sup>	CE	5.6 mM NDA, 2.8 mM NaCN	9.2	LIF	< 30 s	storage at 4 °C for one week
Huynh et al. <sup>67</sup>	CE	0.6 mM NDA, 1.2 mM 2-ME	9.2	LIF	< 30 s	
Wu et al. <sup>68</sup>	CE (MEKC)	1 mM NDA, 0.1 mM KCN	9.2	LIF	15-30 min	

**Table 8:** Reduction potentials and currents from DC-polarography for studies compounds in ACN. Potentials are related to the SCE.

compound	first wave		second wave		third wave	
	i/ $\mu$ A	$E_{1/2}^1$ /V	i/ $\mu$ A	$E_{1/2}^2$ /V	i/ $\mu$ A	$E_{1/2}^3$ /V
OPA	0.837	-1.47	0.475	-2.01	-	-
1,2-DAB	0.290	-1.88	0.400	-2.07	-	-
IPA	0.750	-1.65	0.260	-2.00	0.510	-2.54
1,3-DAB	0.775	-1.95	0.175	-2.32	0.650	-2.65
TPA	0.625	-1.40	0.500	-1.88	-	-
1,4-DAB	0.825	-1.64	0.7375	-2.05	-	-

**Table 9:** Reduction potentials and currents from DC-polarography for studies compounds in DMF. Potentials are related to the SCE.

compound	first wave		second wave		third wave	
	i/ $\mu$ A	$E_{1/2}^1$ /V	i/ $\mu$ A	$E_{1/2}^2$ /V	i/ $\mu$ A	$E_{1/2}^3$ /V
OPA	0.463	-1.38	0.300	-2.05	-	-
1,2-DAB	0.065	-1.81	0.308	-2.03	-	-
IPA	0.480	-1.58	0.050	-2.00	0.350	-2.40
1,3-DAB	0.475	-1.87	0.400	-2.55	-	-
TPA	0.465	-1.30	0.385	-1.89	-	-
1,4-DAB	0.470	-1.55	0.420	-2.04	-	-

## B UV/Vis SEC

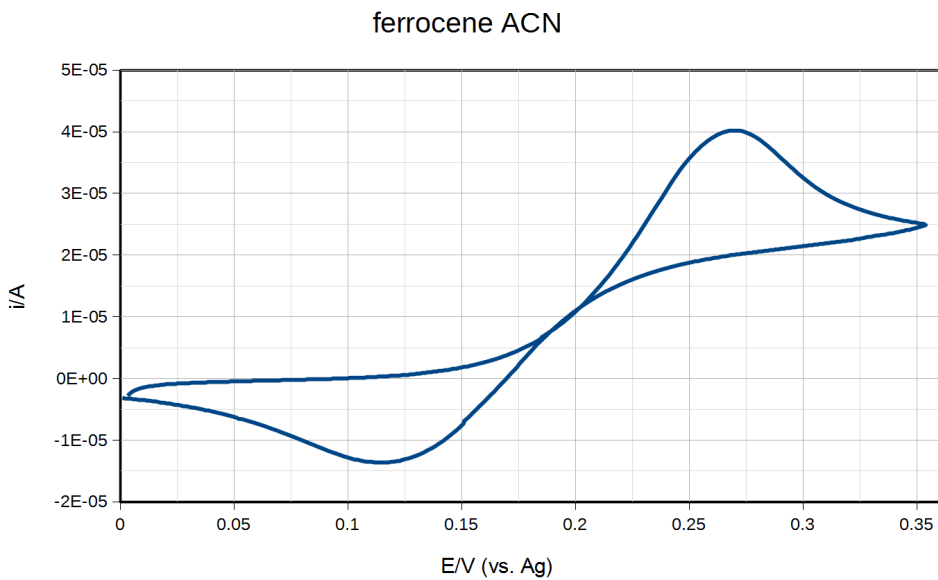


**Figure 58:** CV of ferrocene in ACN in UV/Vis SEC cell ( $c = 0.003 \text{ M}$ ).

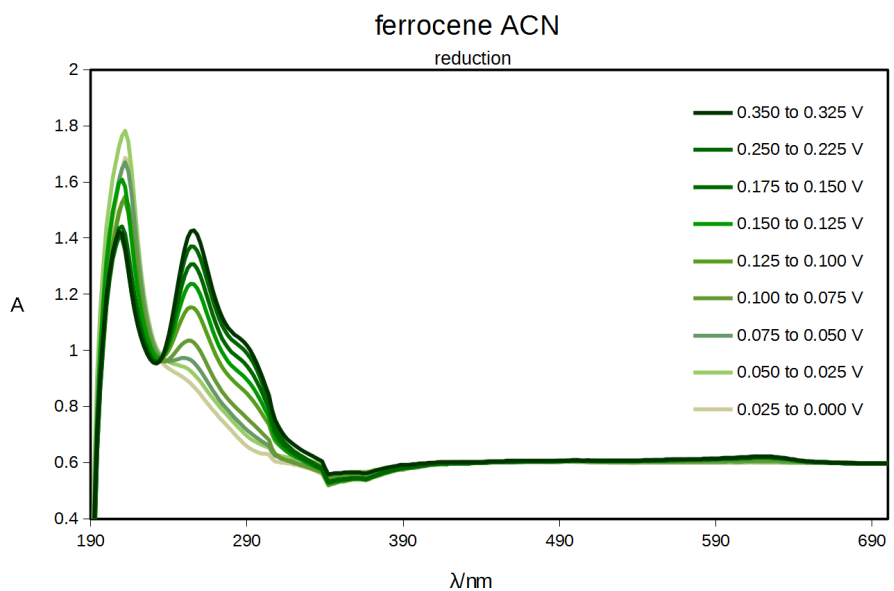


**Figure 59:** Change in UV/Vis spectra of ferrocene ( $c = 0.003 \text{ M}$ ) during electrochemical reduction.

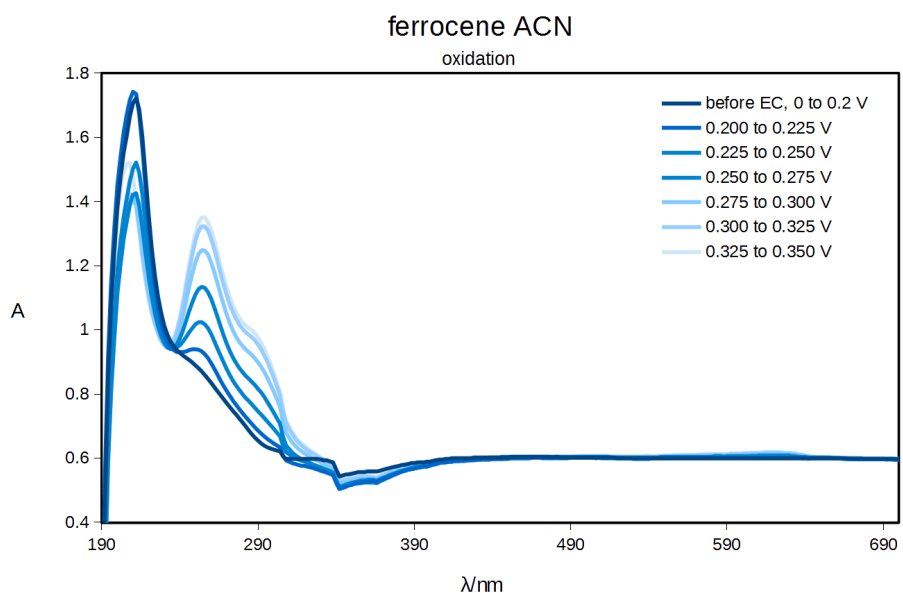


**Figure 60:** Change in UV/Vis spectra of ferrocene ( $c = 0.003 \text{ M}$ ) during electrochemical oxidation.

## C Electrochemical behavior of diacetylbenzenes in ACN, DMF and acetone

In the following text, comparison of electrochemical behavior of diacetylbenzenes with corresponding benzenedialdehydes is presented. The first reduction step of *o*-DAB occurs at more negative potentials than the first reduction of OPA due to the electrodonating methyl groups which reduce the electron withdrawing ability of carbonyls, cf. Table 10. It is completely irreversible and current of the first wave corresponds to uptake of less than one electron/molecule. On UV/Vis SEC spectra shown in Fig. 61, only peak at 240 nm corresponding to  $\pi \rightarrow \pi^*$  and  $n \rightarrow \pi^*$  transitions in carbonyl groups disappears and peak at 200 nm  $\pi \rightarrow \pi^*$  and  $n \rightarrow \pi^*$  transitions in benzene ring slightly increases. The second reduction step then is close to the potential where benzaldehyde is reduced.

**Table 10:** Reduction potentials and currents from CV for *o*-DAB in different solvents and working electrodes. For comparison values for OPA are presented. Potentials are related to the SCE.

compound	solvent/electrode	$E_{pc}^1/V$	$i_{pc}^1/\mu A$	$E_{pc}^2/V$	$i_{pc}^2/\mu A$	$E_{pc}^3/V$	$i_{pc}^3/\mu A$
<i>o</i> -DAB	DMF/Hg	-1.84	0.025	-2.06	1.500	-	-
	DMF/Au	-1.84	0.150	-2.07	1.200	-	-
	ACN/Hg	-1.85	1.375	-2.10	2.050	-	-
	acetone/Hg	-1.87	1.725	-2.08	2.700	-	-
OPA	DMF/Hg	-1.41	1.625	-2.10	1.050	-	-
	DMF/Au	-1.44	1.150	-	-	-	-
	ACN/Hg	-1.51	3.275	-2.02	0.300	-	-

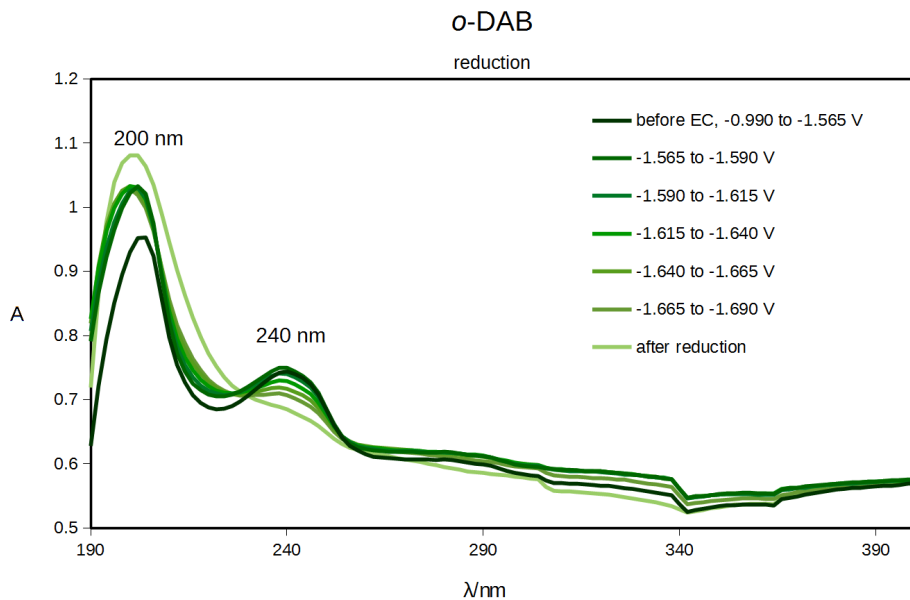


**Figure 61:** Change in UV/Vis spectra of *o*-DAB during the first reduction step in ACN. Potentials are related to the ferrocene system  $\text{Fc}^+/\text{Fc}$ .

Also *m*-DAB is reduced at more negative potentials than the corresponding benzenedialdehyde (IPA), cf. Table 11. In contrast to IPA, reduction steps of *m*-DAB are reversible. Current of the first wave again represents uptake of one electrone/molecule. During UV/Vis SEC experiments (Fig. 62), one can observe disappearance of peak at 220 nm corresponding to  $\pi \rightarrow \pi^*$  and  $n \rightarrow \pi^*$  transitions and two new peaks at 196 and 450 nm ( $\pi \rightarrow \pi^*$  and  $n \rightarrow \pi^*$  transitions in benzene ring and  $\pi \rightarrow \pi^*$  transitions in conjugated double bonds).

**Table 11:** Reduction potentials and currents from CV for *m*-DAB in different solvents and working electrodes. For comparison values for IPA are presented. Potentials are related to the SCE.

compound	solvent/electrode	$E_{pc}^1/V$	$i_{pc}^1/\mu A$	$E_{pc}^2/V$	$i_{pc}^2/\mu A$	$E_{pc}^3/V$	$i_{pc}^3/\mu A$	$E_{pc}^4/V$	$E_{pc}^5/V$
<i>m</i> -DAB	DMF/Hg	-1.92	1.850	-2.33	0.325	-2.64	0.825	-	-
	DMF/Au	-1.91	1.475	-	-	-	-	-	-
	ACN/Hg	-1.97	1.175	-2.33	-	-	-	-	-
	acetone/Hg	-1.95	3.600	-2.16	-	-2.26	-	-	-
IPA	DMF/Hg	-1.64	1.638	-2.07	-	-2.59	-	-2.74	-2.90
	DMF/Au	-1.63	0.143	-	-	-	-	-	-
	ACN/Hg	-1.68	3.000	-2.04	1.150	-	-	-	-
	acetone/Hg	-1.65	0.400	-1.96	1.338	-	-	-	-

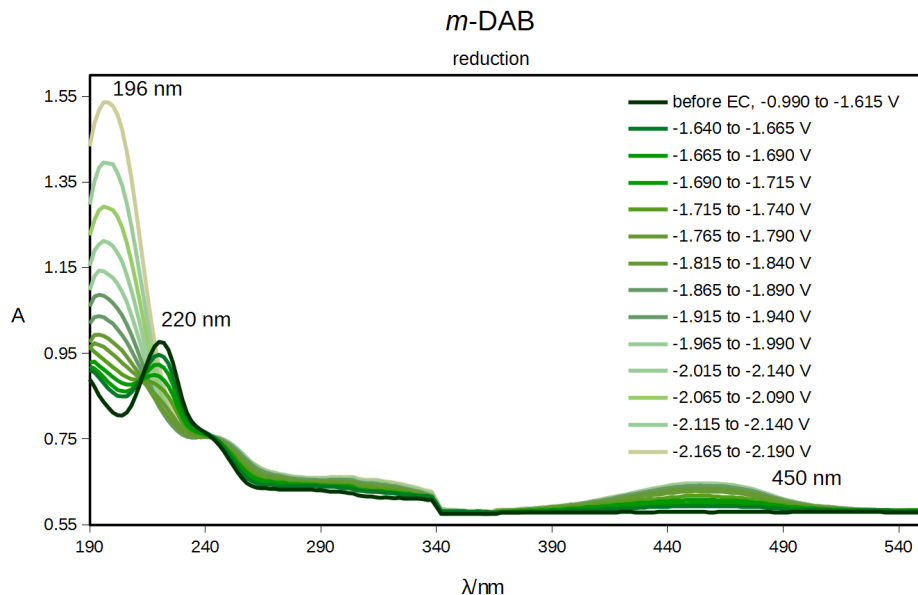


**Figure 62:** Change in UV/Vis spectra of *m*-DAB during the first reduction step in ACN. Potentials are related to the ferrocene system  $\text{Fc}^+/\text{Fc}$ .

Electrochemical behavior of *p*-DAB is very similar to that of TPA, cf. Table 12. The first reduction step occurs approx. at  $-1.65$  V and the second one at approx.  $-2.0$  V. Both steps represent uptake of one electron/molecule and they are completely reversible. The first step was studied also by UV/Vis SEC – the progress of the reduction and the re-oxidation is in Fig. 63 and 64. Peak at 254 nm corresponding to  $\pi \rightarrow \pi^*$  and  $n \rightarrow \pi^*$  transitions in carbonyl groups diminishes as the reduction proceeds and new peaks at 394 and 614 nm appear ( $\pi \rightarrow \pi^*$  transitions in conjugated double bonds). During oxidation the spectrum returns to the original form confirming the fact from CV that the reduction of *p*-DAB is completely reversible. The presence of the radical anion was confirmed by EPR SEC (Fig. 65).

**Table 12:** Reduction potentials and currents from CV for *p*-DAB in different solvents and working electrodes. For comparison values for TPA are presented. Potentials are related to the SCE.

compound	solvent/electrode	$E_{pc}^1/V$	$i_{pc}^1/\mu A$	$E_{pc}^2/V$	$i_{pc}^2/\mu A$	$E_{pc}^3/V$	$i_{pc}^3/\mu A$
<i>p</i> -DAB	DMF/Hg	-1.59	1.950	-1.95	0.325	-2.09	1.750
	DMF/Au	-1.58	1.250	-2.11	–	–	–
	ACN/Hg	-1.68	3.300	-2.06	3.250	–	–
	acetone/Hg	-1.64	2.875	-1.87	2.375	-2.20	2.575
TPA	DMF/Hg	-1.34	1.925	-1.90	1.900	–	–
	DMF/Au	-1.35	0.975	-1.93	0.900	–	–
	ACN/Hg	-1.44	3.150	-1.90	2.850	–	–

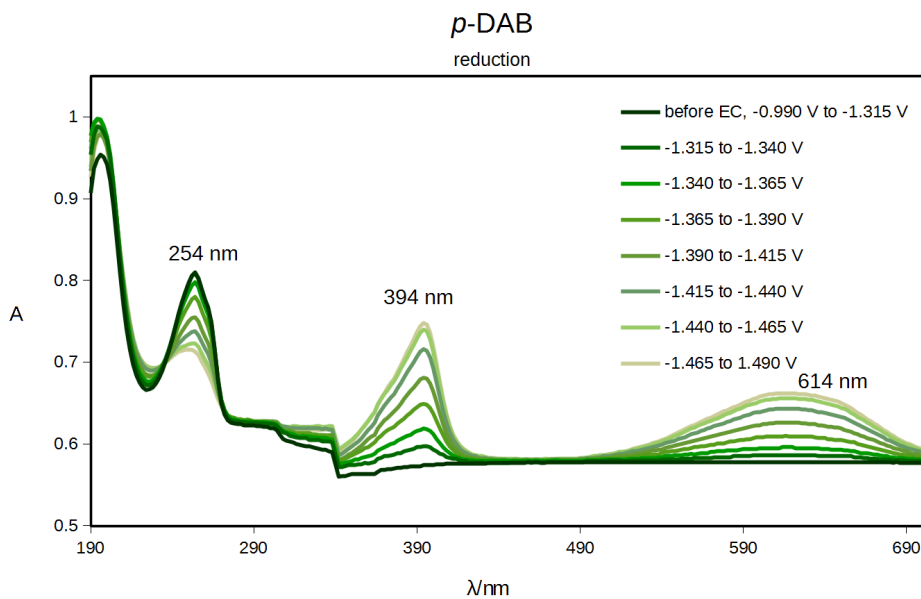


**Figure 63:** Change in UV/Vis spectra of *p*-DAB during the first reduction step in ACN. Potentials are related to the ferrocene system  $\text{Fc}^+/\text{Fc}$ .

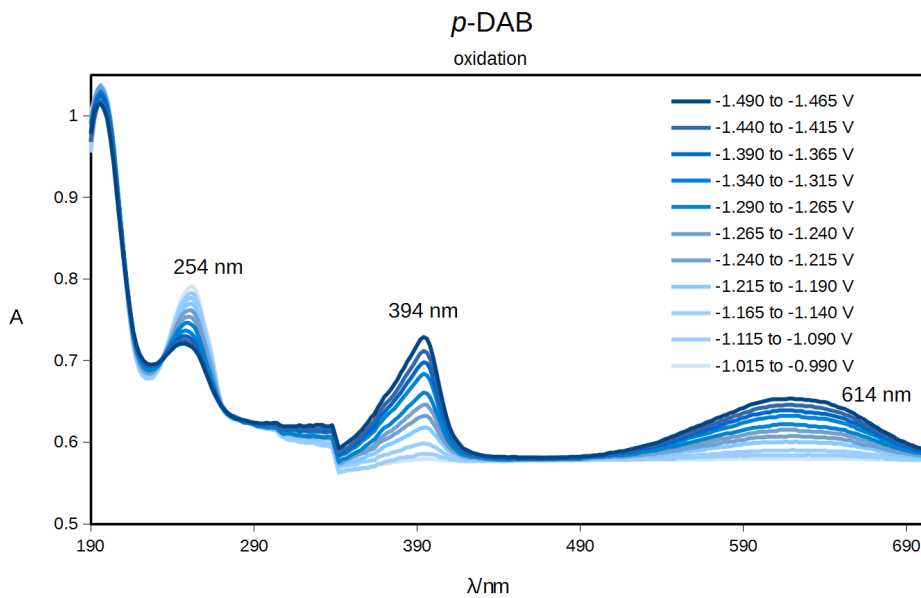


**Figure 64:** Change in UV/Vis spectra of *p*-DAB during oxidation in ACN. Potentials are related to the ferrocene system  $\text{Fc}^+/\text{Fc}$ .

06

EPR spectrum of the p-DAB radical anion

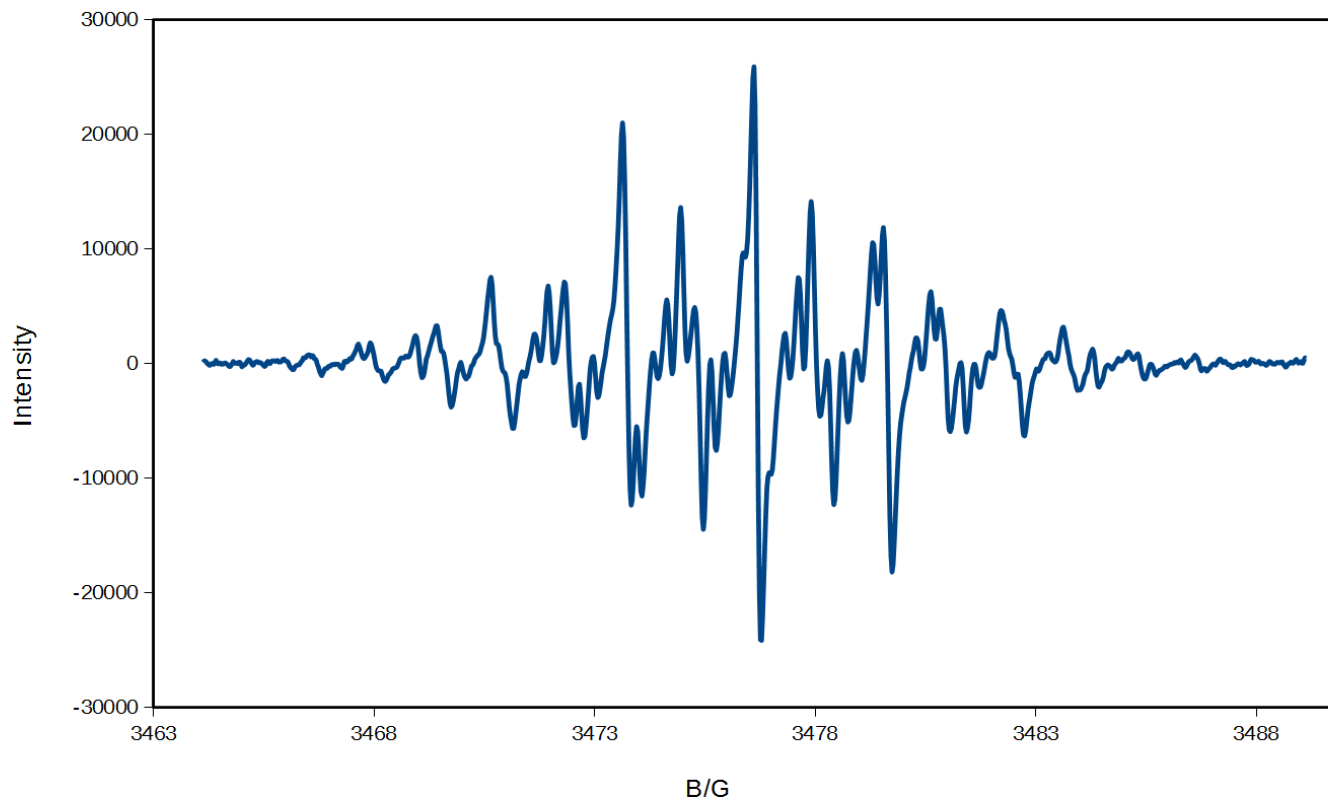


**Figure 65:** EPR spectrum of the *p*-DAB radical anion generated electrochemically *in situ* in the EPR cavity.

## BIBLIOGRAPHY

1. Kantnerová, K.; Ludvík, J. Analytical determination of amino acids using reactions with carbonyl compounds. *Crit. Rev. Clin. Lab. Sci.* **2016**, submitted.
2. Asadpoor, M.; Ansarin, M.; Nemati, M. Amino Acid profile as a feasible tool for determination of the authenticity of fruit juices. *Adv. Pharm. Bull.* **2014**, *4*, 359–62.
3. Peace, R. W.; Gilani, G. S. Chromatographic Determination of Amino Acids in Foods. *J. AOAC Int.* **2005**, *88*, 877–887.
4. Dai, Z.; Wu, Z.; Jia, S.; Wu, G. Analysis of amino acid composition in proteins of animal tissues and foods as pre-column o-phthaldialdehyde derivatives by HPLC with fluorescence detection. *J. Chromatogr. B* **2014**, *964*, 116–27.
5. Rigas, P. G. Review: Liquid Chromatography—Post-Column Derivatization for Amino Acid Analysis: Strategies, Instrumentation, and Applications. *Instrum. Sci. Technol.* **2012**, *40*, 161–193.
6. Friedman, M. Applications of the Ninhydrin Reaction for Analysis of Amino Acids, Peptides, and Proteins to Agricultural and Biomedical Sciences. *J. Agric. Food Chem.* **2004**, *52*, 385–406.
7. Csapó, J.; Albert, C.; Lóki, K.; Csapó-Kiss, Z. Separation and determination of the amino acids by ion exchange column chromatography applying post-column derivatization. *Acta Univ. Sapientiae, Alimentaria* **2008**, *1*, 5–29.
8. Sun, S.-W.; Lin, Y.-C.; Weng, Y.-M.; Chen, M.-J. Efficiency improvements on ninhydrin method for amino acid quantification. *J. Food Compos. Anal.* **2006**, *19*, 112–117.
9. Cernei, N.; Heger, Z.; Veselý, S.; Zítka, O.; Adam, V.; Kizek, R. Chromatografická charakterizace aminokyselinových profilů vzorků moči pacientů s karcinomem prostaty. *Klin. Biochem. Metab.* **2014**, *22*, 196–202.

10. Kaspar, H.; Dettmer, K.; Gronwald, W.; Oefner, P. J. Advances in amino acid analysis. *Anal. Bioanal. Chem.* **2009**, *393*, 445–52.
11. Moulin, M.; Deleu, C.; Larher, F. R.; A., B. High performance liquid chromatography determination of pipecolic acid after precolumn ninhydrin derivatization using-domestic microwave. *Anal. Biochem.* **2002**, *308*, 320–327.
12. Molnár-Perl, I. In *J. Chromatogr. Libr.*; Molnár-Perl, I., Ed.; Elsevier: Amsterdam, 2005; Vol. 70; Chapter Preface, pp VII–VIII.
13. Veledo, M. T.; de Frutos, M.; Diez-Masa, J. C. Amino acids determination using capillary electrophoresis with on-capillary derivatization and laser-induced fluorescence detection. *J. Chromatogr. A* **2005**, *1079*, 335–343.
14. Jelly, R.; Patton, E. L.; Lennard, C.; Lewis, S. W.; Lim, K. F. The detection of latent fingermarks on porous surfaces using amino acid sensitive reagents: a review. *Anal. Chim. Acta* **2009**, *652*, 128–42.
15. Roth, M. Fluorescence Reaction for Amino Acids. *Anal. Chem.* **1971**, *43*, 880–882.
16. Zuman, P. Reactions of Orthophthalaldehyde and Related Compounds with Amino Acids. *Anal. Lett.* **2005**, *38*, 1213–1220.
17. Molnar-Perl, I. Advancement in the derivatizations of the amino groups with the o-phthalaldehyde-thiol and with the 9-fluorenylmethyloxycarbonyl chloride reagents. *J. Chromatogr. B* **2011**, *879*, 1241–69.
18. Ravindran, G.; Bryden, W. L. Tryptophan determination in proteins and feedstuffs by ion exchange chromatography. *Food Chem.* **2005**, *89*, 309–314.
19. McKenzie, J. A. M.; Watson, C. J.; Rostand, R. D.; German, I.; Witowski, S. R.; Kennedy, R. T. Automated capillary liquid chromatography for simultaneous determination of neuroactive amines and amino acids. *J. Chromatogr. A* **2002**, *962*, 105–115.

20. Meussen, B. J.; van Zeeland, A. N. T.; Bruins, M. E.; Sanders, J. P. M. A Fast and Accurate UPLC Method for Analysis of Proteinogenic Amino Acids. *Food Anal. Methods* **2013**, *7*, 1047–1055.
21. Hanczko, R.; Jambor, A.; Perl, A.; Molnar-Perl, I. Advances in the o-phthalaldehyde derivatizations. Comeback to the o-phthalaldehyde-ethanethiol reagent. *J. Chromatogr. A* **2007**, *1163*, 25–42.
22. Körös, A. Analysis of amino acids and amines in biological tissues and food matrices by HPLC. Dissertation, 2008.
23. Boyd, B. W.; Witowski, S. R.; Kennedy, R. T. Trace-Level Amino Acid Analysis by Capillary Liquid Chromatography and Application to in vivo Microdialysis Sampling with 10-s Temporal Resolution. *Anal. Chem.* **2000**, *72*, 865–871.
24. Pereira, V.; Pontes, M.; Camara, J. S.; Marques, J. C. Simultaneous analysis of free amino acids and biogenic amines in honey and wine samples using in loop orthophthalaldehyde derivatization procedure. *J. Chromatogr. A* **2008**, *1189*, 435–43.
25. Tian, M.; Zhang, J.; Mohamed, A. C.; Han, Y.; Guo, L.; Yang, L. Efficient capillary electrophoresis separation and determination of free amino acids in beer samples. *Electrophoresis* **2014**, *35*, 577–84.
26. Sandlin, Z. D.; Shou, M.; Shackman, J. G.; Kennedy, R. T. Microfluidic Electrophoresis Chip Coupled to Microdialysis for in Vivo Monitoring of Amino Acid Neurotransmitters. *Anal. Chem.* **2005**, *77*, 7702–7708.
27. Cellar, N. A.; Burns, S. T.; Meiners, J.-C.; Chen, H.; Kennedy, R. T. Microfluidic Chip for Low-Flow Push-Pull Perfusion Sampling in Vivo with On-Line Analysis of Amino Acids. *Anal. Chem.* **2005**, *77*, 7067–7073.
28. Ptolemy, A. S.; Tran, L.; Britz-McKibbin, P. Single-step enantioselective amino acid flux analysis by capillary electrophoresis using on-line sample preconcentration with chemical derivatization. *Anal. Biochem.* **2006**, *354*, 192–204.

29. Zuman, P. Reactions of Orthophthalaldehyde with Nucleophiles. *Chem. Rev.* **2004**, *104*, 3217–3238.
30. Zuman, P.; Salem, N.; Kulla, E. What Do We Know about Determination of Amino Acids with Orthophthalaldehyde? *Electroanalysis* **2009**, *21*, 645–649.
31. Beale, S. C.; Hsieh, Y.-Z.; Wiesler, D.; Novotny, M. Application of 3-(2-furoyl)quinoline-2-carbaldehyde as a fluorogenic reagent for the analysis of primary amines by liquid chromatography with laser-induced fluorescence detection. *J. Chromatogr.* **1990**, *499*, 579–587.
32. Liu, J.; Hsieh, Y.-Z.; Wiesler, D.; Novotny, M. Design of 3-(4-carboxybenzoyl)-2-quinolinecarboxaldehyde as a reagent for ultrasensitive determination of primary amines by capillary electrophoresis using laser fluorescence detection. *Anal. Chem.* **1991**, *63*, 408–412.
33. Zhang, N.; Zhang, H. S.; Wang, H. Separation of free amino acids and catecholamines in human plasma and rabbit vitreous samples using a new fluorogenic reagent 3-(4-bromobenzoyl)-2-quinolinecarboxaldehyde with CE-LIF detection. *Electrophoresis* **2009**, *30*, 2258–65.
34. Zhang, N.; Guo, X. F.; Wang, H.; Zhang, H. S. Determination of amino acids and catecholamines derivatized with 3-(4-chlorobenzoyl)-2-quinolinecarboxaldehyde in PC12 and HEK293 cells by capillary electrophoresis with laser-induced fluorescence detection. *Anal. Bioanal. Chem.* **2011**, *401*, 297–304.
35. Fukushima, T.; Usui, N.; Santa, T.; Imai, K. Recent progress in derivatization methods for LC and CE analysis. *J. Pharm. Biomed. Anal.* **2003**, *30*, 1655–1687.
36. Poinsot, V.; Rodat, A.; Gavard, P.; Feurer, B.; Couderc, F. Recent advances in amino acid analysis by CE. *Electrophoresis* **2008**, *29*, 207–23.
37. Thongkhao-On, K.; Kottegoda, S.; Pulido, J. S.; Shippy, S. A. Determination of amino acids in rat vitreous perfusates by capillary electrophoresis. *Electrophoresis* **2004**, *25*, 2978–84.

38. McMurry, J. *Organic Chemistry (in Czech Organická chemie)*; 2007; Chapter 26.
39. Baymak, M.; Kulla, E.; Zuman, P. Solvent-solute interactions of isomeric phthalaldehydes in aqueous solutions. *J. Mol. Liq.* **2007**, *131-132*, 24–28.
40. Lund, H.; Hammerich, O. *Organic Electrochemistry*; Marcel Dekker, 2001; Chapter 10.
41. McClelland, R.; Coe, M. Structure-reactivity effects in the hydration of benzaldehydes. *J. Am. Chem. Soc.* **1983**, *105*, 2718–2725.
42. Bover, W.; Johnson, D.; Baymak, M.; Zuman, P. Electroreduction of isophthalaldehyde: An example of simultaneous reduction of two identical electroactive centers. *Indian J. Chem., Sect. A: Inorg., Bio-inorg., Phys., Theor. Anal. Chem.* **2003**, *42*, 744–750.
43. Fijalek, Z.; Pugia, M.; Zuman, P. Polarographic and electrochemical studies of some aromatic nitro compounds: Part VII. Polarographic, voltammetric, and controlled potential electrolytic reduction of meta- and para-nitrobenzaldehyde. *Electroanalysis* **1993**, *5*, 65–78.
44. Furman, N.; Norton, D. Polarographic determination of phthalaldehyde. *Anal. Chem.* **1954**, *26*, 1111–1115.
45. Salem, N.; Andreeescu, S.; Kulla, E.; Zuman, P. Existence and reactivity of three forms of orthophthalaldehyde in aqueous solutions. Polarographic, voltammetric, and spectrophotometric study. *J. Phys. Chem. A* **2007**, *111*, 4658–4670.
46. Stone, E.; Maki, A. ESR study of rotational isomerism in substituted benzaldehyde anions. *J. Chem. Phys.* **1963**, *38*, 1999–2011.
47. Baymak, M.; Vercoe, K.; Zuman, P. Strong covalent hydration of terephthalaldehyde. *J. Phys. Chem. B* **2005**, *109*, 21928–21929.

48. Baymak, M.; Bover, W.; Celik, H.; Zuman, P. Electroreduction and oxidation of terephthalaldehyde and the role of hydration. *Electrochim. Acta* **2005**, *50*, 1347–1359.
49. Kargin, Y. M.; Kondranina, V. Z.; Semakhina, N. I. The electrochemical reduction of bifunctional organic compounds. Communication 4. Aromatic bifunctional compounds in aprotic medium. *Izv. Akad. Nauk SSSR, Ser. Khim.* **1971**, *2*, 278–283.
50. Kargin, Y. M.; Kondranina, V. Z. Effect of proton donors on the mechanism of the electrochemical reduction of some dicarbonyl compounds in dimethylformamide. *Izv. Akad. Nauk SSSR, Ser. Khim.* **1972**, *3*, 665–668.
51. Polarographic behaviour of p-diacetylbenzene ; an example of a compound with two electroactive centers. *J. Electroanal. Chem.* **1966**, *12*, 443 – 461.
52. Asano, T.; Ohkata, K.; Hanafusa, T. Correlation between the reaction of ketones with zinc and their polarographic half-wave reduction potential. *Chem. Lett.* **1974**, 1149–1152.
53. Pragst, F.; Ziebig, R.; Boche, E. Estimation of triplet energies from electrogenerated luminescence: possibilities and restrictions. *J. Lumin.* **1979**, *21*, 21–41.
54. Pragst, F.; Stößer, R. Verwendung von Bis(1,2,4,6-tetramethyl-1,4-dihydro-4-pyridinyl) als Reduktionsmittel zur Erzeugung organischer Radikal-anionen für EPR-Spektroskopie. *Z. Chem.* **1985**, *25*, 222.
55. Heyrovsky, J.; Zuman, P. *Practical Polarography, an Introduction for Chemistry Students*; ACADEMIC PRESS INC., 1968; Chapter I.
56. Bard, A. J.; Faulkner, L. R. *Electrochemical Methods: Fundamentals and Applications*; John Wiley & Sons, Inc., 2001; Chapter 6.5.
57. Krejcik, M.; Danek, M.; Hartl, F. Simple construction of an infrared optically transparent thin-layer electrochemical cell. Applications to the redox reactions of ferrocene, Mn<sub>2</sub>(CO)<sub>10</sub> and Mn(CO)<sub>3</sub>(3,5-di-t-butyl-catecholate)<sup>-</sup>. *J. Electroanal. Chem.* **1991**, *317*, 179–187.

58. Kantnerová, K. Spectroelectrochemical study of the reactivity of orthophthalaldehyde with amino acids. Bachelor thesis, 2014.
59. Izutsu, K. *Electrochemistry in Nonaqueous Solutions*; John Wiley & Sons, 2009; Chapter 4, pp 89–110.
60. Mairanovskii, S. G.; Rubinskaya, T. Y.; Gul'tyai, V. P.; Proskurovskaya, I. V. Electrochemical reduction of benzaldehydes to benzyl alcohol at a mercury cathode. *Bull. Acad. Sci. USSR, Div. Chem. Sci. (Engl. Transl.)* **1976**, *25*, 2203–2205.
61. Hoskovicová, I.; Zvěřinová, R.; Roháčová, J.; Dvořák, D.; Tobrman, T.; Záliš, S.; Ludvík, J. Fischer aminocarbene complexes of chromium and iron: Anomalous electrochemical reduction of p-carbonyl substituted derivatives. *Electrochim. Acta* **2011**, *56*, 6853–6859.
62. Nandi, P.; Scott, D. E.; Desai, D.; Lunte, S. M. Development and optimization of an integrated PDMS based-microdialysis microchip electrophoresis device with on-chip derivatization for continuous monitoring of primary amines. *Electrophoresis* **2013**, *34*, 895–902.
63. Chang, P. L.; Chiu, T. C.; Wang, T. E.; Hu, K. C.; Tsai, Y. H.; Hu, C. C.; Bair, M. J.; Chang, H. T. Quantitation of branched-chain amino acids in ascites by capillary electrophoresis with light-emitting diode-induced fluorescence detection. *Electrophoresis* **2011**, *32*, 1080–3.
64. Kao, Y. Y.; Liu, K. T.; Huang, M. F.; Chiu, T. C.; Chang, H. T. Analysis of amino acids and biogenic amines in breast cancer cells by capillary electrophoresis using polymer solutions containing sodium dodecyl sulfate. *J. Chromatogr. A* **2010**, *1217*, 582–7.
65. Chang, P. L.; Chiu, T. C.; Chang, H. T. Stacking, derivatization, and separation by capillary electrophoresis of amino acids from cerebrospinal fluids. *Electrophoresis* **2006**, *27*, 1922–31.

66. Yassine, O.; Morin, P.; Dispagne, O.; Renaud, L.; Denoroy, L.; Kleimann, P.; Faure, K.; Rocca, J. L.; Ouaini, N.; Ferrigno, R. Electrophoresis PDMS/glass chips with continuous on-chip derivatization and analysis of amino acids using naphthalene-2,3-dicarboxaldehyde as fluorogenic agent. *Anal. Chim. Acta* **2008**, *609*, 215–22.
67. Huynh, B. H.; Fogarty, B. A.; Nandi, P.; Lunte, S. M. A microchip electrophoresis device with on-line microdialysis sampling and on-chip sample derivatization by naphthalene 2,3-dicarboxaldehyde/2-mercaptoethanol for amino acid and peptide analysis. *J. Pharm. Biomed. Anal.* **2006**, *42*, 529–34.
68. Wu, H.; Wheeler, A.; Zare, R. N. Chemical cytometry on a picoliter-scale integrated microfluidic chip. *Proc. Natl. Acad. Sci. U. S. A.* **2004**, *101*, 12809–13.